



Institute of Oceanology Polish Academy of Sciences

ANALYSIS OF MASS, MOMENTUM AND CLIMATE RELEVANT GAS
FLUXES ACROSS THE SEA SURFACE IN THE EUROPEAN ARCTIC

Iwona Niedźwiecka

Series of publications constituting the doctoral dissertation

The thesis prepared under
the supervision of Prof. Jacek Piskozub

Sopot 2019



Instytut Oceanologii Polskiej Akademii Nauk

ANALIZA STRUMIENI MASY, PĘDU ORAZ GAZÓW ISTOTNYCH DLA
KLIMATU PRZEZ POWIERZCHNIĘ MORZA W ARKTYCE EUROPEJSKIEJ

Iwona Niedźwiecka

Cykl publikacji stanowiący rozprawę doktorską

Praca przygotowana

pod kierunkiem prof. dr hab. Jacek Piskozub

Sopot 2019

PhD thesis contents

I.	Abstract	4
	1. List of abbreviations.....	4
	2. English abstract.....	5
	3. Streszczenie (Abstract in Polish).....	15
	References.....	25
II.	List of the attached research papers	28
	<u>Research paper no 1</u>	29
	<i>Effect of gas-transfer velocity parameterization choice on air-sea CO₂ fluxes in the North Atlantic and the European Arctic</i>	
	<u>Wróbel, I., Piskozub, J. 2016. Ocean Science 12, 1091-1103.</u>	
	<u>Research paper no 2</u>	43
	<i>Monthly dynamics of carbon dioxide exchange across the sea surface of the Arctic Ocean in response to changes in gas transfer velocity and partial pressure of CO₂ in 2010</i>	
	<u>Wróbel, I. 2017. Oceanologia 59, 445-459.</u>	
	<u>Research paper no 3</u>	59
	<i>Effect of drag coefficient formula choice on wind stress climatology in the North Atlantic and the European Arctic</i>	
	<u>Wróbel-Niedźwiecka, I., Drozdowska, V., Piskozub, J., 2019. Oceanologia 61, 291-299.</u>	
III.	Authorship statements	75
IV.	Acknowledgements	80

I. Abstract

1. List of abbreviations

Abbreviation	Explanation	Objaśnienia
a.s.l.	above sea level	nad poziomem morza
C_D	drag coefficient	wsp. tarcia
CO_2	carbon dioxide	dwutlenek węgla
Gt	Gigatonnes ($=10^9$)	gigatona
k	gas transfer coefficient	wsp. wymiany gazowej
pCO_2	partial pressure of CO_2	ciśnienie parcjalne CO_2
pCO_{2A}	partial pressure of CO_2 at atmosphere	ciśnienie parcjalne CO_2 w atmosferze
pCO_{2W}	partial pressure of CO_2 at seawater	ciśnienie parcjalne CO_2 w wodzie
ΔpCO_2	difference in partial pressure	różnica ciśnień parcjalnych
Pg	Petagrams ($= 10^{15}$ g)	petagram
ppm	parts per milion	część milionowa
Sc	Schmidt number	liczba Schmidta
SOCAT	Surface Ocean CO_2 Atlas	
SST	sea surface temperature	temperatura powierzchniowa
τ	momentum flux	strumień pędu
u^*	friction velocity	prędkość tarcia

2. English abstract

2.1 Introduction

The extent to which the earth's climate can change, whether due to the actions of mankind or natural variability, is at present major scientific problem to be solved, relevant not only by the scientist. Numerical models of the earth's climate system are being used to determine the quantitative ocean's feedback to progressive climate change. An important aspect of these models is the transfer of energy between the ocean and atmosphere, the air-sea fluxes of mass, momentum, gases (as carbon dioxide (CO₂)), heat and aerosols. These fluxes represent key-processes, which are all irreversible, in the earth's climate system; they establish links and feedbacks between its main components, the ocean and the atmosphere. The efficiencies of these key-processes depend mainly of wind speed, temperature, salinity, and humidity. The average values of the transfer through the sea surface along with the range of their variability shows size of this links as well as illustrate how the atmosphere enforces changes in the ocean circulation. Determine the size of the exchange fluxes is particularly important for polar regions, especially the Arctic Ocean, due to the variability of sea-ice thickness caused directly by atmospheric temperature fluctuation, large summer inputs of fresh water and suspended matter inflow from the surrounding land margin, and high level of primary production inside the Arctic fjords.

Empirical measurements of the air-sea fluxes are too few, to make possible direct calculation of large scale flux fields, so it is important to developing, calibrating, and verifying the parameterization formula used to estimate the fluxes from direct studies and satellite data (SCOR Report, 2000). The gas exchange process is directly connected with the dynamic state of the sea surface, therefore it is important to define the turbulent exchange to fully understand and describe the changes taking place in the Earth's climate system. The values of basics variable used for the parameterization of momentum fluxes are wind speed, temperature and humidity, and in the specific case of the CO₂ fluxes, they are wind speed, temperature, salinity. The choice of the appropriate parameterization which can be used for the high-latitude region study, is not obviously, simply and trivial. In the literature there are at least five various commonly used parameterizations for explaining CO₂ exchange in the air-sea interaction, which differ in exponent of wind speed (two of them used cubic dependence on wind speed, three used quadratic dependency). For explaining surface stress it was not possible to narrow the range of reported C_D or satisfactorily explained that range, despite many years of research to develop a unified parameterization for C_D (Andreas et al., 2012). Since these "bulk formulae" are used for flux estimation not only from *in situ* data, but also from satellites data, and for most circulations models, they are the subject of this dissertation.

Studies on air-sea exchange rates in the Arctic Ocean have recently attracted a great deal of attention due to the increase their values, which is direct indicator of the extremely climate crisis. The North Hemisphere is an extraordinary region where, on the

one hand, there is the North Atlantic, the region best covered by measurements among world's ocean, on the other hand is the adjacent Arctic Ocean, the region insufficient in data, especially in winter. The direction and rates of air-sea CO₂ exchange are determined by the product of the difference in values between partial pressure in seawater ($p\text{CO}_{2W}$) and atmosphere ($p\text{CO}_{2A}$), and by the rate of k . Calculation on air-sea CO₂ flux has to be considered as two individual problems, both solved at this dissertation: the first one is to measure or predict the differences in CO₂ concentration across the sea surface while constraining the uncertainty in the flux calculations. Measurement uncertainty is a parameter related to the measurement result, characterizing the spread of values that can be reasonably attributed to the measured value. The second problem is to investigate the rate of exchange by which this must be multiplied, of k . Transfer velocity is a function primarily of wind speed (U_{10}) and temperature, but is also influence by many minor factors (Matthews, 1999). The most frequent source of inaccuracy and uncertainty in the air-sea gas flux calculations is due to the use of the k parameterizations formula that is unsuitable for the given region. The choice of the wind data product, for calculating k , provides uncertainty, even by 10 - 40 %, while the choice on appropriate wind speed parameterization may cause variability in k by as much as about 50 % (Gregg et al., 2014; Couldrey et al., 2016), whereas the global interannual variability in air-sea CO₂ fluxes can be explain by about 60% due to differences in partial pressure between the air and the sea ($\Delta p\text{CO}_2$) (Couldrey et al., 2016). At the beginning of the industrial era the concentration of CO₂ was approximately 277 ppm (Joos and Spahni, 2008) while in 2017 it increased to 405.0 ± 0.1 ppm (Le Quéré et al., 2018). The Arctic Ocean absorbs a large portion of the atmospheric CO₂, during all year, as the net oceanic uptake. At present, the net air-sea CO₂ fluxes in the Arctic have been estimated at -0.12 ± 0.06 PgC yr⁻¹ with net global ocean CO₂ uptake at 2.2 ± 0.5 PgC yr⁻¹ (PgC = GtC, 10¹⁵gC) (Goddijn-Murphy et al., 2015, Gruber 2009, Takahashi et al., 2009). Additionally, the average air-sea CO₂ flux for the Arctic shelves was estimated as -12 ± 4 gCm⁻¹ a⁻¹ (Cai et al., 2006). “-” downward flux (from the atmosphere to the ocean). A recent study showed that 82 % of the global emissions of CO₂ were caused by fossil carbon emission and 18 % by land-use change, of which 45 % as deposited in the atmosphere, 24 % in the ocean and 30 % in the land biomass (Le Quéré et al., 2018). The growth rate of oceanic and atmospheric concentration of CO₂ increased, since the last 50 years, with faster growth in the atmospheric CO₂ level.

The momentum fluxes drive the oceanic circulation by creating oceanic eddies, gyres and current systems that can redistribute heat in the ocean. The problem of properly describing air-sea fluxes is compound, and simplistic parameterizations are not satisfactory to represent the fluxes in models (Csanady, 2004). It was important to study momentum fluxes over the Arctic Ocean using satellite data as previous studies omitted this region because of the very small amount of *in situ* data. The C_D is an increasing function of the neutral wind speed at 10-m height for moderate wind speeds ($5 - 10$ m s⁻¹) due to increasing sea surface roughness. Despite many years of research there is still

uncertainty with regard to the behavior of the drag coefficient, especially over weak winds (even 30 %). All of the C_D parameterizations are generated from the vertical wind profile, but they differ in the formulas used. In the literature they are formulated as power-law of the relationship between C_D and U_{10} (for example Wu 1969, Andreas et al., 2012) or as linear-law (for example Garratt 1977, Wu 1982) or has a constant value of the relationship (for example NCEP/NCAR). The amount of the parameterizations reflects the difficulties in simultaneously measuring at high sea stress and wind speed. All studies, to properly parameterize the C_D , were based on the laboratory and observations measurements and mostly are divided in accordance with the range of wind speed. The main aim of the drag calculations was characteristics of the boundary layer flow conditions, without specifying the exact values of uncertainty and they were conducted mostly over the North Atlantic. Last studies have showed that results for the drag coefficient are underestimated under the moderate wind speed and overestimated under the high wind speed (Jarosz et al., 2007, Brodeau et al., 2017).

In recent years there has been significant progress in our knowledge of the surface fluxes. Air-sea interaction experiments have refined the formulae used for flux calculation, methods of obtaining fluxes from satellite data have been developed, and weather forecast models have been used to produce a consistent re-analysis of the past state of the atmosphere. Unfortunately, despite these advances, the observational flux data remains limited and various attempts to produce climatologies of the flux fields, and to describe their climatic variability, differ in significant aspects. The air-sea fluxes of CO_2 and momentum are relatively well-know and studied. However, the polar regions are significantly less investigated in this respect than, e.g. mid-latitude regions. Most of the studies on this topic, conducted in the Arctic, focus on estimating the rate of the ocean absorption of atmospheric CO_2 , or comparing different methods for calculating air-sea fluxes, in the case of carbon study. However they ignore estimating the exchange uncertainty as well as omit indicating the major parameter which influence on air-sea CO_2 exchange, except of annual publishing Carbon budget report by Le Quéré et al. In the case of momentum fluxes, most of the studies focus on comparing differences in the drag coefficient values resulting from the choice of used parameterization for unified C_D parameterizations, but without estimating uncertainty of the exchange values. Studies of exchange fluxes in high-latitudes region are sparse and often fragmentary. Therefore the recent development of satellite and other remote sensing systems allow for fluxes to be measured over this hard region, as is the Arctic Ocean.

The subject of my doctoral work is increasing knowledge of the interactions that occur in the European Arctic between the components of the Earth's climate system, and the effects of their impacts as indicator of the progressive climate change. The work is focused on the exchange rates with their efficiencies across the sea surface, and estimating their uncertainties, based on satellite Earth's Observational data.

This doctoral dissertation consists of three original research papers in which subsequent stage of the work are described. The first article [1] focuses on calculation of

average wind speed in polar regions, in order to analyze the influence of the selected k parameterization on air-sea CO_2 fluxes (F). Additionally, annually and monthly mean values of net air-sea CO_2 fluxes were calculated. The second article [2] presents the calculations of the values of individual air-sea CO_2 exchange components in the analyzed year 2010, together with the analysis of spatio-temporal fluctuations of monthly mean values of CO_2 fluxes, depending on changes in $p\text{CO}_{2W}$ and k . The third article [3] documents the calculation of actual wind field from the North Atlantic and the European Arctic in order to determine the magnitude of average monthly and annually momentum transfer through the sea surface depend on selected non-dimensional C_D parameterization.

2.2 Study region

The European sector of the Arctic (closely at the Atlantic sector of the Arctic), referred as the 'European Arctic', consist of the Barents and Greenland seas, was chosen as site for the study (Fig. 1). The Barents Sea is the largest of the Arctic Ocean seas characterized by an inflow of warm, saline Atlantic water via the Norwegian Atlantic Current and minimal freshwater inputs (Omar et al., 2003). The Greenland Sea is a major pathway for the exchange of water between Arctic and Atlantic through the Fram Strait (Nakaoko et al., 2006). Several factors in the Arctic Ocean makes its physical, chemical and biological processes significantly different from the processes in the neighboring the North Atlantic and the Pacific Ocean. The most notable are: coverage by sea ice, high ratio of surrounding shallow seas; large summer inputs of fresh water and suspended and dissolved matter input from the neighboring land margin; high level of primary productivity inside the Arctic fjords. The Arctic Ocean has an important role in the global freshwater cycle and the Atlantic Meridional Overturning Circulation. The outflow of cold and relatively fresh waters, from the Arctic basins has an impact on the large-scale thermohaline circulation and the average global ocean temperature. Arctic waters are driven by the wind and by density differences. Air-sea strongly influences the seasonal sea-ice coverage, as well as interannual changes of sea-ice distributions and thickness, and sea-ice export from the Arctic Ocean.

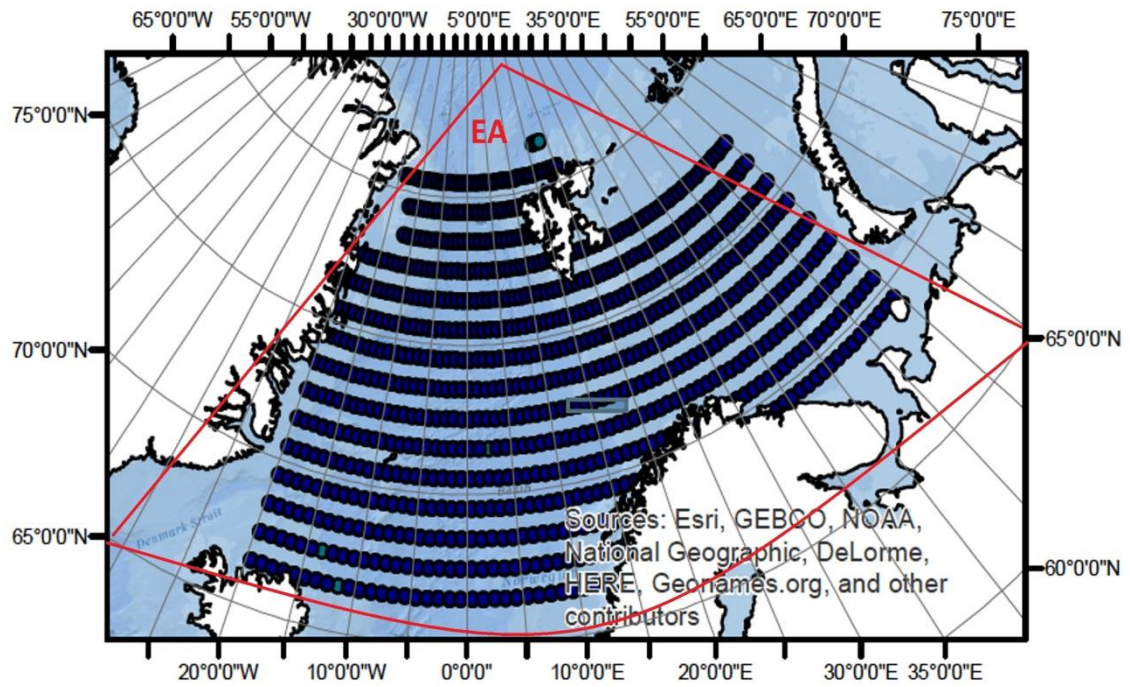


Fig. 1. Study Area – the European Arctic (source: basemap ArcGis) with sampling points.

2.3 Material and methods

To achieve all the research goals the following data were used:

- saline and climatological distribution of surface water $p\text{CO}_2$ - from Takahashi et al. (2009) climatology, which was based on more than 3 million measurements in open ocean environments during non-El Niño conditions [Articles 1,2],
- $p\text{CO}_2$ and associated SST - from SOCAT v1.5 and v2.0 [Articles 1],
- SSTskin - from Advance Along Track Scanning Radiometer (ESA/ARC/(A)ATSR) Global Monthly Sea Surface data set [Articles 1]
- wind speed at 10 m a.s.l. and sea roughness data were obtained from the GlobWave project (available from the European Space Agency (ESA)) [Articles 1,2,3],
- SST data from Ifremer/CERSAT [Articles 2],
- k coefficient was estimated using Nightingale et al. (2000) parameterization [Articles 2].

All inputs data and climatologies were linearly re-interpolated to a $1^\circ \times 1^\circ$ geographical grid from the original resolution, for year 2010, using a set of software processing tools called the 'FluxEngine' (Shutler et al., 2016), which was created as a part of ESA funded OceanFlux Greenhouse Gases project. Data were extracted for the European Arctic from global resolution. Net air-sea CO_2 fluxes and momentum fluxes were calculated.

For analysis of air-sea fluxes, different parameterizations were used. In the case of the air-sea CO_2 fluxes five various parameterizations, differing in the dependence on wind speed, were used [Article 1]:

Table 1 Gas transfer velocity values (k) over the ocean taken from the recent literature. U_{10} is the mean wind speed measured at 10 m above the mean sea surface.

Eq. no.	Source	k
1	Nightingale et al. (2000)	$\sqrt{(660.0 / Sc_{skin})} * (0.212 U_{10}^2 + 0.318 U_{10})$
2	Ho et al. (2006)	$\sqrt{(660.0 / Sc_{skin})} * 0.254 U_{10}^2$
3	Wanninkhof and McGillis (1999)	$\sqrt{(660.0 / Sc_{skin})} * 0.0283 U_{10}^3$
4	Wanninkhof (2014)	$\sqrt{(660.0 / Sc_{skin})} * 0.251 U_{10}^2$
5	McGillis (2001)	$\sqrt{(660.0 / Sc_{skin})} * (3.3 + 0.026 U_{10}^3)$

In the case of the air-sea momentum fluxes [Articles 3] seven different drag coefficient parameterizations (C_D) were used. All of them are generated from vertical wind profile, but differ in formula used:

Table 2 Neutral drag coefficient values over the ocean taken from the recent literature for a reference height of 10 m: C_{D10} is the drag coefficient dependent on surface roughness, C_{DN10} is the expression of neutral-stability (10-m drag coefficient), U_{10N} is the 10-m neutral-stability wind speed, and a and b are proportionality constant.

Eq. no.	Source	Wind speed range [$m s^{-1}$]	$C_{DN(10)} (x10^3)$
6	Wu (1969)	1-15	$0.5 U_{10}^{0.5} 0.5 U_{10}^{0.5}$
7	Garratt (1977)	4-21	$0.75 + 0.067 U_{10}$
8	Wu (1982)	>1	$0.8 + 0.065 U_{10}$
9	Yelland and Taylor (1996)	3-6 6-26	$0.29 + \frac{3.1}{U_{10N}} + \frac{7.7}{U_{10N}^2}$ $0.60 + 0.070 U_{10N}$
10	NCEP/NCAR	everywhere	1.3
11	Large and Yeager (2004)	everywhere	$\frac{2.7}{U_{10N}} + 0.142 + 0.076 U_{10N}$

12	Andreas et al. (2012)	everywhere	$\left(\frac{u^*}{U_{10N}}\right)^2 = a^2 \left(1 + \frac{b}{a} U_{10N}\right)^2$ $a = 0.0583, b = -0.243$
----	--------------------------	------------	---

All analyses were carried out at the Air-Sea Interaction Laboratory of the Institute of Oceanology Polish Academy of Science in Sopot, using the methods described in detail in the articles [1, 2 and 3].

2.4 Results and discussion

As indicated above, the first two publications focus on calculating the monthly, annual and seasonal net air-sea CO₂ sink values, depending on formula used for estimating k , and estimating uncertainty of the values, in the European Arctic and the North Atlantic [1] as well as the spatial and temporal variability [2]. All calculations were made using the FluxEngine software, where at first global gridded monthly net fluxes were produced and subsequently the values for the study regions were extracted. The results presented in Article 1 indicate that the annual net sea CO₂ sink in the Arctic Ocean varies from 0.102 PgC for Nightingale et al. (2000) parameterization to 0.147 PgC for McGillis et al. (2001). In the case of the North Atlantic the values of the net absorption CO₂ by the ocean were 0.38 and 0.56 PgC, respectively, and in the case of global the values were 1.3 and 2.15 Pg C, respectively. The same data “normalized” to the Nightingale et al. (2000) parameterization, in order to visualization the relative differences, shown that results obtained for the European Arctic from the three “quadratic” parameterizations (eqs. 1, 2 and 4) were within 3 - 4 % of each other, and were smaller than results from the “cubic” parameterizations (eqs. 3 and 5), which were within 28 and 44 %, respectively. The calculation results imply smaller relative differences between the parameterizations in the European Arctic, and generally the North Atlantic, than in the global ocean. There may be two reasons for this. The first one is the fact that most of the k formulas intersect close to 9 m s⁻¹, which is annual average wind speed calculating in the North Atlantic, and when comparing quadratic and cubic functions the cubic ones implied higher air-sea flux values for high winds, whereas the quadratic ones lead to higher fluxes for weaker winds. The arithmetic form of this difference is explained in Articles 1. Second reason for smaller inter-parameterization discrepancies in the Northern Hemisphere than many other basins is the lack of seasonal variations in the sign of the air-sea flux, in several basins. The European Arctic and the North Atlantic are characterized by strong fluctuations in fluxes through the year. This confirmed that k parameterizations from eqs. 1, 2 and 4 (Table 1) may be used interchangeably, for the Arctic Ocean and the North Atlantic, with small advantage for Nightingale et al. (2000) parameterization. Monthly mean of air-sea CO₂ fluxes confirm that the Arctic Ocean, as a whole, is a sink of atmospheric CO₂ in every month, with single regions that are net sources for CO₂. Especially close to the North Atlantic Drift and the East Greenland Current. All results were obtained using the Takahashi et al. (2009) pCO₂ climatology but, for better understanding changes in the air-

sea CO₂ fluxes, these data were compared with the data from the SOCAT v1.5 and v2.0 reanalysis. In the European Arctic monthly air-sea CO₂ fluxes calculated for different $p\text{CO}_2$ data sets, using the same k parameterization, resulting in inverse seasonal variability but values from annual net air-sea CO₂ fluxes results were similar: -1.02 Pg C for Takahashi et al. (2009), -0.085 Pg C for SOCAT v1.5 and -0.088 Pg C for SOCAT v2.0. The reason of this discrepancy may be due to the sparse data coverage and possible interpolation artefacts.

The research presented in Article 2 was concentrated on determining the importance of k and $p\text{CO}_2$ on CO₂ budgets in the European Arctic during one year (2010). During the analysis process the statistics of the variability were calculated. The results have shown that in the Arctic the variability in wind speed and, hence, the gas transfer velocity, generally play a major role in determining the temporal variability of CO₂ uptake, while variability in monthly $p\text{CO}_2$ values plays a major role spatially, with some exceptions. The average gas transfer velocity was estimated approximately $13.0 \pm 1.9 \text{ cm h}^{-1}$ with the average wind speed, during the study period, of $8 \pm 0.7 \text{ m s}^{-1}$, and a concentration of $p\text{CO}_{2W}$ $332.4 \pm 11.8 \text{ } \mu\text{atm}$. The SST was approximately $3.0 \pm 1.6 \text{ } ^\circ\text{C}$ and practical salinity 34.3. The $p\text{CO}_{2W}$ varies spatially and temporarily in comparison to $p\text{CO}_{2A}$, what is a reason of strong absorption CO₂ from the atmosphere, and during the study period, the values of ocean $p\text{CO}_2$ were below the atmospheric levels. Calculated oceanic CO₂ uptake were between -6 to -16 $\text{mgC m}^{-2} \text{ day}^{-1}$, and the $p\text{CO}_{2W}$ concentrations varied between 360 to 290 μatm . Zonal mean of $p\text{CO}_2$ values in February and August indicated that during the summertime (from May to September) surface $p\text{CO}_2$ has decreased, in spite to seasonal warming and oceanic CO₂ uptake, thank to high CO₂ exchange, which was counterbalanced by the uptake of CO₂ by phytoplankton. Inside the Arctic fjords the difference between $p\text{CO}_2$ in summer and winter was caused by lower surface-water $p\text{CO}_2$ levels resulting from sea ice melt, dissolution of CaCO₃, primary production. Differences in the $p\text{CO}_2$ characterized of strongly correlation with changes in the $p\text{CO}_{2W}$, especially in wintertime (from October to April), when the average water temperature was higher than the air temperature. Results from the analysis have shown that over spatial scales, the air-sea CO₂ flux values were strongly positively linked to the $p\text{CO}_2$ (much less than with k) during each month ($r=0.757$, $p>0.05$). Over temporal scale air-sea CO₂ fluxes were strongly negative correlated with k ($r = -0.935$, $p<0.05$) with moderate negative correlations in individual months. The variability in k contributes to only approximate 20 % of the Arctic monthly flux variability, while $\Delta p\text{CO}_2$ contributes 50 % of total variability.

The third publication [3] focuses on calculation of actual wind field from the North Atlantic and the European Arctic in order to determine the magnitude of average monthly and annual mean momentum transfer through the sea surface, depending on selected non-dimensional drag coefficient parameterization (C_D) (eqs. 6 - 12, Table 2). Despite many empirical measurements and using satellite data, the C_D parameterizations still have wide spread in values at low and moderate wind speed. The C_D values increased linearly with the increasing of wind speed, when parameterizations (6 – 8, Table 2) were used, with decreasing at the conditions of week winds, when parameterizations (9, 11, 12,

Table 2) were used. The results showed that at low wind values ($<10 \text{ m s}^{-1}$) the differences between particular C_D parameterizations are greater than at higher speeds ($>10 \text{ m s}^{-1}$), and the most outlier results are those obtained from the power law parameterization of Andreas et al. (2012) (12, Table 2). At low winds uncertainty are higher (factor of 0.5 – 1.5, depends on formula used), while at moderate winds it is uncertainty by a factor of 1.5 – 2.0. Direct comparison of the results from the latest C_D parameterizations (11 and 12, Table 2) changing seasonally depending on the research area, with the oldest formula (6, Table 2) showed that formula (12, Table 2) gives results for C_D close to zero at winds 3 – 5 m s^{-1} . This outcome suggests that, results for the C_D may be close to zero for different area but with similar winds speed environmental. Additionally, the oldest C_D parameterizations (6, Table 2) produce higher wind stress values than the newest ones (eq. 12) in both regions with high and low winds, and C_D values are consistently higher for all wind speeds. Mean monthly air-sea momentum flux, calculated for the European Arctic, the North Atlantic and global, showed that region without seasonal wind speed changes, has similar constant values of momentum flux (with annual amplitude approximately 0.02 N m^{-2}). For the European Arctic the situation is more complicated because of strong seasonal wind changes. In the Arctic summer, Andreas et al., (2012) parameterization produces the least wind stress, while all the other parameterizations are very similar qualitatively. The annual European Arctic momentum fluxes, depending on the formula used, varied from 0.329 for Andreas et al. (2012) to 0.375 N m^{-2} for Wu (1969) and are higher than in the North Atlantic and in global. In the case of the North Atlantic annual, the values were 0.290 and 0.333 N m^{-2} and globally 0.283 to 0.322 N m^{-2} , respectively. For better visualization of the relative differences, the data were normalized to the (12, Table 2) parameterization (presented as percentage of this value). The results of the air-sea momentum flux differ to each other, in the range of 1 % in comparison to (11, Table 2) parameterization to 14 % for (6, Table 2). As the value of air-sea momentum flux is important for ocean circulation, its correct calculation in coupled models is very important, especially in the Arctic Ocean, where cold halocline stratification depends on the amount of sea-water mixing. It has been proved that the parameterization formulas used in the NCEP/NCAR and Large and Yeager (2004) climate models, produced stress results differ by about 5 %, with higher monthly values.

2.5 Conclusion

This study made possible the determination of the rate of air-sea exchange in the European Arctic, together with uncertainties resulting from various gas transfer velocity coefficients and drag coefficient. The obtained results significantly improve our knowledge of the role of the Arctic fluxes in global circulation, indicating that the European Arctic is significantly different, in the case of some physical conditions, to the neighboring North Atlantic Ocean. This doctoral dissertation thesis encompasses papers that comprehensively address the transfer processes through the sea surface and coefficients driving the gases and momentum exchange-the gas transfer velocity and the

drag coefficient parameterization-with their uncertainty in monthly and annual scale. The insightful and original aspect of this PhD thesis is using the recently development software, which was created to encourage the use of satellite Earth Observation data for studying air-sea fluxes, which allowed me to estimate the fluxes as an effect of constantly study. Exclusion of gaps in the study period allowed conducting insightful and precision study, which accurately reflects the actual conditions in the Arctic Ocean.

To sum up this doctoral dissertation explores extensively issues concerning the role of the adequately parameterizations for calculating significant parameters in air-sea exchange calculations. Due to the relative small number of data available for the polar regions, those studies are of particular importance and may have broad applicability, for example, in numerical physical models used in the European Arctic.

3. Streszczenie (Abstract in Polish)

3.1 Wstęp

Modele numeryczne w badaniach oceanograficznych wykorzystywane są m.in. do określenia ilościowej odpowiedzi oceanu na postępujące zmiany klimatyczne. Ważnym aspektem tych modeli jest określenie transferu energii między oceanem a atmosferą, wyznaczenie strumieni wymiany masy, pędu oraz gazów (jak na przykład CO₂), ciepła i aerozoli. Efektywność tych transferów przez powierzchnię morza, zależy w dużym stopniu od: prędkości wiatru, temperatury powierzchniowej akwenu, zasolenia, wilgotności. Określenie wielkości strumieni wymiany jest szczególnie ważne dla rejonów polarnych, zwłaszcza Oceanu Arktycznego, ze względu na spadek przyrostu grubości sezonowego lodu morskiego w wyniku wzrostu średniej temperatury powietrza, duże letni dopływ wody słodkiej i zawiesiny z przylegających lądów oraz wysoki poziom produkcji pierwotnej w fiordach Arktycznych.

Gazy atmosferyczne, takie jak azot (N₂), tlen (O₂) i dwutlenek węgla (CO₂), są silnie pochłaniane przez powierzchnie oceanów, zmieniając warunki środowiskowe warstwy granicznej, a w wyniku procesów mieszania się wód oraz prądów morskich, transportowane są do głębszych warstw gdzie są deponowane. W wyniku poboru CO₂ przez oceany, z jednej strony koncentracja CO₂ w atmosferze, wynikająca ze wzrostu antropogenicznych i naturalnych emisji, jest zmniejszona, co bezpośrednio oddziałuje na obserwowane zmiany klimatu, ale z drugiej strony powoduje to zwiększone zakwaszenie oceanów. Procesy wymiany gazowej łączą się bezpośrednio ze stanem dynamicznym powierzchni morza, dlatego ważnym jest, do pełnego opisu zmian zachodzących w systemie klimatycznym Ziemi, wyznaczenie strumieni turbulentnych. Warunki silnych wiatrów nad Oceanem Arktycznym, szczególnie w okresach zimowych oraz duży rozbieg fal powinny warunkować precyzyjne określenie strumieni wymiany pędu, zależnych od gradientu prędkości wiatru przywodnego. Jednak, obliczenia te, pomimo wielu lata badań, nie są dotychczas znane analitycznie, w wyniku niedostatecznych danych empirycznych, w związku z tym powszechne jest stosowanie założeń upraszczających albo wykorzystywanie modeli bazujące na przybliżonych metodach ich rozwiązań. Według raportu IPCC to właśnie brak odpowiedniej liczby danych empirycznych jest podstawowym źródłem niepewności w określeniu globalnego bilansu gazów cieplarnianych (Ciais i in., 2013).

Pomiary empiryczne wykorzystywane do obliczania bezpośrednich pól strumieni okazały się niewystarczające, w związku z tym zostały opracowane i zweryfikowane wzory parametryzacji, umożliwiające wykorzystanie danych zarówno z obserwacji bezpośrednich, jak i satelitarnych (SCOR Report, 2000). Podstawowymi parametrami wykorzystywanymi w formułach parametryzacji dla strumieni turbulentnych są: prędkość wiatru, temperatura i wilgotności, natomiast dla strumieni CO₂: prędkość wiatru, temperatura i zasolenie. Ponieważ wzory te pozwalają na wykorzystanie danych satelitarnych w badaniach strumieni wymiany przez powierzchnię morza, zostały one

użyte w analizach serii publikacji będących składową poniższej pracy doktorskiej. Wybór odpowiedniej parametryzacji możliwej do zastosowania w rejonach polarnych w wyniku, której rezultaty nie będą ani przeszacowane ani niedoszacowane, nie jest oczywisty ani prosty. W literaturze funkcjonuje, co najmniej pięć formuł na obliczanie współczynnika prędkości wymiany gazowej (k), które różnią się między sobą funkcją prędkości wiatru (kwadratowa i sześcienna zależność) oraz wiele formuł w celu wyjaśnienia współczynnika oporu (C_D) dla wiatru, przy określaniu turbulentnej wymiany pędu. Pomimo wieloletnich badań nie udało się stworzyć zunifikowanej formuły na parametryzację C_D (Andreas i in., 2012).

Badania strumieni wymiany przez powierzchnię morza, w Oceanie Arktycznym stały się w ostatnim czasie przedmiotem uwagi, ponieważ zauważono wzrost ich wartości, co jest bezpośrednim indykatorem obserwowanych zmian klimatycznych. Kierunek i prędkość wymiany CO_2 na granicy powierzchni morza warunkowane są przez iloczyn różnicy koncentracji ciśnienia parcjalego (ΔpCO_2) między powierzchniową warstwą wody morskiej a przylegającą warstwą atmosfery oraz współczynnik prędkości wymiany gazowej k . Analiza wymiany gazowej ma na celu rozwiązanie dwóch problemów naukowych (Matthews, 1999), oba zawarte są w poniższej pracy doktorskiej: pierwszy to określenie różnic koncentracji CO_2 na powierzchni morza, przy jednoczesnym ograniczeniu niepewności pomiaru. Drugi problem dotyczy wyboru odpowiedniej formuły parametryzacji wsp. k , która jest bezpośrednią funkcją prędkości wiatru (U_{10}) i temperatury powierzchniowej (SST), wraz z wyznaczeniem dokładnych wartości tego współczynnika. Najczęstszym źródłem niedokładności wyników i niepewności pomiarów, w Oceanie Arktycznym, jest zastosowanie nieodpowiedniej parametryzacji wsp. k , dla tego regionu, powodującym rozbieżność w wynikach nawet na poziomie 50 % (Gregg i in., 2014), natomiast w skali czasowej zmiany strumieni wymiany CO_2 wynikają w znacznym stopniu ze zmienności ΔpCO_2 (nawet 60 % zmienności międzyrocznej) (Couldrey i in., 2016). Na początku ery przemysłowej koncentracja CO_2 wynosiła 277 ppm (Joos i Spahni, 2008), podczas gdy w 2017 r., wzrosła do 405 ppm (Le Quéré i in., 2018). Wody Oceanu Arktycznego pochłaniają CO_2 z atmosfery na poziomie $0.12 \pm 0.06 \text{ PgC rok}^{-1}$ ($\text{Pg} = 10^{15} \text{ g}$), przy globalnym pochłanianiu na poziomie $2.2 \pm 0.5 \text{ PgC rok}^{-1}$ (Goddijn-Murphy i in., 2015, Gruber 2009, Takahashi i in., 2009). Średnia wielkość strumieni w fiordach Arktycznych została oszacowana na poziomie $-12 \pm 4 \text{ gCm}^{-1} \text{ rok}^{-1}$ (Cai i in., 2006). Znak '-' oznacza strumień skierowany pionowo w dół. Najnowsze badania wykazały, że 82 % globalnych emisji CO_2 spowodowanych jest emisją kopalnego węgla a 18 % zmianami w użytkowaniu gruntów. Z tego 45 % CO_2 zdeponowane jest w atmosferze, 24 % w oceanie i 30 % w biomiasie lądowej (Le Quéré i in., 2018).

Turbulentna wymiana pędu napędza cyrkulację oceaniczną, tworząc oceaniczne wiry i systemy prądowe, które mogą redystrybuować ciepło w oceanie. Dokładne opisanie strumieni wymiany pędu na granicy powierzchni morza stanowi złożony problem, a zastosowanie uproszczonych parametryzacji w modelach klimatycznych, nie daje precyzyjnych wyników (Csandy, 2004). W niniejszej pracy doktorskiej skupiłam się na

zbadaniu przepływów pędu nad Oceanem Arktycznym z wykorzystaniem danych satelitarnych, ze względu na pomijanie tego regionu w obliczeniach strumieni wymiany uwarunkowane zbyt małą ilością reprezentatywnych danych empirycznych, a co za tym idzie wysokimi niepewnościami pomiaru (nawet 30 %). C_D jest rosnącą funkcją prędkości wiatru w zakresie umiarkowanych średnich prędkości wiatru (zakres wartości prędkości 5 - 10 m s⁻¹), ze względu na rosnącą szorstkość powierzchni morza, oraz słabo rosnącą przy bardzo silnych wiatrach. Wszystkie parametryzacje na obliczanie wsp. C_D generowane są z pionowych profili wiatru, ale różnią się zastosowanymi formułami zależności pomiędzy C_D a U_{10} . Trzy główne zmienneści opisujące te zależności to zmienność liniowa (jak np. Garratt 1977, Wu 1982), funkcja kwadratowa (jak np. Wu 1969) i wartość stała (model NCEP/NCAR). Dotychczasowe analizy wsp. C_D skupiały się na porównaniach dostępnych parametryzacji w celu zunifikowania i zawężenia kręgu formuł pomiarowych, ale bez określania niepewności pomiarów wynikających z zastosowania odpowiedniej formuły parametryzacji, oraz nie dotyczyły Oceanu Arktycznego. Jako, że niepewność parametryzacji wsp. C_D nadal jest stosunkowo wysoka najnowsze badania do obliczenia wymiany pędu wykorzystują formuły parametryzacji (np. Andreas i in., 2012) bazujące na współczynniku prędkości tarcia (u^*), który również jest funkcją średniej prędkości wiatru. Analizy wyników otrzymanych z użycia formuły C_D i u^* wykazały mniejsze empiryczne niepewności przy wykorzystaniu formuły wsp. u^* .

Głównym celem mojej pracy doktorskiej było poszerzenie wiedzy dotyczącej roli strumieni wymiany między składnikami systemu klimatycznego Ziemi, wraz z skutkami ich oddziaływania, jako współczynnika obrazującego postępujące zmiany klimatyczne. Praca miała na celu określenie wielkości strumieni wymiany i ocenie efektywności tych transferów, w oparciu o dane satelitarne, na granicy oddziaływania morza i atmosfery w zimnych akwenach europejskiego sektora Oceanu Arktycznego. Aby osiągnąć zamierzony cel, koniecznym było:

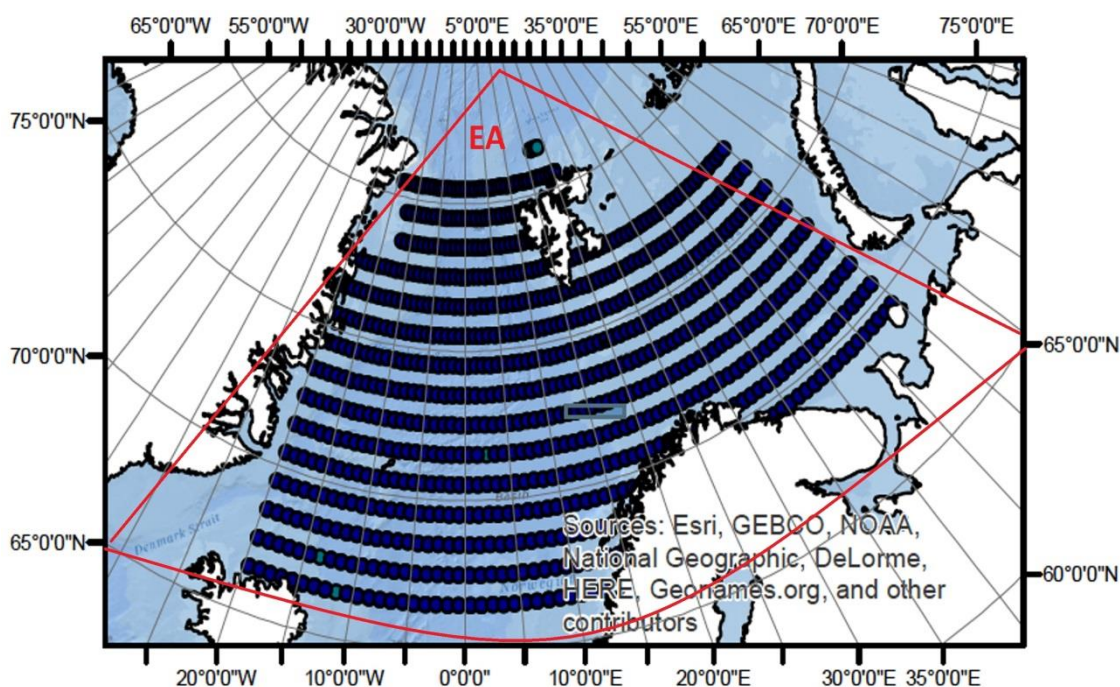
- przeprowadzenie analiz parametryzacji współczynników prędkości wymiany w odniesieniu do warunków panujących w Oceanie Arktycznym,
- wyznaczenie odpowiedniej parametryzacji dla rejonu polarnego, na podstawie niepewności pomiarów,
- obliczenie wielkości zmienności międzyletniej i sezonowej wymiany przez powierzchnie morza,
- określenie głównych czynników powodujących zmiany tempa i wielkości wymiany, zarówno w skali czasowej jak i przestrzennej.

Na pracę doktorską składają się trzy, oryginalne artykuły naukowe, w których opisane są przeprowadzone badania. Pierwszy artykuł [1] skupia się na obliczeniach średniej prędkości wiatru w rejonach polarnych, w celu analizy wybranych parametryzacji współczynnika k wraz z niepewnościami, oraz obliczeniu średnich rocznych wartości strumieni wymiany netto CO₂. Drugi artykuł [2] przedstawia obliczenia wielkości poszczególnych komponentów wymiany CO₂ w analizowanym roku 2010, wraz z analizą fluktuacji czasowych i przestrzennych średnich miesięcznych wartości strumieni CO₂, w

zależności od wahań dwóch podstawowych komponentów, warunkujących kierunek i prędkość transferu przez powierzchnię morza – $\Delta p\text{CO}_2$ i współczynnika k . Trzeci artykuł [3] dokumentuje wyniki analiz rzeczywistych pól wiatrów w Północnym Atlantyku i europejskim sektorze Oceanu Arktycznego, w celu określenia średnich miesięcznych i rocznych wartości transferu pędu, przez powierzchnię morza, w zależności od wybranej formuły parametryzacji współczynnika C_D .

3.2 Rejon badań

Badania były prowadzone w Europejskim sektorze Arktyki, zwanym „europejską Arktyką”, w skład, którego wchodzi Morze Barentsa i Grenlandzkie (Rys. 1). Morze Barentsa jest największym z mórz Oceanu Arktycznego, charakteryzującym się napływem ciepłej, zasolonej wody atlantyckiej niesionej przez prąd Norweski, wyodrębniający się z prądu Północnoatlantyckiego, i minimalnymi nakładami wody słodkiej (Omar i in. 2003). Morze Grenlandzkie stanowi główną drogę wymiany wód, przez Cieśninę Fram, między Oceanem Arktycznym a Północnym Atlantykiem (Nakaoko i in.,) 2016. Kilka czynników w Oceanie Arktycznym sprawia, że procesy fizyczne, chemiczne i biologiczne znacznie różnią się od procesów w sąsiednim Oceanie Atlantyckim i Pacyficznym. Należą do nich: sezonowe pokrycie lodem morskim, wysoki współczynnik otaczających płytkich mórz, duże letnie dopływy świeżej wody i spływ zawiesiny i rozpuszczonej substancji z sąsiadujących lądów, jak również wysoki poziom produkcji pierwotnej wewnątrz fiordów Arktycznych. Odpływ zimnych i „świeżych” wód z basenu arktycznego wpływa na cyrkulację termohalinową (THC) i średnią globalną temperaturę oceanu światowego.



Rys. 1 Mapa zaznaczonego rejonu badań – Arktyka Europejska (źródło: basemap ArcGis).

3.3 Materiały i metody badań

Aby zrealizować wyznaczone cele badawcze przeprowadzono analizy przy wykorzystaniu poniższych danych:

- praktyczne zasolenie i klimatologia rozkładu koncentracji $p\text{CO}_2$ w wodzie morskiej z klimatologii Takahashi i in. (2009). Klimatologia ta opiera się na ponad 3 milionach pomiarów w otwartych wodach oceanicznych, w warunkach braku występowania zjawiska El Niño [Artykuł 1],
- $p\text{CO}_2$ i powiązana wartość temperatury powierzchniowej [SST] wód z SOCAT v1.5 i v2.0 [Artykuł 1],
- temperatura górnej warstwy powierzchniowej wód [SST_{skin}] z radiometru skanującego będącego na wyposażeniu satelity Europejskiej Agencji Kosmicznej [Artykuł 1],
- prędkość wiatru na 10 m n.p.m. i chropowatość morza z projektu GlobWave [Artykuł 1, 2, 3],
- SST z baz Ifremer/CERT [Artykuł 2],
- formuła współczynnika k z parametryzacji Nightingale i in. (2000) [Artykuł 2].

Wszystkie powyższe dane wejściowe i klimatologie, zostały liniowo zinterpolowane do siatki $1^\circ \times 1^\circ$, dla roku 2010, przy użyciu oprogramowania 'FluxEngine' (Shutler i in., 2016) stworzonego w ramach grantu ufundowanego przez Europejską Agencję Kosmiczną – Greenhouse Gases Project. Wyodrębnione dane zostały użyte w celu obliczenia strumieni wymiany CO_2 i pędu dla Arktyki Europejskiej.

W analizach strumieni CO_2 [Artykuł 1, 2] wykorzystano pięć powszechnie używanych parametryzacji stworzonych do obliczania współczynnika k , różniących się pomiędzy sobą stopniem zależności od prędkości wiatru.

Tabela 1. Formuły parametryzacji współczynnika k , funkcjonujące w literaturze. Sc – liczba Schmidta, U_{10} – prędkość wiatru na 10 m n.p.m.

Nr.	źródło	wzór na wsp. k
1	Nightingale et al. (2000)	$\sqrt{(660.0 / Sc_{\text{skin}})} * (0.212 U_{10}^2 + 0.318 U_{10})$
2	Ho et al. (2006)	$\sqrt{(660.0 / Sc_{\text{skin}})} * 0.254 U_{10}^2$
3	Wanninkhof and McGillis (1999)	$\sqrt{(660.0 / Sc_{\text{skin}})} * 0.0283 U_{10}^3$
4	Wanninkhof (2014)	$\sqrt{(660.0 / Sc_{\text{skin}})} * 0.251 U_{10}^2$
5	McGillis (2001)	$\sqrt{(660.0 / Sc_{\text{skin}})} * (3.3 + 0.026 U_{10}^3)$

W celu obliczenia strumieni wymiany pędu [Artykuł 3] wykorzystano siedem różnych parametryzacji na obliczanie współczynnika oporu. Wszystkie parametryzacje generowane są z pionowego profilu wiatru, ale różnią się zastosowaną formułą.

Tabela 2. Wybrane formuły parametryzacji współczynnika tarcia (C_D), funkcjonujące w literaturze.

Nr.	źródło	Zakres prędkości wiatru [m s ⁻¹]	$C_{DN(10)} (x10^3)$
6	Wu (1969)	1-15	$0.5U_{10}^{0.5} 0.5 U_{10}^{0.5}$
7	Garratt (1977)	4-21	$0.75 + 0.067U_{10}$
8	Wu (1982)	>1	$0.8 + 0.065U_{10}$
9	Yelland and Taylor (1996)	3-6 6-26	$0.29 + \frac{3.1}{U_{10N}} + \frac{7.7}{U_{10N}^2}$ $0.60 + 0.070U_{10N}$
10	NCEP/NCAR	w każdych warunkach	1.3
11	Large and Yeager (2004)	w każdych warunkach	$\frac{2.7}{U_{10N}} + 0.142 + 0.076U_{10N}$
12	Andreas et al. (2012)	w każdych warunkach	$(\frac{u^*}{U_{10N}})^2 = a^2 (1 + \frac{b}{a} U_{10N})^2$ $a = 0.0583, b = -0.243$

Wszystkie analizy zostały przeprowadzone w Pracowni Wzajemnego Oddziaływania Morza i Atmosfery w Instytucie Oceanologii Polskiej Akademii Nauk w Sopocie, wykorzystując metody szczegółowo opisane w artykułach [1, 2, 3].

3.4 Wyniki i dyskusja

Jak już wspomniano wyżej, pierwsze dwie publikacje skupiają się na obliczaniu miesięcznych, sezonowych i rocznych wartości netto pochłaniania CO₂ przez powierzchnię oceanu, wraz z oszacowaniem niepewności pomiarów, w Arktyce Europejskiej [1] wraz z wyznaczeniem zmienności czasowo-przestrzennych wielkości strumieni wymiany [2]. Wyniki przedstawione w publikacji [1] wykazują, że roczna wartość pochłanianego CO₂ przez Ocean Arktyczny waha się od 0.102 PgC dla parametryzacji Nightingale i in. (2000) do 0.147 PgC dla parametryzacji McGillis i in. (2001). W Północnym Atlantyku ilość

pochłanianego CO₂, netto, wynosiła odpowiednio 0.38 i 0.56 PgC, a globalne wartości wahały się od 1.3 do 2.15 PgC. Niepewności tych samych danych, znormalizowane do parametryzacji Nightingale i in. (2000) w celu wizualizacji różnic względnych, wykazały, że wyniki uzyskane dla europejskiego sektora Arktyki z formuł używających kwadratowe funkcje prędkości wiatru (równania 1,2 i 4, Tabela 1) różniły się między sobą o ok. 3 - 4 % i były mniejsze niż wyniki z formuł funkcji sześciennych, które wynosiły odpowiednio 28 i 44 %. Dodatkowo, wyniki prowadzonych obliczeń dowodzą mniejsze względne różnice niepewności rezultatów w Arktyce Europejskiej i Północnym Atlantyku aniżeli globalnie. Wyniki te były zaskakujące ze względu na wyższe średnie prędkości wiatru na półkuli północnej, niż globalnie. Powodem takiego stanu rzeczy jest fakt, że wartości wsp. k , dla różnych parametryzacji, są jednakowe dla prędkości wiatru, ok. 9 m s^{-1} , która to jest średnią roczną prędkością wiatru Północnego Atlantyku. Funkcja kwadratowa i sześcienna wiatru musi się przecinać, aby uzyskać podobne średnie globalne wartości. W ten sposób wyższe wartości funkcji sześciennych dla silnych wiatrów są równoważone przez wyższe wartości kwadratowych dla wiatrów słabych. Prędkość wiatru na skrzyżowaniu musi być wyższa niż średnia globalna prędkość wiatru, ponieważ rozbieżności między różnymi parametrami wzrastają wraz z prędkością wiatru. Region Północnego Atlantyku wraz z Oceanem Arktycznym wydaje się przez przypadek mieć idealną średnią prędkość wiatru, aby wszystkie parametryzacje skutkowały podobnymi rocznymi strumieniami. Formuła arytmetyczna tych różnic jest dokładnie opisana w publikacji [1]. Drugim powodem jest zmienność sezonowa kierunku przepływu strumieni CO₂. W wielu regionach świata kierunek przepływu zmienia się między zimą a latem, a prędkość wiatru jest znacznie większa w zimnej porze roku. Używając matematycznych rozwiązań zostało wykazane, że w przypadku sezonowości strumieni, różnice między parametryzacjami częściowo się anulują, co nie ma miejsca, gdy strumienie nigdy nie zmieniają swojego kierunku. Badania potwierdziły, że parametryzacje wsp. k z równań (1, 2, 4, Tabela 1) mogą być używane zamiennie, dla obliczeń zmian w Oceanie Arktycznym i Północnym Atlantyku, z niewielką przewagą mniejszych niepewności dla parametryzacji Nightingale i in. (2000). Potwierdzone zostało stwierdzenie, że Ocean Arktyczny, jako całość, silnie pochłania atmosferyczny CO₂, z nielicznymi miejscami, na styku z Prądem Północnoatlantyckim i Prądem Wschodniogrenlandzkim, gdzie CO₂ jest oddawany do atmosfery. Wszystkie wyniki uzyskano za pomocą klimatologii $p\text{CO}_2$ Takahashi i in. (2009), jednak dla lepszego zrozumienia zmian i ich wizualizacji, dane te zestawiono z danymi z reanaliz SOCAT v1.5 i v2.0. W europejskim sektorze Arktyki, miesięczne wartości strumieni CO₂, obliczone na podstawie różnych danych $p\text{CO}_2$ ale dla tych samych parametryzacji, skutkowały odwrotną zmiennością sezonową, przy zbliżonych wartościach średnich rocznych strumieni wynoszących: -1.02 PgC dla Takahashi i in. (2009), -0.085 PgC dla SOCAT v1.5 i -0.088 PgC dla SOCAT v2.0. Przyczyną tych rozbieżności może być różnica przestrzenna danych i możliwe artefakty interpolacji.

Badania przedstawione w artykule [2] koncentrowały się na obliczeniach wartości poszczególnych komponentów strumienia wymiany CO₂ oraz określeniu stopnia wpływu

oddziaływania wsp. k i $p\text{CO}_2$ na budżet CO_2 w Arktyce Europejskiej. Wyniki wykazały, że w Oceanie Arktycznym zmienność prędkości wiatru, a co za tym idzie fluktuacja wsp. k , na ogół odgrywają główną rolę w określaniu wielkości pochłaniania CO_2 przez powierzchnię styku, w skali czasowej, podczas gdy miesięczna fluktuacja $p\text{CO}_2$ wpływa na wahania wartości netto CO_2 w skali przestrzennej. Średnią prędkość przenoszenia gazu oszacowano na około $13.0 \pm 1.9 \text{ cm h}^{-1}$ z średnią prędkością wiatru, w analizowanym roku 2010, wynoszącą $8 \pm 0.7 \text{ m s}^{-1}$ i stężeniem $p\text{CO}_{2W}$ $332.4 \pm 11.8 \mu\text{atm}$. Wartość temperatury powierzchniowej Oceanu Arktycznego wyniosła około $3.0 \pm 1.6 \text{ }^\circ\text{C}$ a praktyczne zasolenie 34.3. $p\text{CO}_{2W}$ charakteryzuje się fluktuacjami w skali czasowo-przestrzennej, w porównaniu do $p\text{CO}_{2A}$, co wynika z faktu silnego pochłaniania CO_2 przez ocean. W badanym okresie koncentracji $p\text{CO}_2$ w oceanie była poniżej poziomu atmosferycznego. Obliczony pobór CO_2 wynosił od -6 do $-16 \text{ mgC m}^{-2} \text{ dzień}^{-1}$, a koncentracja $p\text{CO}_{2W}$ wahała się od 360 do 290 μatm . Średnia wartość $p\text{CO}_2$ w lutym i sierpniu wskazywała, że w okresie letnim (zdefiniowanym jako czas od maja do września) nastąpił spadek koncentracji w warstwie powierzchniowej, pomimo absorpcji CO_2 przez ocean, dzięki wysokiej wymianie z powietrzem, która została zrównoważona przez absorpcję CO_2 przez fitoplankton. W fiordach Arktyki różnica między $p\text{CO}_2$ latem i zimą była spowodowana niższą koncentracją $p\text{CO}_{2W}$ wynikającą z topnienia lodu morskiego, rozpuszczania CaCO_3 i zwiększonej produkcji pierwotnej. Różnice w $p\text{CO}_2$ charakteryzują się silną korelacją ze zmianami w $p\text{CO}_{2W}$, zwłaszcza w okresie zimowym (od października do kwietnia), kiedy średnia temperatura wody jest wyższa niż temperatura powietrza. Wyniki analizy pokazały, że w skali przestrzennej wartości strumienia CO_2 powietrze-morze były silnie dodatnio skorelowane z $p\text{CO}_2$ (znacznie mniej niż z k) podczas każdego miesiąca ($r = 0.757$, $p > 0.05$). a w skali czasowej silnie ujemnie skorelowane z k ($r = -0.935$, $p < 0.05$) z umiarkowanymi ujemnymi korelacjami w poszczególnych miesiącach. Zmienność k przyczynia się do wyjaśnienia jedynie około 20 % wahań miesięcznego strumienia CO_2 w Arktyce, podczas gdy $\Delta p\text{CO}_2$ przyczynia się do wyjaśnienia 50 % całkowitej zmienności.

Trzecia publikacja [3] koncentruje się na obliczeniu rzeczywistych pól wiatru z Północnego Atlantyku i europejskiej Arktyki w celu określenia średnich miesięcznych i rocznych wartości strumieni pędu przez powierzchnię morza, w zależności od wybranej parametryzacji na obliczanie bezwymiarowego współczynnika oporu (C_D) (równania 6 – 12, Tabela 2). Mimo prowadzenia ciągłych analiz pomiarów empirycznych, oraz wykorzystywania danych satelitarnych, rozrzut wartości wyników obliczeń wsp. C_D wciąż ma szeroki zakres, zarówno dla niskich i umiarkowanych średnich prędkości wiatru. Rezultat badań wykazał, rozrzut wartości C_D w zależności od użytej formuły. Wielkość wsp. C_D rośnie liniowo z wzrostem prędkości wiatru przy użyciu formuł (6-8), natomiast przy użyciu formuł 9, 11,12 (Tabela 2) maleje przy niskich średnich prędkościach wiatrów. Udowodniono, że przy niższych wartościach średnich prędkości wiatru ($< 10 \text{ m s}^{-1}$) różnice między poszczególnymi parametryzacjami C_D są większe, niż przy wyższych prędkościach ($> 10 \text{ m s}^{-1}$) a najbardziej odstającymi wynikami są te uzyskane z zastosowania parametryzacji (12). W warunkach słabych wiatrów niepewność pomiarów jest większa

(współczynnik 0.5 – 1.5, w zależności od użytej formuły), niż w warunkach umiarkowanych prędkościach (niepewność o współczynnik 1.5 – 2.0). Bezpośrednie porównanie wartości wyników z najnowszych parametryzacji C_D (11 i 12, Tabela 2), zmieniających się sezonowo w zależności od rejonu badań, z najstarszą formułą (6, Tabela 2) wykazało, że formuła (12, Tabela 2) daje wyniki blisko zerowemu współczynnikowi oporu, dla wiatrów o sile 3-5 m s⁻¹. Wyniki te sugerują, że średnie wartości współczynnika oporu dla różnych rejonów o podobnych prędkościach wiatru, mogą być bliskie zeru. Dodatkowo dowiedziono, że najstarsze parametryzacje C_D (6,7, Tabela 2) uległy „przedawnieniu” i skutkują zawyżonymi wynikami strumieni wymiany, w każdych warunkach, aniżeli parametryzacje stosunkowo nowe (11, 12, Tabela 2). Średnie miesięczne wartości obliczone dla Arktyki Europejskiej, Północnego Atlantyku i globalnie, w celu porównania, wykazały, że rejon, gdzie nie występują sezonowe zmienności prędkości wiatru, charakteryzują się podobnymi, stałymi wielkościami strumieni pędu (ok. 0.28 – 0.34 N m⁻², w zależności od użytej formuły, przy rocznej amplitudzie ok. 0.02 N m⁻²). W Arktyce Europejskiej ze względu na duże roczne amplitudy prędkości wiatru, sytuacja jest znacznie skomplikowana. W miesiącach letnich, formuła (12, Tabela 2) daje wyniki najniższe, podczas gdy pozostałe wyniki wartości C_D są zbliżone, dla każdej zastosowanej formuły. Średnie roczne strumienie wymiany pędu w Oceanie Arktycznym wahają się od 0.329 dla formuły Andreasa i in. (2012) do 0.375 N m⁻² dla Wu (1969) i są wyższe niż w Północnym Atlantyku i globalnie. W Północnym Atlantyku wartości te wynosiły, odpowiednio, 0.290 i 0.333 N m⁻² i globalnie 0.283 do 0.322 N m⁻². Dane, znormalizowane do formuły Andreas i in. (2012) dowiodły względne różnice pomiędzy zastosowanymi parametryzacjami wahające się od 1 % (11) do 14 % (6). Ponieważ określenie wielkości strumieni wymiany jest istotne przy opisie cyrkulacji oceanicznej, stosowanie ich poprawnych wartości w modelach numerycznych jest kluczowe, szczególnie dla modeli Oceanu Arktycznego, ze względu na występowanie halokliny. Dowiedziono, że formuły parametryzacji zastosowane w modelach klimatycznych NCEP/NCAR i Large and Yeager (2004), dają niepewności średnich wartości na poziomie 5 % z jeszcze większymi w skali miesięcznej.

3.5 Podsumowanie

Przeprowadzone badania pozwoliły określić wielkość strumieni wymiany CO₂ i pędu przez powierzchnię morza w europejskim sektorze Arktyki, wraz z niepewnościami wynikającymi z zastosowania różnych parametryzacji na współczynniki prędkości transferu k i współczynnika oporu C_D . Uzyskane wyniki znacząco poszerzyły wiedzę dotyczącą roli poszczególnych komponentów transferu przez warstwę styku, oraz wzbogaciły obecny stan wiedzy w ciągłe dane o tempie zmian klimatu. Wskazują one, że europejska Arktyka znacznie różni się pod względem badanych wartości, od sąsiadującego Północnego Atlantyku, pomimo stałej wymiany wód zachodzącej pomiędzy tymi oceanami. Niniejsza rozprawa doktorska obejmuje artykuły, które kompleksowo odnoszą się zarówno do procesów jak i współczynników napędzających strumienie wymiany CO₂ i pędu, prędkości przenoszenia gazu i parametryzacji współczynnika oporu, z

niepewnościami wartości w miesięcznych i rocznych obliczeniach. Ponadto określono stopień wpływu poszczególnych komponentów strumieni CO₂ na wielkości wymiany, w zależności od rozpatrywanej skali. Wnikliwym i oryginalnym aspektem tej pracy doktorskiej jest wykorzystanie danych satelitarnych w niedawno opracowanym modelu numerycznym FLuxEngine, co pozwoliło na zmniejszenie niepewności wynikające z niewystarczającej ilości danych oraz na wykluczenie luk, w badanym okresie, dzięki czemu opisane warunki odzwierciedlają rzeczywiste warunki w Arktyce Europejskiej

Podsumowując, praca doktorska z dużą dokładnością analizuje kwestię zastosowania odpowiednich parametryzacji w obliczeniach oddziaływania morza i atmosfery. Ze względu na stosunkowo niewielką liczbę danych dostępnych dla rejonów polarnych badania te, mają szczególne znaczenie i mogą mieć szerokie zastosowanie, na przykład w numerycznych modelach fizycznych stosowanych w europejskiej Arktyce.

- Andreas, E. L., Mahrt, L., Vickers, D., 2012. A new drag relation for aerodynamically rough flow over the Ocean. *J. Atmos. Sci.*, 69 (8), 2520-2539, doi:10.1175/JAS-D-11-0312.1.
- Brodeau, L., Barnier, B., Gulev, S.K., Woods, C., 2017. Climatologically significant effects of some approximations in the bulk parameterizations of turbulent air-sea fluxes. *J. Phys. Oceanogr.*, 47(1), 5-28, doi:10.1175/JPO-D-16-0169.1.
- Cai, W. J., Dai, M., Wang, Y., 2006. Air-sea exchange of carbon dioxide in ocean margins: a province-based synthesis. *Geophys. Res. Lett.* 33 (12), L12603, doi:10.1029/2006GL0226219.
- Ciais, P., Sabine, C., Bala, G., Bopp, L., Brovkin, V., Canadell, J., Chhabra, A., DeFries, R., Galloway, J., Heimann, M., Jones, C., Le Quéré, C., Myneni, R. B., Piao, S., Thornton, P., 2013. Carbon and Other Biogeochemical Cycles, [w:] T. F. Stocker, D. Qin, G. -K. Plattner, M. Tignor, S. K. Allen, J. Boschung, A. Nuels, Y. Xia, V. Bex, P. M. Midgley (red.) Climate Change 2013: The physical Science Basis, Contribution of Working Group I to the Fifth Assessment report of the Intergovernmental Panel on Climate Change. Cambridge University Press, Cambridge, United Kingdom and New York, NY, USA.
- Couldrey, M. P., Oliver, K. I. C., Yool, A., Halloran, P. R., and Achterberg, E. P., 2016. On which timescale do gas transfer velocity control North Atlantic CO₂ flux variability?. *Global Biogeochem. Cyc.*, 30, 787-802, doi:10.1002/2015GB005267.
- Csanady, G. T., 2004. The transfer laws of the air-sea interface. [w:] G. T. Csanady (red.). Air-sea interaction: Laws and Mechanism, Cambridge University Press, Cambridge, United Kingdom and New York, NY, USA, pp 1-3.
- Doney, S. C., Fabry, V. J., Feely, R.A., Kleypas, J. A., 2009. Ocean acidification: the other CO₂ problem. *Annu. Rev. Marine Sci.*, (1), 169-192, doi:10.1146/aanurev.marine.010908.163834.
- Final report of the Joint WCRP/SCOR Working Group on Air-SeaFluxes (SCOR Working Group 110), 2000. Intercomparison and validation of ocean-atmosphere energy flux fields. P. K. Taylor [red.]
- Garratt, J. R., 1977. Review of drag coefficients over oceans and continents. *Mon. Weather Rev.*, 105 (7), 915-929, doi:10.1175/1520-0493(1977)105<0915:RODCOO>2.0.CO;2.
- Goddijn-Murphy, L., Woolf, D. K., Land P. E., Shutler, J. D., Dinlon, C., 2015. The OceanFlux Greenhouse gases methodology for deriving a sea surface climatology of CO₂ fugacity in support of air-sea gas flux studies. *Ocean Sci.* 11(4), 519-541., doi:10.5194/05-11-519-2015.
- Gregg, W. W., Casey, N. W., and Rosseaux, C. S., 2014. Sensitivity of simulated global ocean carbon flux estimates to forcing by reanalysis products, *Ocean Model.*, 80, 24–35, doi:10.1016/j.ocemod.2014.05.002.
- Gruber, N., 2009. Carbon cycle: fickle trends in the ocean. *Nature* 458 (7235), 155-156, doi:10.1038/458155a.

- Ho, D. T., Law, C. S., Smith, M. J., Schlosser, P., Harvey, M. and Hill, P., 2006. Measurements of air-sea gas exchange at high wind speeds in the Southern Ocean: Implications for global parameterizations, *Geophys. Res. Lett.*, 33, 16611, doi: 10.1029/2006/GL026817.
- Jarosz, E., Mitchell, D.A., Wang, D. W., and Teague, W. J., 2007. Bottom-up determination of air-sea momentum exchange under a major tropical cyclone. *Science*, 315, 1707-1709.
- Joos, E, and Spahni, R., 2008. Rates of change in natural and anthropogenic radiative forcing over the past 20 000 years. *P Natl. Acad. Sci. USA*, 105,142-1430. Doi:10.1073/pnas/0707386105.
- Kalnay, E., Kanamitsu, M., Kistler R., Collins, W., Daeven, D., Gandin, L., Iredell, M., Saha, S., White, G., Woollen, J., Zhu, Y., Chelliah, M., Ebisuzaki, W., Higgins, W., Janowiak, J., Mo, K. C., Ropelewski, C., Wang, J., Leetmaa, A., Reynolds, R., Jenne, R., Joseph, D., 1996. The NCEP/NCAR 40-year reanalysis project. *Bull. Am. Meteor Soc.*, 77 (3), 437–471.
- Large, W. G., Yeager, S. G., 2004. Diurnal to decadal global forcing for ocean and sea-ice models: the data sets and flux climatologies. *Technical Note NCAR/TN-460+STR*, NCAR, Boulder, CO.
- Le Quéré, C., Andrew, R.M., Friedlingstein, P., Sitch, S., Hauck, J., Pongratz, J., Pickers, P. A., Korsbakken, J. I., Peters, G. P., Canadell, J. G., Arneeth, A., Arora, V. K., Barbero, L., Bastos, A., Bopp, L., Chevallier, F., Chini, L.P., Ciais, P., Doney, S. C., Gkritzalis, T., Goll, D. S., Harris, I., Haverd, V., Hoffman, F. M., Hoppema, M., Houghton, R. A., hurt, G., Ilyina, T., Jain, A. K., Johannessen, T., Jones, C. D., Kato, E., Kelling, R. F., Goldewijk, Landschützer, P., Lefèvre, N., Lienert, S., Liu, Z., Lombardozzi, D., Metzl, N., Munro, D. R., Nabel, J. E. M. S., Nakaoko, S. I., Neil, C., Olsen, A., Ono, T., Patra, P., Peregon, A., Peters, W., Peylin, P., Pfeil, B., Pierrot, D., Poulter, B., Rehder, G., Resplandy, L., Robertson, E., Rocher, M., Rödenbeck, C., Schuster, U., Schwinger, J., Séférian, R., Skjelvan, I., Stinhoff, T., Sutton, A. J., Tans, P. P., Tian, H., Tilbrook, B., Tubiello, F., N., van der Laan-Luijkx, I. T., van der Werf, G. R., Viovy, N., Walker, A. P., Wiltshire, A. J., Wright, R., Zaehle, S., and Zheng, B., 2018. Global Carbon budget 2018. *Ocean Sci*, 10, 2141-2194, doi:10.5194/essd-10-2141-2018.
- Matthews, B. J. H., 1999. The rate of air-sea CO₂ exchange: chemical enhancement and catalysis by marine microalgae. PhD Thesis (web edition), University of East Anglia, Norwich.
- McGillis, W. R., and Edson, J. B., Hare, J. E., Fairall, C. W., 2001. Direct covariance air-sea CO₂ fluxes, *J. Geophys. Res.*, 106, C8 16729-16745.
- Nightingale, P. D., Malin, G., Law, C. S., Watson, A. J., Liss, P. S., Liddicoat, M. I., Boutin, J., and Upstill-Goddard, R. C., 2000. In situ evaluation of air-sea gas exchange parameterizations using novel conservative and volatile tracers, *Global Biogeochem. Cyc.*, 14, 373-387, <http://dx.doi.org/10.1029/1999GB900091>.

- Nakaoko, S. I., Aoki, A., Nakazawa, T., Hashida, G., Morimoto, S., Yamanouchi, T., Yoshikawa-Inoue, H., 2006. Temporal and spatial variations of oceanic pCO₂ and air—sea CO₂ flux in Greenland Sea and Barents Sea. *Tellus B* 58 (2), 148—616, <http://dx.doi.org/10.1111/j.1600-0889.2006.00178>.
- Omar, A. M., Johannessen, T., Kaltin, S., Olsen, A., 2003. Anthro-po-genic increase of oceanic pCO₂ in the Barents Sea surface water. *J. Geophys. Res.*, 108 (C12), 18-1—18-8, <http://dx.doi.org/10.1029/2002JC001628>.
- Schuster, U. and Watson, A. J., 2007. A variable and decreasing sink for atmospheric CO₂ in the North Atlantic, *J. Geophys. Res.*, 112, C11006, doi:10.1029/2006JC003941.
- Shutler, J. D., Piolle, J.-F., Land, P. E., Woolf, D. K., Goddijn-Murphy, L., Paul, F., Girard-Ardhuin, F., Chapron, B., Donlon, C. J., 2016. FluxEngine: a flexible processing system for calculating atmo-sphere—ocean carbon dioxide gas fluxes and climatologies. *J. Atmos. Ocean. Technol.* 33 (4), 741—756, <http://dx.doi.org/10.1175/JTECH-D-14-00204.1>.
- Takahashi, T., Sutherland, S. C., Wanninkhof, R., Sweeney, C., Feely, R. A., Chipman, D. W., Hales, B., Friederich, G., Chavez, F., Sabine, C., Watson, A., Bakker, D. C. E., Schuster, U., Metzl, N., Yoshikawa-Inoue, H. Y., Ishii, M., Midorikawa, T., Nojiri, Y., Köert-zinger, A., Steinhoff, T., Hoppema, M., Olafsson, J., Arnarson, T. S., Tilbrook, B., Johannessen, T., Olsen, A., Bellerby, R., Wong, C. S., Delille, B., Bates, N. R., de Baar, H. J. W., 2009. Climatological mean and decadal change in surface ocean pCO₂ and net sea—air CO₂ flux over the global oceans. *Deep-Sea Res. II*, 56 (8—10), 554— 577, <http://dx.doi.org/10.1016/j.dsr2.2008.12.009>.
- Wanninkhof, R., 2007. The impact of difference gas exchange formulations and wind speed products on global air-sea CO₂ fluxes. [w:] C. S. Garbe, R. A. Handler, B. Jähne (red.). *Transport at the air-sea interface*, Springer, pp. 1-23.
- Wanninkhof, R., 2014. Relationship between wind speed and gas exchange over the ocean revisited, *Limnol. Oceanogr. Methods*, 12, 351—362, doi: 10.4319/lom.2014.12.351.
- Wanninkhof, R., and McGillis, W. R., 1999. A cubic relationship between air-sea CO₂ exchange and wind speed, *Geophys. Res. Lett.*, 26, 1889-1892.
- Wu, J., 1969. Wind stress and surface roughness at air-sea interface. *J. Geophys. Res.*, 74 (2), 444-455, doi:10.1029/JB074i002p00444.
- Wu, J., 1982. Wind-stress coefficients over sea surface from breeze to hurricane. *J. Geophys. Res.*, 87 (C12), 9704-9706, doi: 10.1029/JC087iC12p09704.
- Yelland, M., Taylor, P. K., 1996. Wind stress measurements from the open ocean. *J. Phys. Oceanogr.*, 26 (4), 541-558, doi:10.1175/1520-0485(1996)026<0541:WSMFTO>2.0.CO;2.

II. List of the attached research paper

1. Research paper no 1

Wróbel, I., Piskozub, J. 2016. *Effect of gas-transfer velocity parameterization choice on air-sea CO₂ fluxes in the North Atlantic and the European Arctic*. Ocean Science, 12, 1091-1103, doi: 10.5194/os-12-1091-2016.

(IF¹ = 2.289; MNiSW² = 30)

2. Research paper no 2

Wróbel, I. 2017. *Monthly dynamics of carbon dioxide exchange across the sea surface of the Arctic Ocean in response to changes in gas transfer velocity and partial pressure of CO₂ in 2010*. Oceanologia, 59, 445-459, doi:10.1016/j.oceano.2017.05.001.

(IF = 1.614; MNiSW = 20)

3. Research paper no 3

Wróbel-Niedźwiecka, I., Drozdowska, V., Piskozub, J. 2019. *Effect of drag coefficient formula choice on wind stress climatology in the North Atlantic and the European Arctic*. Oceanologia, 61, 291-299, doi:10.1016/j.oceano.2019.02.002.

(IF = 1.614; MNiSW = 20)

¹ Journal Impact Factor (IF) according to the Journal Citation Reports

² Journal Score according to the list of the Polish Ministry of Science and Higher Education

1. Research paper no 1

Wróbel, I., Piskozub, J. 2016. *Effect of gas-transfer velocity parameterization choice on air-sea CO₂ fluxes in the North Atlantic and the European Arctic*. Ocean Science, 12, 1091-1103, doi: 10.5194/os-12-1091-2016



Effect of gas-transfer velocity parameterization choice on air–sea CO₂ fluxes in the North Atlantic Ocean and the European Arctic

Iwona Wrobel and Jacek Piskozub

Institute of Oceanology, Polish Academy of Sciences, Sopot, Poland

Correspondence to: Iwona Wróbel (iwrobel@iopan.gda.pl)

Received: 22 September 2015 – Published in Ocean Sci. Discuss.: 3 November 2015

Revised: 2 September 2016 – Accepted: 14 September 2016 – Published: 30 September 2016

Abstract. The oceanic sink of carbon dioxide (CO₂) is an important part of the global carbon budget. Understanding uncertainties in the calculation of this net flux into the ocean is crucial for climate research. One of the sources of the uncertainty within this calculation is the parameterization chosen for the CO₂ gas-transfer velocity. We used a recently developed software toolbox, called the FluxEngine (Shutler et al., 2016), to estimate the monthly air–sea CO₂ fluxes for the extratropical North Atlantic Ocean, including the European Arctic, and for the global ocean using several published quadratic and cubic wind speed parameterizations of the gas-transfer velocity. The aim of the study is to constrain the uncertainty caused by the choice of parameterization in the North Atlantic Ocean. This region is a large oceanic sink of CO₂, and it is also a region characterized by strong winds, especially in winter but with good in situ data coverage. We show that the uncertainty in the parameterization is smaller in the North Atlantic Ocean and the Arctic than in the global ocean. It is as little as 5 % in the North Atlantic and 4 % in the European Arctic, in comparison to 9 % for the global ocean when restricted to parameterizations with quadratic wind dependence. This uncertainty becomes 46, 44, and 65 %, respectively, when all parameterizations are considered. We suggest that this smaller uncertainty (5 and 4 %) is caused by a combination of higher than global average wind speeds in the North Atlantic ($> 7 \text{ ms}^{-1}$) and lack of any seasonal changes in the direction of the flux direction within most of the region. We also compare the impact of using two different in situ pCO₂ data sets (Takahashi et al. (2009) and Surface Ocean CO₂ Atlas (SOCAT) v1.5 and v2.0, for the flux calculation. The annual fluxes using the two data sets differ by 8 % in the North Atlantic and 19 % in the European Arctic. The seasonal fluxes in the Arctic computed from the two data sets

disagree with each other possibly due to insufficient spatial and temporal data coverage, especially in winter.

1 Introduction

The region of extratropical North Atlantic Ocean, including the European Arctic, is a region responsible for the formation of deep ocean waters (see Talley, 2013, for a recent review). This process, part of the global overturning circulation, makes the area a large sink of atmospheric carbon dioxide (CO₂) (Takahashi et al., 2002, 2009; Landschützer et al., 2014; Le Quéré et al., 2015; Orr et al., 2001). Therefore, there is a widespread interest in tracking the changes in the North Atlantic net CO₂ fluxes, especially as models appear to predict a decrease in the sink volume later this century (Halloran et al., 2015).

The trend and variations in the North Atlantic CO₂ sinks has been intensively studied since observations have shown it appeared to be decreasing (Lefèvre et al., 2004). This decrease on interannual timescales has been confirmed by further studies (Schuster and Watson, 2007) and this trend has continued in recent years north of 40° N (Landschützer et al., 2013). It is not certain how many of these changes are the result of long-term changes, decadal changes in atmospheric forcing – namely the North Atlantic Oscillation (González-Dávila et al., 2007; Thomas et al., 2008; Gruber, 2009; Watson et al., 2009), or changes in meridional overturning circulations (Pérez et al., 2013). Recent assessments of the Atlantic and the Arctic net sea–air CO₂ fluxes (Schuster et al., 2013) and the global ocean net carbon uptake (Wanninkhof et al., 2013) show that the cause is still unknown.

Published by Copernicus Publications on behalf of the European Geosciences Union.

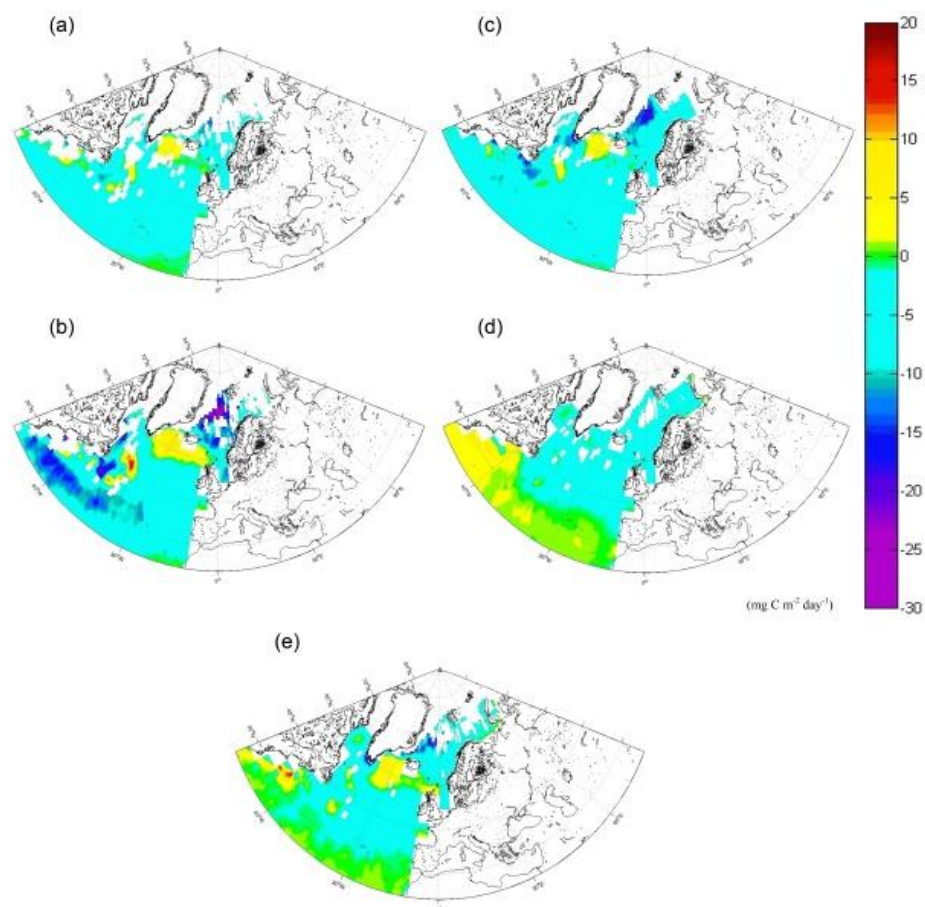


Figure 1. Seasonal and annual mean air-sea fluxes of CO_2 ($\text{mg C m}^{-2} \text{ day}^{-1}$) in the North Atlantic, using Nightingale et al. (2000), k parameterization and Takahashi et al. (2009) climatology: (a) annual, (b) DJF (winter), (c) MAM (spring), (d) JJA (summer), and (e) SON (autumn). The gaps (white areas) are due to missing data, land, and ice masks.

Table 1. Annual air-sea CO_2 fluxes (in Pg) using different k parameterizations. The values in parentheses are fluxes normalized to Nightingale et al. (2000; as in Fig. 7).

	Global	Arctic	North Atlantic	Southern Ocean
Nightingale et al. (2000)	−1.30 (1.00)	−0.102 (1.00)	−0.382 (1.00)	−0.72 (1.00)
Ho et al. (2006)	−1.42 (1.09)	−0.106 (1.04)	−0.402 (1.05)	−0.76 (1.06)
Wanninkhof and McGillis (1999)	−1.73 (1.33)	−0.130 (1.28)	−0.490 (1.29)	−0.93 (1.30)
Wanninkhof (2014)	−1.40 (1.08)	−0.105 (1.03)	−0.398 (1.04)	−0.76 (1.05)
McGillis et al. (2001)	−2.15 (1.65)	−0.147 (1.44)	−0.557 (1.46)	−1.08 (1.49)
OceanFlux GHG wind driven	−1.98 (1.52)	−0.138 (1.36)	−0.560 (1.47)	−1.14 (1.58)
OceanFluxGHG backscatter	−1.88 (1.44)	−0.130 (1.27)	−0.526 (1.38)	−1.09 (1.51)

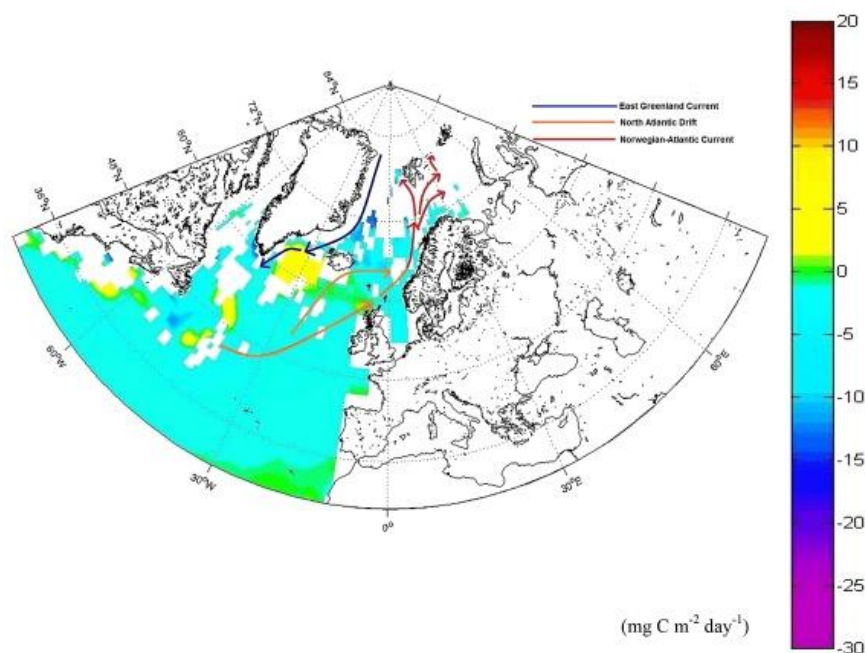


Figure 2. Some relevant surface ocean currents in the North Atlantic Ocean and the European Arctic against the background of the annual mean air–sea CO_2 fluxes ($\text{mg C m}^{-2} \text{ day}^{-1}$) as in Fig. 1. The North Atlantic Drift continues as the Norwegian–Atlantic Current in the Nordic Seas.

To study the rate of the ocean CO_2 sink and especially its long-term trend, one needs to first constrain the uncertainty in the flux calculation. The global interannual variability in air–sea CO_2 fluxes can be about 60 % due to differences in $p\text{CO}_2$ and 35 % by gas-transfer velocity k parameterization (Couldrey et al., 2016). Sources of uncertainty include sampling coverage, the method of data interpolation, data quality of the fugacity of CO_2 ($f\text{CO}_2$), the method used for normalization of fugacity data to a reference year in a world of ever increasing atmospheric CO_2 , the measurement uncertainty in all the parameters used to calculate the fluxes (partial pressure in water and air, bulk and skin water temperatures, air temperatures, wind speed, etc.), and some which are not usually included in the calculations but most probably influence the flux values (sea state parameters, air bubble void fraction, surfactant effects, etc.) as well as the choice of the gas-transfer velocity k parameterization formula (Landschützer et al., 2014). It has also been identified that the choice of the wind data product provides an additional source of uncertainty in gas-transfer velocity, even by 10–40 %, and the choice of the wind speed parameterization may cause variability in k by as much as about 50 % (Gregg et al., 2014;

Couldrey et al., 2016). In this work we have analysed solely the effects of the choice between various published empirical wind-driven gas-transfer parameterizations. The North Atlantic is one of the regions of the world ocean best covered by CO_2 fugacity measurements (Watson et al., 2011), the coverage of the Arctic seas is much poorer, especially in winter (Schuster et al., 2013).

In the literature there are many different parameterizations to choose from and most depend on a cubic or quadratic wind speed relationship. The choice of the appropriate parameterization is not trivial as indicated by the name of an international meeting, which focused on this topic (“ k conundrum” workshop, COST-735 Action organized meeting in Norwich, February 2008). The conclusions from this meeting have been incorporated into a recent review book chapter (Garbe et al., 2014). This paper concentrates on quantifying the uncertainty caused by the choice of the gas-transfer velocity parameterization in the North Atlantic and the European Arctic. These regions were chosen as they are the areas for which many of the parameterizations were originally derived. They are also regions with wind fields skewed towards higher winds (in comparison to the global average) enabling

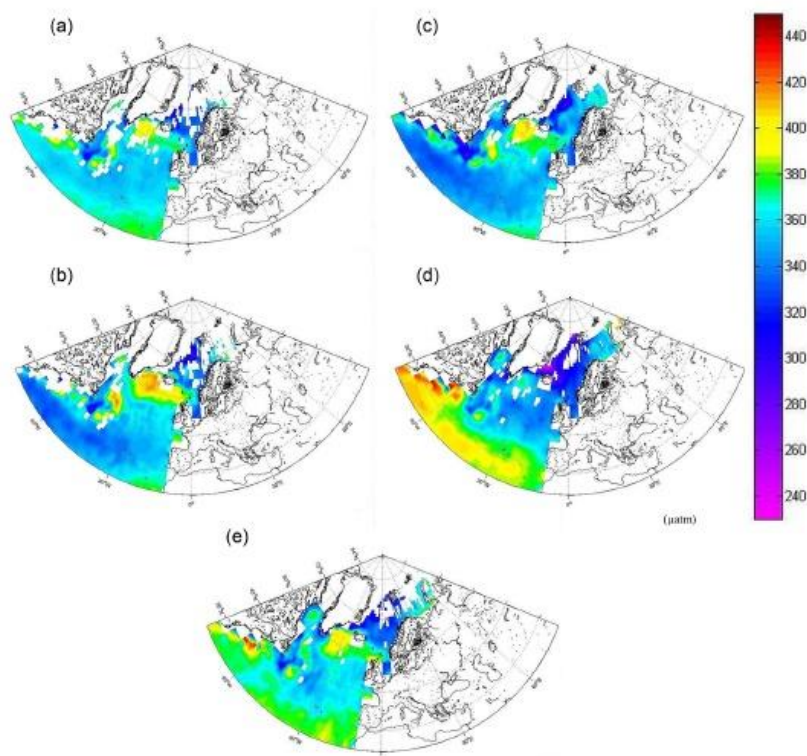


Figure 3. Seasonal and annual $p\text{CO}_2$ values (μatm) in surface waters of the North Atlantic, estimated using the Takahashi et al. (2009) climatology: (a) annual, (b) DJF (winter), (c) MAM (spring), (d) JJA (summer), and (e) SON (autumn). The gaps (white areas) are due to missing data, land and ice masks.

the effect of stronger winds on the net flux calculations to be investigated by using published gas-transfer velocity formulas.

2 Methods

2.1 Data sets

We calculated net air–sea CO_2 fluxes using a set of software processing tools called the “FluxEngine” (Shutler et al., 2016), which was created as part of European Space Agency funded OceanFlux Greenhouse Gases (GHGs) project (<http://www.oceanflux-ghg.org>). The tools were developed to provide the community with a verified and consistent toolbox and to encourage the use of satellite Earth observation (EO) data for studying air–sea fluxes. The toolbox source code can be downloaded or alternatively there is a version that can be

run through a web interface. Within the online web interface, a suite of re-analysis data products, in situ and model data are available as input to the toolbox. The FluxEngine allows the users to select several different air–sea flux parameterizations producing monthly global gridded net air–sea fluxes products with $1^\circ \times 1^\circ$ spatial resolution. The output consists of twelve NetCDF files (one file per month). One monthly composite file includes the mean (first-order moment), median, standard deviation, and the second-, third-, and fourth-order moments. There is also information (metadata) about origin of data inputs. For example, the monthly EO input data include rain intensity, wind speed and direction, % of sea ice cover from monthly model data, ECMWF (European Centre for Medium-Range Weather Forecast) air pressure, whitecapping (Goddijn-Murphy et al., 2011), two options for monthly data sets of $p\text{CO}_2$, sea surface temperature (SST), and salinity. The user then needs to choose the different com-

ponents and structure of the net air–sea gas flux calculation and choose the transfer velocity parameterization.

For the calculations, we used $p\text{CO}_2$ and salinity values from Takahashi et al. (2009) climatology, which was based on more than 3 million measurements of surface water $p\text{CO}_2$ in open-ocean environments during non-El Niño conditions. For some calculations, we used, as an alternative, Surface Ocean CO_2 Atlas (SOCAT) v1.5 and v2.0 (Sabine et al., 2013; Pfeil et al., 2013; Bakker et al., 2014) $p\text{CO}_2$, and associated SST data. SOCAT is a community-driven data set containing 6.3 and 10.1 million surface water CO_2 fugacity values for v1.5 and v2.0, respectively, with a global coverage. The SOCAT databases have been re-analysed and then converted to climatologies using the methodology described in Goddijn-Murphy et al. (2015). All the climatologies were calculated for year 2010 with the FluxEngine toolset. The SSTskin (defined within Group for High Resolution SST (GHRSSST) as temperature of the surface measured by an infrared radiometer operating at the depth of $\sim 10\text{--}20\ \mu\text{m}$) values were taken from the Advance Along Track Scanning Radiometer (ESA/ARC/(A)ATSR) Global Monthly Sea Surface data set (Merchant et al., 2012) in the case of both data sets, and have been preprocessed in the same way for use with the FluxEngine (Shutler et al., 2016).

We used EO wind speed and sea roughness (σ_0 – altimeter backscatter signal in Ku-band from GlobWave L2P products) data obtained from the European Space Agency (ESA). The GlobWave satellite products give a “uniform” set of along track satellite wave data from all available Altimeters (spanning multiple space agencies) and from ESA Synthetic Aperture Radar (SAR) data and are publicly available at the Ifremer/CERSAT cloud (<http://globwave.ifremer.fr/products/data-access>). Wave data are collected from six altimeter missions (Topex/POSEIDON, Jason-1/22, CryoSAT, GEOSAT, and GEOSAT Follow On) and from ESA SAR missions, namely ERS-1/2 and ENVISAT. All data come in netCDF-3 format.

All analyses were performed using global data contained in the FluxEngine software. From the gridded product ($1^\circ \times 1^\circ$) we extracted data from the extratropical North Atlantic Ocean (north of 30°N), and its subset, the European Arctic (north of 64°N). For comparison, we also calculated fluxes in the Southern Ocean (south of 40°S). Hereafter, we follow the convention of that sources of CO_2 (upward ocean-to-atmosphere gas fluxes) are positive and sinks (downward atmosphere-to-ocean gas fluxes) are negative. We give all results of net CO_2 fluxes in the SI unit of Pg (Pg is 10^{15} g , which is numerically identical to Gt).

2.2 k parameterizations

The flux of CO_2 at the interface of air and the sea is controlled by wind speed, sea state, SST, and other factors. We estimate the net air–sea flux of CO_2 (F , $\text{mg C m}^{-2}\text{ day}^{-1}$) as the product of gas-transfer velocity (k , ms^{-1}) and the dif-

ference in CO_2 concentration (gm^{-3}) in the sea water and its interface with the air (Land et al., 2013). The concentration of CO_2 in sea water is the product of its solubility (α , $\text{gm}^{-3}\text{ atm}^{-1}$) and its fugacity ($f\text{CO}_2$, atm). Solubility is, in turn, a function of salinity and temperature. Hence F is defined as

$$F = k(\alpha_W f\text{CO}_{2W} - \alpha_S f\text{CO}_{2A}), \quad (1)$$

where the subscripts denote values in water (W) and the air–sea interface (S) and in the air (A). We can exchange fugacity with the partial pressure (their values differ by $<0.5\%$ over the temperature range considered; McGillis et al., 2001). So Eq. (1) now becomes

$$F = k(\alpha_W p\text{CO}_{2W} - \alpha_S p\text{CO}_{2A}). \quad (2)$$

One can also ignore the differences between the two solubilities, and just use the waterside solubility α_W . Equation (2) will then become

$$F = k\alpha_W(p\text{CO}_{2W} - p\text{CO}_{2A}). \quad (3)$$

This formulation is often referred to as the “bulk parameterization”.

In this study we chose to analyse the air–sea gas fluxes using five different gas-transfer parameterizations (k). All of them are wind speed parameterizations, but differ in the formula used:

$$k = \sqrt{(660.0/S_{c\text{skin}}) \cdot (0.212U_{10}^2 + 0.318U_{10})} \quad (4)$$

(Nightingale et al., 2000),

$$k = \sqrt{(660.0/S_{c\text{skin}}) \cdot 0.254U_{10}^2} \quad (5)$$

(Ho et al., 2006),

$$k = \sqrt{(660.0/S_{c\text{skin}}) \cdot 0.0283U_{10}^3} \quad (6)$$

(Wanninkhof and McGillis, 1999),

$$k = \sqrt{(660.0/S_{c\text{skin}}) \cdot 0.251U_{10}^2} \quad (7)$$

(Wanninkhof, 2014),

$$k = \sqrt{(660.0/S_{c\text{skin}}) \cdot (3.3 + 0.026U_{10}^3)} \quad (8)$$

(McGillis et al., 2001),

where $S_{c\text{skin}}$ stands for the Schmidt numbers at the skin surface, a function of SST ($[= (\text{kinematic viscosity of water})/(\text{diffusion coefficient of } \text{CO}_2 \text{ in water})]$), 660.0 is the Schmidt number corresponding to values of CO_2 at 20°C in seawater, and U_{10} is the wind speed 10 m above the sea surface.

In addition to the purely wind-driven parameterizations, we have used the combined Goddijn-Murphy et al. (2012) and Fangohr and Woolf (2007) parameterization, which was developed as a test algorithm within of OceanFlux GHG Evolution project. This parameterization separates contributions from direct- and bubble-mediated gas transfer as suggested by Woolf (2005). Its purpose is to enable a sepa-

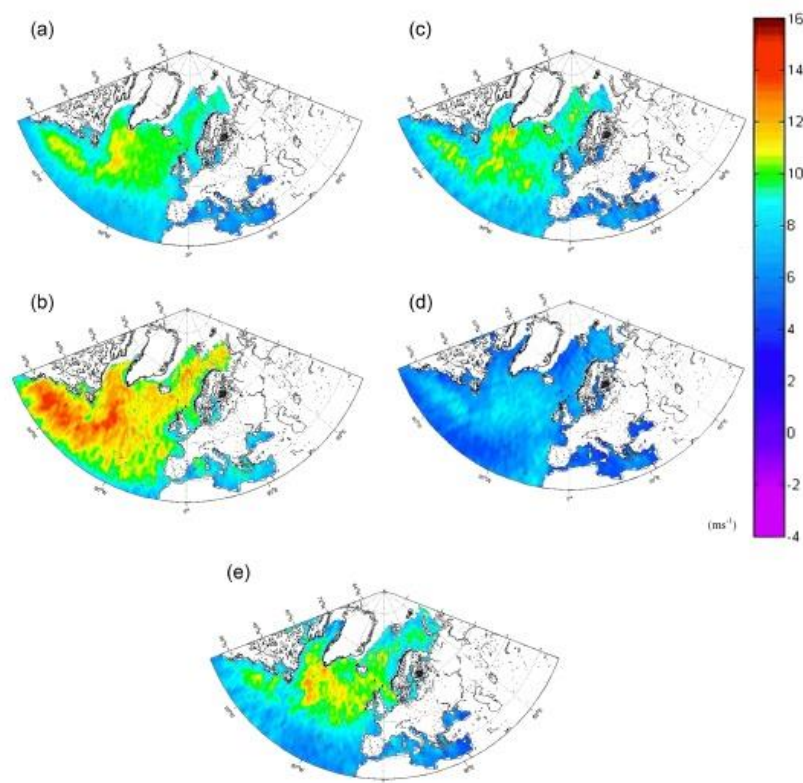


Figure 4. Wind speed distribution U_{10} (ms^{-1}) in the North Atlantic used to determine the relationship between gas-transfer velocity and air–sea CO_2 fluxes: (a) annual, (b) DJF (winter), (c) MAM (spring), (d) JJA (summer), and (e) SON (autumn). The gaps (white areas) are due to missing data, land, and ice masks.

rate evaluation of the effect of the two processes on air–sea gas fluxes and it is an algorithm that has yet to be calibrated. We used two versions of this parameterization: wind-driven direct transfer (using the U_{10} wind fields) and radar backscatter-driven direct transfer (using mean wave square slope) as described in Goddijn-Murphy et al. (2012).

3 Results

Using the FluxEngine software, we have produced global gridded monthly net CO_2 air–sea fluxes and from these we have extracted the values for the two study regions, the extratropical North Atlantic Ocean and separately for its subset – the European Arctic seas. Figure 1 shows maps of the monthly mean air–sea CO_2 fluxes for the North Atlantic, calculated with Nightingale et al. (2000; hereafter called

N2000) k parameterization and the Takahashi et al. (2009) climatology for the whole year and for each season. The area, as a whole, is a sink of CO_2 but some regions close to North Atlantic Drift and East Greenland Current (Fig. 2) are net sources. At the seasonal maps one can see more variability caused by physical process (with temperature changes causing maximum oceanic $p\text{CO}_2$ in summer) or biological activity (with phytoplankton blooms causing summer values to be lowest in the annual cycle). For example, the areas close to the North Atlantic Drift and East Greenland Current are sinks of CO_2 in the summer (likely due to the growth of phytoplankton) while the southern most areas of the region become CO_2 sources in summer and autumn (which is likely to be due to the effect of sea-water temperature changes). Much of this variability is caused by changes in the surface water $p\text{CO}_2$ values, shown in Fig. 3 for the whole year and for each

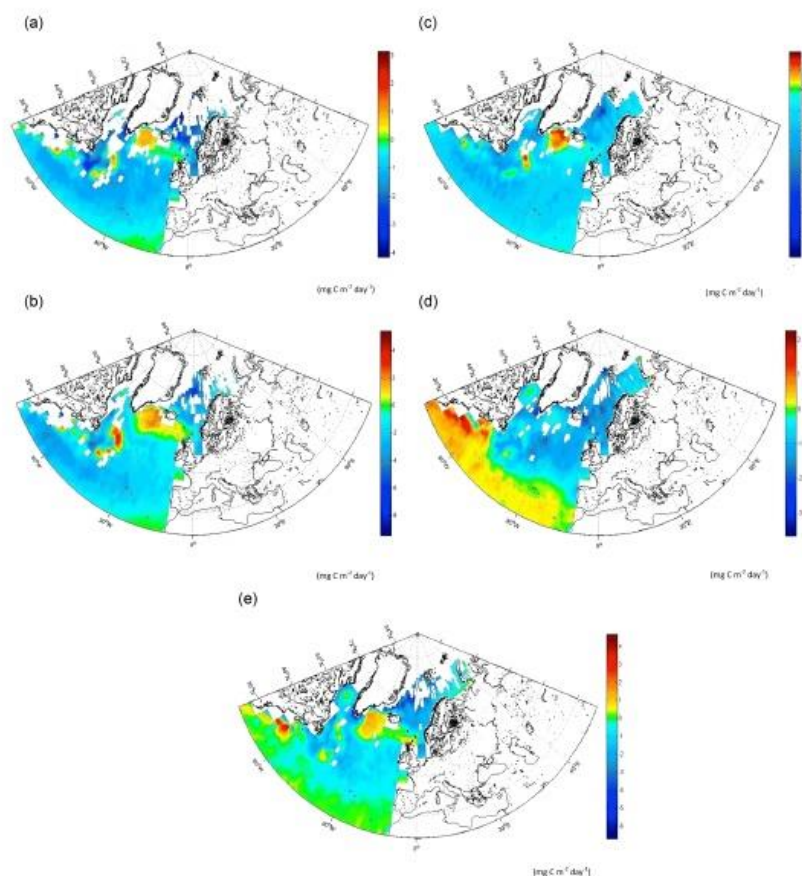


Figure 5. Difference maps for the air–sea CO_2 fluxes ($\text{mg C m}^{-2} \text{ day}^{-1}$) in the North Atlantic, between a cubed and a squared parameterization (Wanninkhof and McGillis, 1999 and Wanninkhof, 2014): (a) annual, (b) DJF (winter), (c) MAM (spring), (d) JJA (summer) and (e) SON (autumn). The gaps (white areas) are due to missing data, land, and ice masks.

season (and variability in atmospheric CO_2 partial pressure, not shown). However, the flux is proportional to the product of $\Delta p\text{CO}_2$ and k . In most parameterizations k is a function of wind speed (Eqs. 4–8). The mean wind speed U_{10} for the whole year and each season are shown in Fig. 4. The wind speeds in the North Atlantic are higher than the mean value in the world ocean (which is 7 m s^{-1} ; Couldrey et al., 2016), with mean values higher than 10 m s^{-1} in many regions of the study area in all seasons except for the summer (with the highest values in winter). This is important because the air–sea flux depends not only on average wind speed but also on its distribution (see Discussion below). This effect is especially visible between formulas with different powers of U_{10} .

Figure 5 shows the difference in the air–sea CO_2 fluxes calculated using two example parameterizations: one proportional to U_{10}^3 (Eq. 6) and one to U_{10}^2 (Eq. 7), namely Wanninkhof and McGillis (1999; hereafter called WMcG1999) and Wanninkhof (2014; hereafter called W2014). It can be seen that the “cubic” function results in higher absolute air–sea flux values when compared to the “quadratic” function in the regions of high winds, and lower absolute air–sea flux values in weaker winds.

Figure 6 shows the monthly values of air–sea CO_2 fluxes for the five parameterizations (Eqs. 4–8) for the North Atlantic and the European Arctic. The regions are sinks of CO_2 in every month, although August is close to neutral for

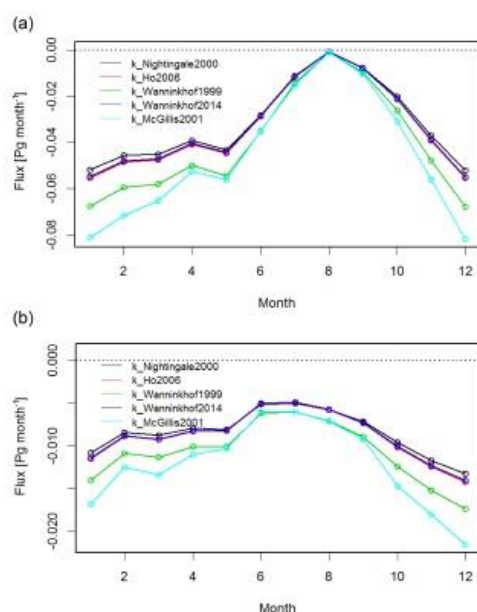


Figure 6. Monthly values of CO_2 air-sea fluxes (Pg month^{-1}) for the five parameterizations (Eqs. 4–8); (a) the North Atlantic, (b) the European Arctic.

the North Atlantic. The results using cubic parameterizations (Eqs. 6 and 8) are higher in absolute values, by up to 30 % for WMcG1999 and 55 % for McGillis et al. (2001; hereafter called McG2001), in comparison to the “quadratic” of N2000 (Eq. 4). The other two “quadratic” parameterizations W2014 and Ho et al. (2006; hereafter called H2006; Eqs. 5 and 7) resulted in fluxes within 5 % of N2000. In addition to the five parameterizations, Fig. 7 presents results for both of the OceanFlux GHG Evolution formulas (using wind and radar backscatter data). The mean and standard deviations of the parameterization ensemble are shown as grey vertical lines. The standard deviation in global fluxes is similar to previous estimates (Sweeney et al., 2007; Landschützer et al., 2014) but they cannot be directly compared due to different parameterization choices and methodologies. Annual net fluxes for the North Atlantic, Southern and global oceans, as well as for the European Arctic, are shown in Table 1. The results show that the annual North Atlantic net air-sea CO_2 sink, depending on the formula used, varies from -0.38 for N2000 to -0.56 Pg C for McG2001. In the case of global net air-sea CO_2 sink the values are -1.30 and -2.15 Pg C , respectively. Table 1 as well as Fig. 7 shows the same data “normalized” to the N2000 data (divided by value), which allows us to visualize the relative differences (in Table 1 values in parenthe-

ses). In the case of the North Atlantic, using the “quadratic” W2014 and H2006 parameterizations results in net air-sea fluxes that are 4 and 5 % higher in absolute values, respectively, than the equivalent N2000 result, while the “cubic” WMcG1999 and McG2000 result in values that are 28 and 44 % higher, respectively, than the N2000 results for this region. The respective values for the Arctic are 3 % for W2014 and 4 % for H2006, as well as 28 % for WMcG1999 and 44 % for McG2001 than N2000. In the case of global net air-sea CO_2 fluxes the equivalent values are 8 % (W2014) and 9 % (H2006) higher than the N2000 result for the quadratic functions as well as 33 % (WMcG1999) and 65 % (McG2001) for cubic ones. The OceanFlux GHG parameterization for the backscatter and wind-driven versions, results in net air-sea CO_2 fluxes higher for North Atlantic Ocean than the N2000, that are 38 and 47 %, respectively, and in the global case the values, for those two versions, were 44 and 52 % higher, respectively, than N2000 values. The spread of the Arctic values was lower than that of the Atlantic values (see Table 1). On the other hand, the values for the Southern Ocean were slightly higher than for the North Atlantic but lower than the global values, with the exception of the OceanFlux GHG parameterizations.

All the above results were obtained with the Takahashi et al. (2009) $p\text{CO}_2$ climatology and for comparison, we have also calculated the air-sea CO_2 fluxes using the re-analysed SOCAT v1.5 and v2.0 data (which were converted to climatologies using methodology described in Goddijn-Murphy et al., 2015). Figure 8 shows the results using the N2000 k parameterization for all three of the data sets (Takahashi et al., 2009 and both SOCAT versions). In the case of the North Atlantic Ocean study area, although the monthly values show large differences (using both SOCAT data sets results in a larger sink in summer and smaller in winter compared to Takahashi et al., 2009), the annual values are similar: -0.38 Pg C for both Takahashi et al. (2009) and SOCAT v1.5 and -0.41 Pg C for SOCAT v2.0. In the case of the European Arctic, the situation is very different, with Takahashi et al. (2009) and SOCAT data set-derived climatologies resulting in inverse seasonal variability but with annual net air-sea CO_2 fluxes results that are similar: -0.102 Pg C for Takahashi et al. (2009), -0.085 Pg C for SOCAT v1.5, and -0.088 Pg C for SOCAT v2.0.

4 Discussion

Our results show that the three “quadratic” parameterization (Nightingale et al., 2000; Ho et al., 2006 and Wanninkhof, 2014) air-sea fluxes are within 5 % of each other in the case of the North Atlantic (Table 1, values in parentheses). This discrepancy is smaller than the 9 % difference identified for the global case (Table 1 and Fig. 7). This confirms that at present, these different parameterizations are interchangeable for the North Atlantic as this range is within

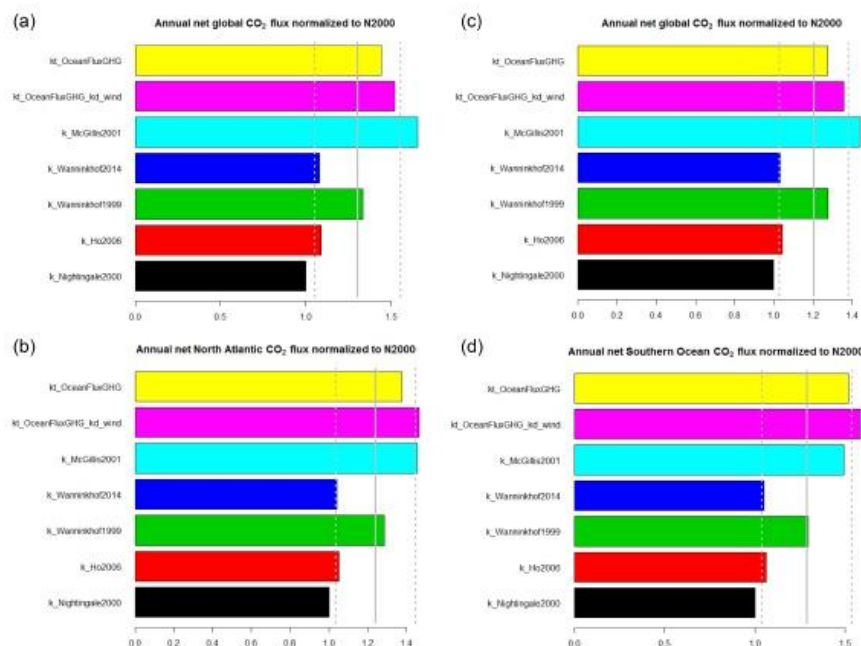


Figure 7. Annual air–sea fluxes of CO_2 for the five (Eqs. 4–8) parameterizations as well as for backscatter (default) and wind-driven OceanFlux GHG parameterizations normalized to flux values of Nightingale et al. (2000) k parameterization (see text): (a) globally, (b) the North Atlantic, (c) the European Arctic, and (d) the Southern Ocean. Average values for all parameterization and standard deviations are marked as vertical grey lines.

the experimental uncertainty (Nightingale, 2015). The three parameterizations were derived using different methods and data from different regions, namely passive tracers and dual-tracer experiments in the North Sea in the case of Nightingale et al. (2000), dual tracers in the Southern Ocean in the case of Ho et al. (2006), and global ocean ^{14}C inventories in the case of Wanninkhof (2014). The differences between the quadratic and cubic parameterization are large, and instead of the quadratic functions that are supported by several lines of evidence (see Garbe et al., 2014 for discussion), the cubic function are not completely refuted by the available observation. Therefore, it is important to notice that a choice of one of the available cubic functions may lead to net air–sea CO_2 fluxes that are considerably larger in absolute values, by up to 33 % in the North Atlantic Ocean and more than 50 % in the global ocean.

The above results imply smaller relative differences between the parameterizations in the North Atlantic Ocean than in the global ocean. This is interesting because the North Atlantic is the region of strong winds and over most of its area there are no seasonal changes in the air–sea flux direction

(Fig. 1). For example in the South Atlantic, the annual mean wind speed is 8.5 m s^{-1} , which is lower than in the North Atlantic (9 m s^{-1}), and the range of seasonal changes in the air–sea CO_2 fluxes are from -0.05 to $+0.05 \text{ Pg C yr}^{-1}$ with the difference between parameterizations being lower than in the North Atlantic (Le Quéré et al., 2007; Takahashi et al., 2009). Takahashi et al. (2009) also indicate that the air–sea CO_2 flux difference in the Southern Ocean is strongly dependent on the choice of the gas-transfer parameterizations and wind speed. Smaller differences in the North Atlantic Ocean than in the global ocean are surprising, given that at least some of the older parameterizations (e.g. W2009 or WMcG1999) were developed using a smaller range of winds than what occurs in the North Atlantic. There may be two reasons for this. First, when comparing quadratic and cubic parameterizations (Fig. 9), the cubic parameterization implies higher air–sea fluxes for high winds, whereas the quadratic ones lead to higher fluxes for weaker winds. This difference can be presented in arithmetic terms. Let us assume two func-

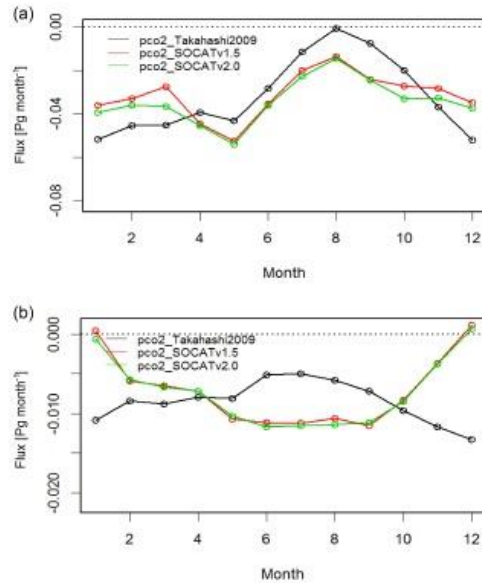


Figure 8. Comparison of monthly air-sea CO₂ fluxes calculated with different pCO₂ data sets (Takahashi et al., 2009; SOCAT v1.5 and v2.0) using the same k parameterization (Nightingale et al., 2000): (a) the North Atlantic, (b) the European Arctic.

tions of wind speed U , $F_1(U)$ quadratic and $F_2(U)$ cubic:

$$F_1(U) = aU^2, \quad (9)$$

$$F_2(U) = bU^3. \quad (10)$$

The difference between the two functions ΔF is equal to

$$\begin{aligned} \Delta F &= F_2 - F_1 = bU^3 - aU^2 \\ &= bU^2(U - ab^{-1}) = bU^2(U - U_x), \end{aligned} \quad (11)$$

where $U_x = ab^{-1}$. The difference is positive for wind speeds greater than U_x and negative for winds less than U_x . U_x is the value of wind speed for which the two functions intersect. In the case of Eqs. (6) and (7), where $a = 0.251$ and $b = 0.0283$, they imply that $U_x = 8.87 \text{ m s}^{-1}$. In fact all of the functions presented in Fig. 9 produce very similar values for U_x , all of which are close to 9 m s^{-1} . This value is very close to average wind speed in the North Atlantic (Fig. 4). This is one of the reasons for the small relative difference in net air-sea fluxes. The spread of flux values for the Southern Ocean seems to support this conclusion, being larger than that in the North Atlantic. The Southern Ocean has on average stronger winds than the North Atlantic (including also the Arctic seas), which seems to have the smallest spread of flux values for different parameterizations. The other reason

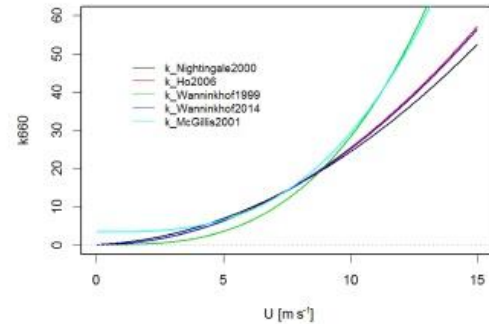


Figure 9. Different k_{660} parameterizations as a function of wind speed.

of smaller relative differences between the parameterizations in the North Atlantic than in the global ocean is the lack of seasonal variation in the sign of the air-sea flux. In the case of seasonal changes in the air-sea flux direction (caused by seasonal changes in water temperature or primary productivity), with winds stronger than U_x in some seasons and weaker in others (usually strong winds in winter and weak in summer), the fluxes partly cancel each other. The difference between cubic and quadratic parameterizations adds to each other due to simultaneous changes in the sign of both fluxes itself and the $U - U_x$ term. This effect of seasonal variation has been suggested to us based on available observations (A. Watson, University of Exeter, personal communication, 2015) but we are unaware of any paper investigating it or even describing it explicitly.

In addition to the five parameterizations described above, we calculated the air-sea fluxes using the OceanFlux GHG Evolution combined formula, which is based on knowledge that air-sea exchange is enhanced by air-entraining wave breaking and bubble-mediated transfer, especially for the less soluble gases than CO₂. Goddijn-Murphy et al. (2016) assume a linear wind relationship for dimethyl sulphide (DMS) and an additional bubble-mediated term for less soluble gases, parameterized with whitecap coverage. The resulting air-sea fluxes are higher in absolute terms, than all of the quadratic functions considered in this study, and are closer in value to cubic parameterization. This may mean that the bubble-mediated term of Fangohr and Woolf (2007) is overestimating the bubble component, implying the need for a dedicated calibration effort. This question will be the subject of further studies in the OceanFlux GHG Evolution project.

Using both Takahashi et al. (2009) climatology and SOCAT data sets (Fig. 8) results in similar annual net air-sea CO₂ fluxes in the North Atlantic; however it should be noted that they show different seasonal variations. This may have been caused by slightly different time periods of the data sets, as the SOCAT-based data set contains more recent data. It

should be noted that a significant part of the data from Takahashi et al. (2009) are included in SOCAT; therefore, the differences in the European Arctic may be due to the sparse data coverage and possible interpolation artefacts (Goddijn-Murphy et al., 2015) or to processing of the data through the FluxEngine. A recent paper (Couldrey et al., 2016) using even more high latitude data than were available in the SOCAT v1.5 and v2.0, which we used, shows a similar seasonal pattern to SOCAT. Still, this discrepancy makes us treat the net air–sea CO₂ fluxes results from the Arctic with much less confidence than the values for the whole North Atlantic. It is impossible to decide in this study which data set is more accurate as only new data can settle this. However, new data, not included in the SOCAT versions we used, have been available due to the recent analysis by Yasunaka et al. (2016). The observed *p*CO₂ data (Fig. 4 in Yasunaka et al., 2016), especially since 2005, have clearly shown an annual cycle compatible with the SOCAT seasonal flux variability.

5 Conclusions

In this paper we have studied the effect of the choice of gas-transfer velocity parameterization on the net CO₂ air–sea gas fluxes in the North Atlantic and the European Arctic using the recently developed FluxEngine software. The results show that the uncertainty caused by the choice of the *k* formula is smaller in the North Atlantic and in the Arctic than it is globally. The difference in the annual net air–sea CO₂ fluxes caused by the choice of the parameterization is 5 % in the North Atlantic and 4 % in the European Arctic, compared to 9 % globally for the studied functions with quadratic wind dependence. It is up to 46 % different for the North Atlantic, 36 % for the Arctic and 65 % globally when comparing cubic and quadratic functions. In both cases the uncertainty in the North Atlantic and the Arctic regions are smaller than the global case. We explain the smaller North Atlantic variability to be a combination of, first, higher than global average wind speeds in the North Atlantic, close to 9 m s^{−1}, which is the wind speed at which most *k* parameterization have similar values, and, second, the all-season CO₂ sink conditions in most North Atlantic areas. We repeated the analysis using Takahashi et al. (2009) and SOCAT *p*CO₂-derived climatology and find that although the seasonal variability in the North Atlantic is different the annual net air–sea CO₂ fluxes are within 8 % in the North Atlantic and 19 % in the European Arctic. The seasonal flux calculated from the two *p*CO₂ data sets in the Arctic have inverse seasonal variations, indicating possible under sampling (aliasing) of the *p*CO₂ in this polar region and therefore highlighting the need to collect more polar *p*CO₂ observations in all months and seasons.

6 Data availability

Several relevant data sets have been collected from various sources for the OceanFlux project. They have been processed in order to provide consistent and homogeneous composite files, on the same grid and temporal resolution, as well as multi-year climatologies. All these input and processed data sets are available in the OceanFlux FTP repository at <ftp://efp.ifremer.fr>. Some of these data sets are at present restricted to project partners for reasons related to the original provider distribution policy. Therefore the access to the FTP site is protected: any user interested in the data sets should send a request to the CERSAT help desk (fpaf@ifremer.fr) in order to get a login and password.

Acknowledgements. The publication has been financed from the funds of the Leading National Research Centre (KNOW) received by the Centre for Polar Studies for the period 2014–2018; OceanFlux Greenhouse Gases Evolution, a project funded by the European Space Agency, ESRIN contract no. 4000112091/14/LG; and GAME “Growing of Marine Arctic Ecosystem”, funded by Narodowe Centrum Nauki grant DEC-2012/04/A/NZ8/00661. We would also like to thank Jamie Shutler for important advice on the FluxEngine and for correcting the manuscript for English language. The authors are very grateful to those who have produced and made freely available the LDEO Flux Climatology base, FluxEngine software funded by European Space Agency, Surface Ocean CO₂ Atlas (SOCAT), GlobWave Project funded by European Space Agency, as well as Centre de Recherche et d’Exploitation Satellitaire (CERSAT) at IFREMER.

Edited by: M. Hoppema

Reviewed by: three anonymous referees

References

- Bakker, D. C. E., Pfeil, B., Smith, K., Hankin, S., Olsen, A., Alin, S. R., Cosca, C., Harasawa, S., Kozyr, A., Nojiri, Y., O’Brien, K. M., Schuster, U., Telszewski, M., Tilbrook, B., Wada, C., Akl, J., Barbero, L., Bates, N. R., Boutin, J., Bozec, Y., Cai, W.-J., Castle, R. D., Chavez, F. P., Chen, L., Chierici, M., Currie, K., de Baar, H. J. W., Evans, W., Feely, R. A., Fransson, A., Gao, Z., Hales, B., Hardman-Mountford, N. J., Hoppema, M., Huang, W.-J., Hunt, C. W., Huss, B., Ichikawa, T., Johannessen, T., Jones, E. M., Jones, S. D., Jutterström, S., Kitidis, V., Körtzinger, A., Landschützer, P., Lauvset, S. K., Lefèvre, N., Manke, A. B., Mathis, J. T., Merlivat, L., Metzl, N., Murata, A., Newberger, T., Omar, A. M., Ono, T., Park, G.-H., Pateron, K., Pierrot, D., Ríos, A. F., Sabine, C. L., Saito, S., Salisbury, J., Sarma, V. V. S. S., Schlitzer, R., Sieger, R., Skjelvan, I., Steinhoff, T., Sullivan, K. F., Sun, H., Sutton, A. J., Suzuki, T., Sweeney, C., Takahashi, T., Tjiputra, J., Tsurushima, N., van Heuven, S. M. A. C., Vandemark, D., Vlahos, P., Wallace, D. W. R., Wanninkhof, R., and Watson, A. J.: An update to the Surface Ocean CO₂ Atlas (SOCAT version 2), *Earth Syst. Sci. Data*, 6, 69–90, doi:10.5194/essd-6-69-2014, 2014.

- Couldrey, M. P., Oliver, K. I. C., Yool, A., Halloran, P. R., and Achterberg, E. P.: On which timescale do gas transfer velocities control North Atlantic CO₂ flux variability?, *Global Biogeochem. Cy.*, 30, 787–802, doi:10.1002/2015GB005267, 2016.
- Fangohr, S. and Woolf, D. K.: Application of new parameterizations of gas transfer velocity and their impact on regional and global marine CO₂ budgets, *J. Marine Syst.*, 66, 195–203, doi:10.1016/j.jmarsys.2006.01.012, 2007.
- Garbe, C. S., Rutgersson, A., Boutin, J., de Leeuw, G., Delille, B., Fairall, C. W., Gruber, N., Hare, J., Ho, D. T., Johnson, M. T., Nightingale, P. D., Pettersson, H., Piskozub, J., Sahlée, E., Tsai, W., Ward, B., Woolf, D. K., and Zappa, C. J.: Transfer across the air-sea interface, in: *Ocean-atmosphere interactions of gases and particles*, edited by: Liss, P. S. and Johnson, M. T., *Earth Sys. Sci.*, Springer, Berlin, Heidelberg, 55–111, 2014.
- Goddijn-Murphy, L., Woolf, D. K., and Callaghan, A. H.: Parameterizations and algorithms for oceanic whitecap coverage, *J. Phys. Oceanogr.*, 41, 742–756, doi:10.1175/2010JPO4533.1, 2011.
- Goddijn-Murphy, L. M., Woolf, D. K., and Marandino, C.: Space-based retrievals of air-sea gas transfer velocities using altimeters: Calibration for dimethyl sulfide, *J. Geophys. Res.*, 117, C08028, doi:10.1029/2011JC007535, 2012.
- Goddijn-Murphy, L. M., Woolf, D. K., Land, P. E., Shutler, J. D., and Donlon, C.: The OceanFlux Greenhouse Gases methodology for deriving a sea surface climatology of CO₂ fugacity in support of air-sea gas flux studies, *Ocean Sci.*, 11, 519–541, doi:10.5194/os-11-519-2015, 2015.
- Goddijn-Murphy, L., Woolf, D. K., Callaghan, A. H., Nightingale, P. D., and Shutler, J. D.: A reconciliation of empirical and mechanistic models of the air-sea gas transfer velocity, *J. Geophys. Res.-Oceans*, 121, 818–835, doi:10.1002/2015JC011096, 2016.
- González-Dávila, M., Santana-Casiano, J. M., and González-Dávila, E. F.: Interannual variability of the upper ocean carbon cycle in the northeast Atlantic Ocean, *Geophys. Res. Lett.*, 34, L07608, doi:10.1029/2006GL028145, 2007.
- Gregg, W. W., Casey, N. W., and Rosseaux, C. S.: Sensitivity of simulated global ocean carbon flux estimates to forcing by reanalysis products, *Ocean Model.*, 80, 24–35, doi:10.1016/j.ocemod.2014.05.002, 2014.
- Gruber, N.: Carbon cycle: Fickle trends in the ocean, *Nature*, 458, 155–156, doi:10.1038/458155a, 2009.
- Halloran, P. R., Booth, B. B. B., Jones, C. D., Lambert, F. H., McNeall, D. J., Totterdell, I. J., and Völker, C.: The mechanisms of North Atlantic CO₂ uptake in a large Earth System Model ensemble, *Biogeosciences*, 12, 4497–4508, doi:10.5194/bg-12-4497-2015, 2015.
- Ho, D. T., Law, C. S., Smith, M. J., Schlosser, P., Harvey, M., and Hill, P.: Measurements of air-sea gas exchange at high wind speeds in the Southern Ocean: Implications for global parameterizations, *Geophys. Res. Lett.*, 33, 16611, doi:10.1029/2006GL026817, 2006.
- Landschützer, P., Gruber, N., Bakker, D. C. E., Schuster, U., Nakaoka, S., Payne, M. R., Sasse, T. P., and Zeng, J.: A neural network-based estimate of the seasonal to inter-annual variability of the Atlantic Ocean carbon sink, *Biogeosciences*, 10, 7793–7815, doi:10.5194/bg-10-7793-2013, 2013.
- Landschützer, P., Gruber, N., Bakker, D. C. E., and Schuster, U.: Recent variability of the global ocean carbon sink, *Global Biogeochem. Cy.*, 28, 927–949, doi:10.1002/2014GB004853, 2014.
- Le Quéré, C., Rödenbeck, C., Buitenhuis, E. T., Conway, T. J., Langenfelds, R., Gomez, A., Labuschagne, C., Ramonet, M., Nakazawa, T., Metzl, N., Gillett, N., and Heimann, M.: Saturation of the Southern Ocean CO₂ sink due to recent climate change, *Science*, 316, 1735–1738, doi:10.1126/science.1136188, 2007.
- Le Quéré, C., Moriarty, R., Andrew, R. M., Peters, G. P., Ciais, P., Friedlingstein, P., Jones, S. D., Sitch, S., Tans, P., Arneeth, A., Boden, T. A., Bopp, L., Bozec, Y., Canadell, J. G., Chini, L. P., Chevallier, F., Cosca, C. E., Harris, I., Hoppema, M., Houghton, R. A., House, J. I., Jain, A. K., Johannessen, T., Kato, E., Keeling, R. F., Kitidis, V., Klein Goldewijk, K., Koven, C., Landa, C. S., Landschützer, P., Lenton, A., Lima, I. D., Marland, G., Mathis, J. T., Metzl, N., Nojiri, Y., Olsen, A., Ono, T., Peng, S., Peters, W., Pfeil, B., Poulter, B., Raupach, M. R., Regnier, P., Rödenbeck, C., Saito, S., Salisbury, J. E., Schuster, U., Schwinger, J., Séférian, R., Segsneider, J., Steinhoff, T., Stocker, B. D., Sutton, A. J., Takahashi, T., Tilbrook, B., van der Werf, G. R., Viovy, N., Wang, Y.-P., Wanninkhof, R., Wiltshire, A., and Zeng, N.: Global carbon budget 2014, *Earth Syst. Sci. Data*, 7, 47–85, doi:10.5194/essd-7-47-2015, 2015.
- Lefèvre, N., Watson, A. J., Olsen, A., Rios, A. F., Perez, F. F., and Johannessen, T.: A decrease in the sink for atmospheric CO₂ in the North Atlantic, *Geophys. Res. Lett.*, 31, L07306, doi:10.1029/2003GL018957, 2004.
- McGillis, W. R. and Edson, J. B.: Hare, J. E., Fairall, C. W.: Direct covariance air-sea CO₂ fluxes, *J. Geophys. Res.*, 106, 16729–16745, 2001.
- Merchant, C. M., Embury, O., Rayner, N. A., Berry, D. I., Corlett, G. K., Lean, K., Veal, K. L., Kent, E. C., Llewellyn-Jones, D. T., Remedios, J. J., and Saunders, R.: A 20 year independent record of sea surface temperature for climate from Along-Track Scanning Radiometers, *J. Geophys. Res.*, 117, C12, doi:10.1029/2012JC008400, 2012.
- Nightingale, P. D., Malin, G., Law, C. S., Watson, A. J., Liss, P. S., Liddicoat, M. I., Boutin, J., and Upstill-Goddard, R. C.: In situ evaluation of air-sea gas exchange parameterizations using novel conservative and volatile tracers, *Global Biogeochem. Cy.*, 14, 373–387, 2000.
- Nightingale, P. D.: Relationship between wind speed and gas exchange over the ocean: which parameterisation should I use? Report from Discussion Session at SOLAS Open Science conference in Kiel, available at: <http://goo.gl/TrMQkg> (last access: 12 August 2016), 2015.
- Orr, J. C., Maier-Reimer, E., Mikolajewicz, U., Monfray, P., Sarmiento, J. L., Toggweiler, J. R., Taylor, N. K., Palmer, J., Gruber, N., Sabine, C. L., Le Quéré, C., Key, R. M., and Boutin, J.: Estimates of anthropogenic carbon uptake from four three-dimensional global ocean models, *Global Biogeochem. Cy.*, 15, 43–60, doi:10.1029/2000GB001273, 2001.
- Pérez, F. F., Mercier, H., Vázquez-Rodríguez, M., Lherminier, P., Velo, A., Pardo, P. C., Rosón, G., and Ríos, A. F.: Atlantic Ocean CO₂ uptake reduced by weakening of the meridional overturning circulation, *Nat. Geosci.*, 6, 146–152, doi:10.1038/NGEO1680, 2013.

- Pfeil, B., Olsen, A., Bakker, D. C. E., Hankin, S., Koyuk, H., Kozyr, A., Malczyk, J., Manke, A., Metzl, N., Sabine, C. L., Akl, J., Alin, S. R., Bates, N., Bellerby, R. G. J., Borges, A., Boutin, J., Brown, P. J., Cai, W.-J., Chavez, F. P., Chen, A., Cosca, C., Fassbender, A. J., Feely, R. A., González-Dávila, M., Goyet, C., Hales, B., Hardman-Mountford, N., Heinze, C., Hood, M., Hoppema, M., Hunt, C. W., Hydes, D., Ishii, M., Johannessen, T., Jones, S. D., Key, R. M., Körtzinger, A., Landschützer, P., Lauvset, S. K., Lefèvre, N., Lenton, A., Laurantou, A., Merlivat, L., Midorikawa, T., Mintrop, L., Miyazaki, C., Murata, A., Nakadate, A., Nakano, Y., Nakaoka, S., Nojiri, Y., Omar, A. M., Padin, X. A., Park, G.-H., Paterson, K., Perez, F. F., Pierrot, D., Poisson, A., Rios, A. F., Santana-Casiano, J. M., Salisbury, J., Sarma, V. V. S. S., Schlitzer, R., Schneider, B., Schuster, U., Sieger, R., Skjelvan, I., Steinhoff, T., Suzuki, T., Takahashi, T., Tedesco, K., Telszewski, M., Thomas, H., Tilbrook, B., Tjiputra, J., Vandemark, D., Veness, T., Wanninkhof, R., Watson, A. J., Weiss, R., Wong, C. S., and Yoshikawa-Inoue, H.: A uniform, quality controlled Surface Ocean CO₂ Atlas (SOCAT). *Earth Syst. Sci. Data*, 5, 125–143, doi:10.5194/essd-5-125-2013, 2013.
- Sabine, C. L., Hankin, S., Kozyr, H., Bakker, D. C. E., Pfeil, B., Olsen, A., Metzl, N., Kozyr, A., Fassbender, A., Manke, A., Malczyk, J., Akl, J., Alin, S. R., Bellerby, R. G. J., Borges, A., Boutin, J., Brown, P. J., Cai, W.-J., Chavez, F. P., Chen, A., Cosca, C., Feely, R. A., González-Dávila, M., Goyet, C., Hardman-Mountford, N., Heinze, C., Hoppema, M., Hunt, C. W., Hydes, D., Ishii, M., Johannessen, T., Key, R. M., Körtzinger, A., Landschützer, P., Lauvset, S. K., Lefèvre, N., Lenton, A., Laurantou, A., Merlivat, L., Midorikawa, T., Mintrop, L., Miyazaki, C., Murata, A., Nakadate, A., Nakano, Y., Nakaoka, S., Nojiri, Y., Omar, A. M., Padin, X. A., Park, G.-H., Paterson, K., Perez, F. F., Pierrot, D., Poisson, A., Rios, A. F., Salisbury, J., Santana-Casiano, J. M., Sarma, V. V. S. S., Schlitzer, R., Schneider, B., Schuster, U., Sieger, R., Skjelvan, I., Steinhoff, T., Suzuki, T., Takahashi, T., Tedesco, K., Telszewski, M., Thomas, H., Tilbrook, B., Vandemark, D., Veness, T., Watson, A. J., Weiss, R., Wong, C. S., and Yoshikawa-Inoue, H.: Surface Ocean CO₂ Atlas (SOCAT) gridded data products, *Earth Syst. Sci. Data*, 5, 145–153, doi:10.5194/essd-5-145-2013, 2013.
- Schuster, U. and Watson, A. J.: A variable and decreasing sink for atmospheric CO₂ in the North Atlantic, *J. Geophys. Res.*, 112, C11006, doi:10.1029/2006JC003941, 2007.
- Schuster, U., McKinley, G. A., Bates, N., Chevallier, F., Doney, S. C., Fay, A. R., González-Dávila, M., Gruber, N., Jones, S., Krijnen, J., Landschützer, P., Lefèvre, N., Manizza, M., Mathis, J., Metzl, N., Olsen, A., Rios, A. F., Rödenbeck, C., Santana-Casiano, J. M., Takahashi, T., Wanninkhof, R., and Watson, A. J.: An assessment of the Atlantic and Arctic sea-air CO₂ fluxes, 1990–2009, *Biogeosciences*, 10, 607–627, doi:10.5194/bg-10-607-2013, 2013.
- Shutler, J. D., Piolle, J.-F., Land, P. E., Woolf, D. K., Goddijn-Murphy, L., Paul, F., Girard-Ardhuin, F., Chapron, B., and Donlon, C. J.: FluxEngine: a flexible processing system for calculating air-sea carbon dioxide gas fluxes and climatologies, *J. Atmos. Ocean. Technol.*, 33, 741–756, doi:10.1175/JTECH-D-14-00204.1, 2016.
- Sweeney, C., Gloor, E., Jacobson, A. R., Key, R. M., McKinley, G., Sarmiento, J. L., and Wanninkhof, R.: Constraining global air-sea gas exchange for CO₂ with recent bomb ¹⁴C measurements, *Global Biogeochem. Cy.*, 21, doi:10.1029/2006GB002784, 2007.
- Takahashi, T., Sutherland, S. C., Sweeney, C., Poisson, A., Metzl, N., Tilbrook, B., Bates, N., Wanninkhof, R., Feely, R. A., Sabine, C., Olafsson, J., and Nojiri, Y.: Global sea-air CO₂ flux based on climatological surface ocean pCO₂, and seasonal biological and temperature effects, *Deep-Sea Res. Pt. II*, 49, 1601–1622, 2002.
- Takahashi, T., Sutherland, S. C., Wanninkhof, R., Sweeney, C., Feely, R. A., Chipman, D. W., Hales, B., Friederich, G., Chavez, F., Sabine, C., Watson, A., Bakker, D. C. E., Schuster, U., Metzl, N., Yoshikawa-Inoue, H., Ishii, M., Midorikawa, T., Nojiri, Y., Körtzinger, A., Steinhoff, T., Hoppema, M., Olafsson, J., Arnarson, T. S., Tilbrook, B., Johannessen, T., Olsen, A., Bellerby, R., Wong, C. S., Delille, B., Bates, N. R., and de Baar, H. J. W.: Climatological mean and decadal change in surface ocean pCO₂ and net sea-air CO₂ flux over the global oceans, *Deep-Sea Res. Pt. II*, 56, 554–577, doi:10.1016/j.dsr2.2008.12.009, 2009.
- Talley, L. D.: Closure of the global overturning circulation through the Indian, Pacific, and Southern Oceans: schematics and transports, *Oceanography*, 26, 80–97, doi:10.5670/oceanog.2013.07, 2013.
- Thomas, H., Friederike Prowe, A. E., Lima, I. D., Doney, S. C., Wanninkhof, R., Greatbatch, R. J., Schuster, U., and Corbière, A.: Changes in the North Atlantic Oscillation influence CO₂ uptake in the North Atlantic over the past 2 decades, *Global Biogeochem. Cy.*, 22, GB4027, doi:10.1029/2007GB003167, 2008.
- Wanninkhof, R.: Relationship between wind speed and gas exchange over the ocean revisited, *Limnol. Oceanogr.-Meth.*, 12, 351–362, doi:10.4319/lom.2014.12.351, 2014.
- Wanninkhof, R. and McGillis, W. R.: A cubic relationship between air-sea CO₂ exchange and wind speed, *Geophys. Res. Lett.*, 26, 1889–1892, 1999.
- Wanninkhof, R., Park, G.-H., Takahashi, T., Sweeney, C., Feely, R., Nojiri, Y., Gruber, N., Doney, S. C., McKinley, G. A., Lenton, A., Le Quééré, C., Heinze, C., Schwinger, J., Graven, H., and Khaliwala, S.: Global ocean carbon uptake: magnitude, variability and trends, *Biogeosciences*, 10, 1983–2000, doi:10.5194/bg-10-1983-2013, 2013.
- Watson, A. J., Schuster, U., Bakker, D. C. E., Bates, N. R., Corbière, A., González-Dávila, M., Friedrich, T., Hauck, J., Heinze, C., Johannessen, T., Körtzinger, A., Metzl, N., Olafsson, J., Olsen, A., Oschlies, A., Padin, X. A., Pfeil, B., Santana-Casiano, J. M., Steinhoff, T., Telszewski, M., Rios, A. F., Wallace, D. W., and Wanninkhof, R.: Tracking the variable North Atlantic sink for atmospheric CO₂, *Science*, 326, 1391–1393, doi:10.1126/science.1177394, 2009.
- Watson, A. J., Metzl, N., and Schuster, U.: Monitoring and interpreting the ocean uptake of atmospheric CO₂, *Philos. T. R. Soc. A*, 369, 1997–2008, doi:10.1098/rsta.2011.0060, 2011.
- Woolf, D. K.: Parameterization of gas transfer velocities and sea-state dependent wave breaking, *Tellus B*, 57, 87–94, 2005.
- Yasunaka, S., Murata, A., Watanabe, E., Chierici, M., Fransson, A., van Heuven, S., Hoppema, M., Ishii, M., Johannessen, T., Kosugi, N., Lauvset, S. K., Mathis, J. T., Nishino, S., Omar, A. M., Olsen, A., Sasano, D., Takahashi, T., and Wanninkhof, R.: Mapping of the air-sea CO₂ flux in the Arctic Ocean and its adjacent seas: Basin-wide distribution and seasonal to interannual variability, *Polar Sci.*, doi:10.1016/j.polar.2016.03.006, 2016.

2. Research paper no 2

Wróbel, I. 2017. *Monthly dynamics of carbon dioxide exchange across the sea surface of the Arctic Ocean in response to changes in gas transfer velocity and partial pressure of CO₂ in 2010*. Oceanologia, 59, 445-459, doi:10.1016/j.oceano.2017.05.00



ORIGINAL RESEARCH ARTICLE

Monthly dynamics of carbon dioxide exchange across the sea surface of the Arctic Ocean in response to changes in gas transfer velocity and partial pressure of CO₂ in 2010

Iwona Wrobel*

Institute of Oceanology, Polish Academy of Sciences, Sopot, Poland

Received 5 July 2016; accepted 17 May 2017

Available online 7 June 2017

KEYWORDS

Partial pressure of CO₂;
Gas transfer velocity;
Arctic fjord;
Air–sea CO₂ fluxes;
Greenland and Barents seas

Summary The Arctic Ocean (AO) is an important basin for global oceanic carbon dioxide (CO₂) uptake, but the mechanisms controlling air–sea gas fluxes are not fully understood, especially over short and long timescales. The oceanic sink of CO₂ is an important part of the global carbon budget. Previous studies have shown that in the AO differences in the partial pressure of CO₂ ($\Delta p\text{CO}_2$) and gas transfer velocity (k) both contribute significantly to interannual air–sea CO₂ flux variability, but that k is unimportant for multidecadal variability. This study combined Earth Observation (EO) data collected in 2010 with the in situ $p\text{CO}_2$ dataset from Takahashi et al. (2009) (T09) using a recently developed software toolbox called FluxEngine to determine the importance of k and $\Delta p\text{CO}_2$ on CO₂ budgets in two regions of the AO – the Greenland Sea (GS) and the Barents Sea (BS) with their continental margins. Results from the study indicate that the variability in wind speed and, hence, the gas transfer velocity, generally play a major role in determining the temporal variability of CO₂ uptake, while variability in monthly $\Delta p\text{CO}_2$ plays a major role spatially, with some exceptions.

© 2017 Institute of Oceanology of the Polish Academy of Sciences. Production and hosting by Elsevier Sp. z o.o. This is an open access article under the CC BY-NC-ND license (<http://creativecommons.org/licenses/by-nc-nd/4.0/>).

* Correspondence address: Institute of Oceanology Polish Academy of Sciences, Powstańców Warszawy 55, 81-712 Sopot, Poland.

Tel.: +48 587311801.

E-mail address: iwrobel@iopan.gda.pl.

Peer review under the responsibility of Institute of Oceanology of the Polish Academy of Sciences.



Production and hosting by Elsevier

<http://dx.doi.org/10.1016/j.oceano.2017.05.001>

0078-3234/© 2017 Institute of Oceanology of the Polish Academy of Sciences. Production and hosting by Elsevier Sp. z o.o. This is an open access article under the CC BY-NC-ND license (<http://creativecommons.org/licenses/by-nc-nd/4.0/>).

1. Introduction

The global carbon cycle plays an important role in energy and mass exchange in the Earth System and links the components of this system (land, ocean, atmosphere) (Garbe et al., 2014; Thomas et al., 2004). Increases in atmospheric carbon dioxide (CO_2) concentrations caused mainly by the burning fossil fuels, cement production and growing urbanization are directly responsible for 60% of the average global air temperature increase (IPCC, 2013; Kulinski and Pempkowiak, 2011). Half of the CO_2 emitted remains in the atmosphere while the rest is absorbed by the oceans and land biomass (Le Quéré et al., 2010, 2016; Omar et al., 2003; Sabine et al., 2004; Yasunaka et al., 2016). Relevant knowledge of air–sea CO_2 fluxes and their spatial and temporal variability is essential to gain the necessary understanding of the global carbon cycle and to fully resolve the ocean's role in climate variability (Le Quéré et al., 2013; Wanninkhof et al., 2009; Woolf et al., 2013). It is well known that the Arctic Ocean (AO) is an overall sink for CO_2 throughout the year even though continental shelves can either be regional or seasonal sinks or sources of atmospheric CO_2 . However, there is a lot of uncertainty in calculating the CO_2 budgets of marginal and coastal shelf seas especially in the Polar Ocean margins (Cai et al., 2006; Doney et al., 2009; Landschützer et al., 2014). At present, the net air–sea CO_2 fluxes in the AO have been estimated at $-0.12 \pm 0.06 \text{ PgC yr}^{-1}$ with net global ocean CO_2 uptake at $-2.2 \pm 0.5 \text{ PgC yr}^{-1}$ (Goddijn-Murphy et al., 2015; Gruber, 2009; Schuster et al., 2013; Takahashi et al., 2009; Wanninkhof et al., 2013). Additionally, Cai et al. (2006) have shown that the average sea–air CO_2 flux for Arctic shelves is estimated as $-12 \pm 4 \text{ gC m}^{-2} \text{ a}^{-1}$. Arctic shelves are greatly influenced by sea ice cover and the age of terrestrial inputs resulting in large CO_2 sinks during ice-free periods (Bates and Mathis, 2009; Cai et al., 2006).

Projections of trends in net carbon dioxide air–sea fluxes suggest that, in the future, CO_2 uptake by the ocean will increase because of sea ice loss (IPCC, 2013; Rödenbeck, 2005; Schuster et al., 2013). Reports have also been published, indicating that the seawater partial pressure of CO_2 ($p\text{CO}_{2w}$) in the North Atlantic has increased at a rate higher than the atmospheric $p\text{CO}_2$ ($p\text{CO}_{2a}$) (Lefèvre et al., 2004; Olsen et al., 2003).

Currently, there are several different approaches for estimating air–sea CO_2 fluxes. The first involves measuring direct fluxes using eddy correlation techniques (Else et al., 2011; Kondo and Tsukamoto, 2012; Repina et al., 2007). Another method focuses on calculating net air–sea CO_2 exchange with a mass balance assessment of carbon stocks and the inputs/outputs of carbon or vertical variations in DIC (Dissolved Inorganic Carbon) (Arrigo et al., 2010; MacGilchrist et al., 2014). The third approach takes into account differences in atmospheric and seawater $p\text{CO}_2$ combined with gas transfer velocity parameterizations (k) (Bates and Mathis, 2009; Boutin et al., 2002; Land et al., 2013; Landschützer et al., 2014; Takahashi et al., 2009). This final approach can employ the neural network technique, the advantage of which is that it can “notice” and exploit unpredicted correlations in the data (Lefèvre et al., 2005; Telszewski et al., 2009; Yasunaka et al., 2016).

In this article, the net CO_2 flux across the sea surface is calculated by multiplying $\Delta p\text{CO}_2$ by the CO_2 gas transfer

velocity coefficient (k), which depends primarily on the degree of turbulence near the interface. The direction and rates of net air–sea CO_2 exchange are determined by the product of the difference in values between $p\text{CO}_2$ in seawater and the atmosphere, and also by the rate of k . Positive $\Delta p\text{CO}_2$ values indicate that the sea is a source of atmospheric carbon dioxide, whereas negative values indicate that it is a sink. Choosing the appropriate formula for gas transfer velocity is the key when calculating net air–sea gas fluxes. The main difficulty in quantifying k is its dependence on several physicochemical elements of the environment, such as surfactants, wind speed, sea state, surface roughness and breaking waves (Ho et al., 2006; McGillis et al., 2001; Shutler et al., 2016; Takahashi et al., 2009; Wanninkhof et al., 2009). In the literature, a wide range of different gas transfer parameterizations can be found that were derived using a number of techniques, e.g., Wanninkhof and McGillis (1999), Nightingale et al. (2000), McGillis et al. (2001), Ho et al. (2006), and Wanninkhof et al. (2013). At present, parameterizations with a quadratic wind speed relationship are interchangeable in the Arctic as Wrobel and Piskozub (2016) have shown. Fluxes resulting from using these functions (Ho et al., 2006; Wanninkhof et al., 2013) are only 3–4% higher (Fig. 1), respectively, than the most accurate parameterization applied to the study region, which is Nightingale et al. (2000) (see also Wrobel and Piskozub, 2016). Earlier studies showed that over interannual and shorter timescales, both components of the right hand side of Eq. (1) are significant in controlling air–sea fluxes, with only a few exceptions (Couldrey et al., 2016; Doney et al., 2009). Over longer, interannual to multidecadal timescales, flux variability is controlled only by $\Delta p\text{CO}_2$ (Bates, 2012; Couldrey et al., 2016; Doney et al., 2009; Gruber et al., 2003; Le Quéré et al., 2000). The high uncertainty in the size of the net AO sink stems from the lack of coordinated in situ measurements in the winter; data are interpolated for the rest of the year. A potential alternative solution lies in exploiting satellite data from EO techniques (Boutin et al., 2002).

When studying air–sea CO_2 exchange across the sea surface in the AO, one has to remember the important role of extensive ice coverage in this process. Because of this, the monthly dynamics of air–sea interactions were analyzed in this paper during a one year period. Seasonal sea ice cover can reduce the exchange of CO_2 across the sea surface, but it

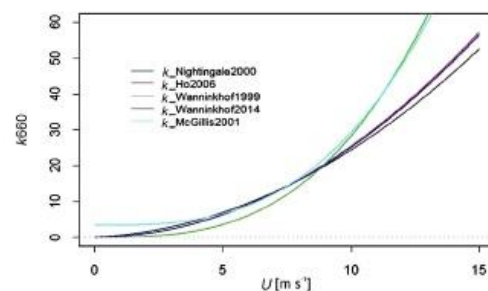


Figure 1 Gas transfer velocity [m s^{-1}] using different parameterizations as a function of wind speed [m s^{-1}].

also influences biogeochemical processes in surface water, especially inside Arctic fjords. The decrease of sea ice cover can result in an increase in outgassing in shallow shelf areas when surface waters are mixed deeper during the spring and winter. As was demonstrated in earlier studies by Olsen et al. (2003), Arrigo et al. (2008), Sejvar et al. (2011), and others, sea ice loss in the AO produces a large area of open, ice-free water that is favorable for phytoplankton growth. Thinner seasonal sea ice cover replaces thick multi-year sea ice which makes it a weaker barrier for sea ice exchange, which means that phytoplankton spring blooms can absorb more CO_2 (Arrigo et al., 2008). Decreases of sea ice extent also cause water surface warming and, thus, act to reduce the CO_2 uptake by the ocean (Bates and Mathis, 2009). We do not yet fully understand whether decreased sea ice extent will indirectly affect higher CO_2 uptake by the ocean in the Arctic or not.

Trends and variability in the Arctic CO_2 sink have been studied intensively. Observations suggest its decrease is caused by increased in-water $p\text{CO}_2$ (Ashton et al., 2016; Boutin et al., 2002; Goddijn-Murphy et al., 2016; Lefèvre et al., 2004; MacGilchrist et al., 2014; Schuster et al., 2013). Marine $p\text{CO}_2$ seems to have been rising faster than atmospheric $p\text{CO}_2$, especially in the summer (Couldrey et al., 2016). The results from the FluxEngine-based Earth Observation (EO) data obtained from the European Space Agency OceanFlux Greenhouse Gases (GHG) Evolution project (<http://www.oceanflux-ghg.org/>) to evaluate how flux variability is controlled on short timescales. The present study examines the following testable hypothesis: air–sea CO_2 fluxes on a one year timeframe are dependent on both $\Delta p\text{CO}_2$ and k .

1.1. Study area

The AO (Fig. 2) is relatively small ($\sim 10.7 \times 10^6 \text{ km}^2$), and belongs to a class of ocean basins known as Mediterranean seas, with broad, shallow (<200 m deep) continental shelves surrounding a central basin. The AO has limited pathways of communication with Atlantic and Pacific waters, through the Bering Strait, the Canadian Archipelago, the Fram Strait and the Norwegian Sea gateways. Thermohaline forcing is the dominant driver (Piechura and Walczowski, 2009). Seasonal sea ice cover, especially in winter, reduces the exchange of energy, mass, and gases between the atmosphere and the

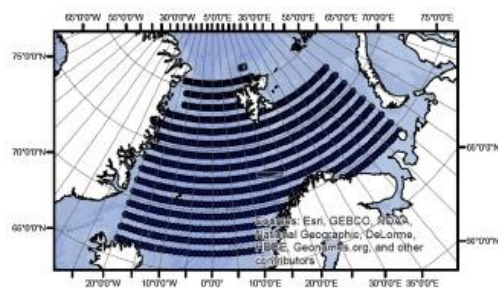


Figure 2 Study area (source: ArcGIS basemap) – Greenland Sea and Barents Sea with sampling points.

ocean, and it also has a negative effect on sunlight penetration into the ocean that is needed for photosynthesis. Whether the Arctic acts as a sink or a source of CO_2 is controlled by many variables that are, themselves, influenced by climate change, including biological activity (Arrigo et al., 2010), temperature (Polyakov et al., 2004), riverine inputs (Dai et al., 2009), and sea ice melt (Bates and Mathis, 2009).

The Barents Sea (BS) is the largest of the AO seas (1,424,000 km^2 area with a volume of about 316,000 km^3) and covers broad, shallow continental shelves with a maximum depth of $\sim 600 \text{ m}$ (average depth $\sim 229 \text{ m}$) (Gurgul, 2002). It is characterized by an inflow of warm, saline Atlantic water via the Norwegian Atlantic Current and minimal freshwater inputs (Omar et al., 2003). Maximum wind speeds over the BS are about 20 m s^{-1} , with an average of approximately 6 m s^{-1} (Gurgul, 2002). Warm, saline Atlantic water is transformed into subsurface water by the process of brine rejection from sea ice formation or the cooling of surface water, and it is then transported to the Kara Sea and the central basin of the AO (Omar et al., 2007).

The Greenland Sea (GS) covers an area of 1,205,000 km^2 with an average depth of 1450 m and a maximum depth of approximately 5500 m. It lies south of the Arctic Basin and is a major pathway for the exchange of Arctic water with warm, saline Atlantic water through the Fram Strait via the deep East Greenland Current. Greenland Sea Deep Water is formed in the central GS, and it aerates the North Atlantic Deep Water (Nakaoko et al., 2006).

2. Methods

2.1. Data sets

Net air–sea CO_2 fluxes were calculated using the FluxEngine toolset (Shutler et al., 2016), which was created as a part of the European Space Agency funded OceanFlux Greenhouse Gases project (<http://www.oceanflux-ghg.org/>) to encourage the use of satellite Earth Observation data. The toolbox allows its users to create their own climatology from the data available. After choosing the relevant data and formulae, users can create monthly global flux datasets. FluxEngine is available publicly on the Ifremer/CERSAT (Centre d'Exploitation et de Recherche Satellitaire) Nephelae Cloud (no specific skills are required to use it), and can be run through a web interface (<http://cersat.ifremer.fr/data/collections/oceanflux/>) or it can also be downloaded. The source code can be downloaded from a GitHub server (Goddijn-Murphy et al., 2015; Shutler et al., 2016; Wrobel and Piskozub, 2016).

The calculations for this study were based on the climatological mean distribution of surface water $p\text{CO}_2$ and salinity values from Takahashi et al. (2009) (T09) climatology, archived at the Carbon Dioxide Information and Analysis Centre (CDIAC, Oak Ridge, National Laboratory (Takahashi et al., 2008)) in non-El Niño conditions. T09 data were normalized to 2010 to evaluate seasonal variations in air–sea CO_2 fluxes (the calculations were based on Olsen et al. (2003), Omar et al. (2003), Nakaoko et al. (2006), Goddijn-Murphy et al. (2015) approaches, that assumed the partial CO_2 pressure in seawater has increased at a rate of $1.5 \mu\text{atm yr}^{-1}$, on average observed for CO_2 partial pressure

in the air). Wind speed data at 10 m a.s.l. were obtained from the GlobWave project (<http://globwave.ifremer.fr/>), which produced a 20-plus year time series of global coverage multi-sensor cross-calibrated wave and wind data. The Sea Surface Temperature (SST) data were obtained from Ifremer/CERSAT and produced OceanFlux from ARC/(A)ATRS (Advance Along Track Scanning Radiometer measurements) carried out by the Envisat satellite (Merchant et al., 2012). SST_{skin} data are defined as the “radiometric temperature of the surface measured by an infrared radiometer operating in the 1–12 μm waveband (10–20 μm depth” according to definition in The Global Ocean Data Assimilation Experiment (GODAE) high-resolution sea surface temperature pilot project; Minnett and Kaiser-Weiss, 2012). The (A)ATRS is a self-calibrating radiometer that provides estimates of SST and exhibits a very small standard deviation of error. The *k* coefficient was estimated using the Nightingale et al. (2000) parameterization (hereafter called N2000, Fig. 1), which best fits the AO (Wrobel and Piskozub, 2016). All input data and climatologies were linearly re-interpolated to a 1° × 1° geographical grid from the original resolution, and calculated for 2010 using the FluxEngine toolset. Data were extracted for the AO (north of 66°) from global resolution.

2.2. Parameterizations

The air–sea CO₂ flux is controlled by wind speed, SST, Sea Surface Salinity (SSS), sea state, and biological activity (Godijn-Murphy et al., 2016). The calculations of CO₂ flux between the air and the sea [*F*, mgC m^{−2} day^{−1}] are given based on the Δ*p*CO₂ [μatm] across a thin (~10–250 μm) mass boundary layer at the sea surface and the solubility of CO₂ [*α*, g m^{−3} μatm^{−1}] multiplied by the gas transfer velocity [*k*, cm h^{−1}] as a function of wind speed. The concentration of CO₂ in the sea water is a function of SSS and SST, its solubility [*α*, g m^{−3} μatm^{−1}], and its fugacity [*f*CO₂, μatm]. Hence, the standard bulk formula for the flux (*F*) was defined as:

$$F = k(\alpha_W pCO_{2W} - \alpha_S pCO_{2A}), \quad (1)$$

where *S* is the air–sea interface, *A* is the air, and *W* is water. We can replace fugacity with partial pressure (their values differ by < 0.5% over the temperature range considered) (McGillis et al., 2001). So Eq. (1) becomes:

$$F = k(\alpha_W pCO_{2W} - \alpha_S pCO_{2A}), \quad (2)$$

$$F = k\alpha\Delta pCO_2. \quad (3)$$

Gas transfer velocity was mainly parametrized as:

$$k_W = Sc^{-n}(a_0 + a_1U + a_2U^2 + a_3U^3), \quad (4)$$

(Wanninkhof et al., 2009) where (*a*₀...*a*_{*n*}) are coefficients (one or more of which may be set to zero) of polynomials in wind-speed *U* [m s^{−1}], *Sc* is the Schmidt number of dissolved gas. Schmidt numbers at the skin surface (*Sc*_{skin}) are a function of SST [= (kinematic viscosity of water)/(diffusion coefficient of CO₂ in water)]. The Schmidt number for CO₂ in seawater at 20 °C is equal to 660.0. The calculations were based on the Nightingale et al. (2000) parameterization:

$$k = \sqrt{(600.0/Sc_{skin}) * (0.222 U_{10}^2 + 0.333 U_{10})}. \quad (5)$$

The parameterization was based on multiple trace experiment conducted in the southern North Sea during one month in 1992 and 1993 and based on data from March and October 1989.

3. Results and discussion

The global monthly air–sea CO₂ flux variability, the partial pressure of CO₂ in seawater (*p*CO_{2W}), and gas transfer velocity rates (*k*) were estimated using FluxEngine software. Values were extracted from these for the two study regions – the GS and BS in the AO (north of 66°) (Fig. 2). The periods from October to April were defined as wintertime and from May to September as summertime. Since wind velocity was used to estimate *k*, Fig. 1 shows a wide range of empirical formulas. The N2000 quadratic dependence of *k* on wind speed, which fit the best to AO air–sea interaction measurements (Wrobel and Piskozub, 2016), was chosen for this study. In the AO where the average wind speed during the study period was approximately 8 ± 0.7 m s^{−1} (see Table 1), the average gas transfer velocity rate was 13.0 ± 1.9 cm h^{−1} (Fig. 1). For better proof of results, a statistical summary of the data was calculated (Table 1). The area, as a whole, is a sink of CO₂ with an annual average wind speed of approximately 8 ± 0.7 m s^{−1}, an annual average *k* of 13.0 ± 1.9 cm h^{−1}, and a concentration of *p*CO_{2W} (332.4 ± 11.8 μatm) lower than the annual partial pressure of CO₂ in the atmosphere for the year 2010 (382 ± 0.6 μatm). The SST was approximately 3.0 ± 1.6 °C and salinity was 34.3.

Table 2 shows the mean monthly variability of the estimated variables. Despite the AO acting as a sink for atmospheric CO₂, considerable variability in Δ*p*CO₂ was observed

Table 1 Statistics of data used for calculations. Descriptions in rows: *k* – gas transfer coefficient, *U*₁₀ – 10-m wind speed, *p*CO_{2W} and *p*CO_{2A} – seawater and atmospheric partial pressure of CO₂, respectively, Δ*p*CO₂ – difference in partial pressure, SST – sea surface temperature.

	<i>N</i>	Ave.	Min	Max	St. error	Var.	St. dev
<i>F</i> [mgC m ^{−2} day ^{−1}]	576	−8.0	−15.4	−4.2	0.1	2.6	1.6
<i>k</i> [cm h ^{−1}]	576	13.0	7.9	17.9	0.1	3.5	1.9
<i>U</i> ₁₀ [m s ^{−1}]	576	8.3	5.8	9.7	0.0	0.4	0.7
<i>p</i> CO _{2W} [μatm]	576	332.4	292.7	354.6	0.5	139.2	11.8
Δ <i>p</i> CO ₂ [μatm]	576	−50.1	−91.1	−27.7	0.5	152.2	12.3
<i>p</i> CO _{2A} [μatm]	576	382.5	381.2	384.1	0.0	0.4	0.6
SST [°C]	576	3.0		6.5	0.1	2.7	1.6

in space and time (Fig. 6 and Table 2). The $p\text{CO}_{2W}$ varies considerably, both spatially and temporarily, as has been shown in recent studies, e.g., Olsen et al. (2003), Omar et al. (2003), Nakaoko et al. (2006), Takahashi et al. (2009), and Sejr et al. (2011). The mean values of partial CO_2 pressure in the air range from $372.5 \pm 0.6 \mu\text{atm}$ in August to $389.1 \pm 0.6 \mu\text{atm}$ in May, while values of partial CO_2 pressure in seawater varied from $309.1 \pm 11.8 \mu\text{atm}$ in August to $348.2 \pm 11.8 \mu\text{atm}$ in February. Bates and Mathis (2009) showed that when SST rises by 1°C $p\text{CO}_{2W}$ should increase by up to 8 to $12 \mu\text{atm}/^\circ\text{C}$. Nakaoko et al. (2006) reported that monthly $p\text{CO}_{2W}$ values increased proportionately to increasing SST (in 1994–2001), except in May and June. In June, when SST was above 2°C , $p\text{CO}_{2W}$ was higher than $250 \mu\text{atm}$, while lower $p\text{CO}_{2W}$ was observed when SST was about 1°C . The results from FluxEngine show that when SST increased above 2.5°C , $p\text{CO}_{2W}$ was lower than $340 \mu\text{atm}$, and when SST decreased below 2.5°C , $p\text{CO}_{2W}$ was higher than $340 \mu\text{atm}$, except in May. Calculations from FluxEngine indicate the opposite relationship to that demonstrated in Bates and Mathis (2009). During the study period, gas transfer velocity varied from $19.9 \pm 1.9 \text{ cm h}^{-1}$ in December, when values of wind speed were higher than 10 m s^{-1} , to $6.6 \pm 1.9 \text{ cm h}^{-1}$ in July when wind speed was lower than 5 m s^{-1} . The strongest winds in the AO were from October to April at mean values of $9.0 \pm 0.7 \text{ m s}^{-1}$, while from May to September the values were $6.0 \pm 0.7 \text{ m s}^{-1}$.

Fig. 3 shows the relationships between annual mean $p\text{CO}_{2W}$ concentrations and air–sea CO_2 fluxes to the north. Over spatial scales, the air–sea CO_2 flux values were strongly positively linked to the partial pressure of CO_2 in seawater (much less than with k) (see Table 3). Regions from the Arctic Circle to the North Pole were sinks of CO_2 , and all surface $p\text{CO}_2$ values were below atmospheric levels ($p\text{CO}_2$ in the atmosphere was $380 \mu\text{atm}$ in 2010), although the Arctic Circle regions were close to equilibrium. The calculated oceanic CO_2 uptake varied between -6 to $-16 \text{ mg C m}^{-2} \text{ day}^{-1}$, and $p\text{CO}_{2W}$ concentrations varied between 360 and $290 \mu\text{atm}$ to the northward. Variations in $p\text{CO}_{2W}$ mainly stemmed from biological activity, changes in sea surface temperature, and water mass transport, which are clearly indicated in Fig. 3 (Garbe et al., 2014; Nakaoko

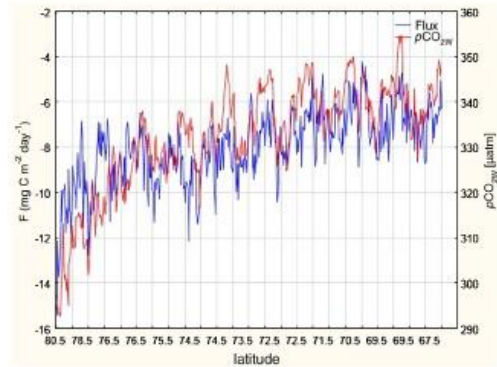


Figure 3 Annual mean $p\text{CO}_2$ in seawater [μatm] and air–sea CO_2 fluxes [$\text{mg C m}^{-2} \text{ day}^{-1}$].

et al., 2006). The SST of the GS and BS was dominated by the inflow of warm North Atlantic Ocean water.

Fig. 4 illustrates maps of the zonal mean $p\text{CO}_{2W}$ in February and August, and Fig. 5 indicates differences between them. In summer, all the $p\text{CO}_{2W}$ values in the GS and BS were below atmospheric levels, while in winter $p\text{CO}_{2W}$ was close to or higher than atmospheric levels in the BS. These results are in good agreement with those obtained by Cai et al. (2006), Nakaoko et al. (2006) for 1992–2001, and Sejr et al. (2011) for 2006–2009. Calculations from FluxEngine indicate that annual mean values of $p\text{CO}_{2W}$ in 2010 were $332.4 \pm 11.8 \mu\text{atm}$ (see Table 1), with mean values in August of $295 \pm 11.8 \mu\text{atm}$ in the GS and $355 \pm 11.8 \mu\text{atm}$ in the BS. Weiss et al. (1992) showed in July 1981 and 1990 that $p\text{CO}_{2W}$ concentrations were around 225 – $230 \mu\text{atm}$, while in August 1994–2001 they were around $255 \mu\text{atm}$ in the GS and $280 \mu\text{atm}$ in the BS (Nakaoko et al., 2006). During 1995–2003, the annual mean $p\text{CO}_2$ was $313 \pm 4.1 \mu\text{atm}$ in the GS and $292 \pm 6.1 \mu\text{atm}$ in the BS (Arrigo et al., 2010), and in 1995 it was only $282 \pm 31 \mu\text{atm}$ (Takahashi et al., 2002). Generally, the AO is a strong net CO_2 sink; however, there

Table 2 Monthly dynamics of the datasets in the AO. Descriptions in columns: k – gas transfer coefficient, U_{10} – 10-m wind speed, $p\text{CO}_{2W}$ and $p\text{CO}_{2A}$ – seawater and atmospheric partial pressure of CO_2 , respectively, $\Delta p\text{CO}_2$ – difference in partial pressure, SST – sea surface temperature.

	F [$\text{mg C m}^{-2} \text{ day}^{-1}$]	k [cm h^{-1}]	U_{10} [m s^{-1}]	$p\text{CO}_{2W}$ [μatm]	$\Delta p\text{CO}_2$ [μatm]	$p\text{CO}_{2A}$ [μatm]	SST [$^\circ\text{C}$]
Jan	−10.9	18.4	10.6	341.7	−44.2	385.9	2.24
Feb	−8.5	16.6	10	348.2	−39.5	387.8	2.2
Mar	−8.8	16	9.8	346.2	−39.5	385.6	1.92
Apr	−8.4	13.5	8.8	341.5	−44.6	387	1.72
May	−6.9	9.1	7	334.6	−56.5	389.1	2.01
Jun	−4.4	6.8	5.8	328.1	−57.7	384.6	3.44
Jul	−4	6.6	5.2	314.6	−63	377.6	4.99
Aug	−5	7.4	5.9	309.1	−59.4	372.5	4.55
Sep	−6	9.4	6.9	321.3	−52.4	373.11	4.14
Oct	−8.2	16.5	9.4	335.1	−39.1	376.1	3.99
Nov	−11.7	17.5	10	334.2	−48.5	382.7	2.67
Dec	−13.6	19.9	10.9	335	−49	385.2	2.71

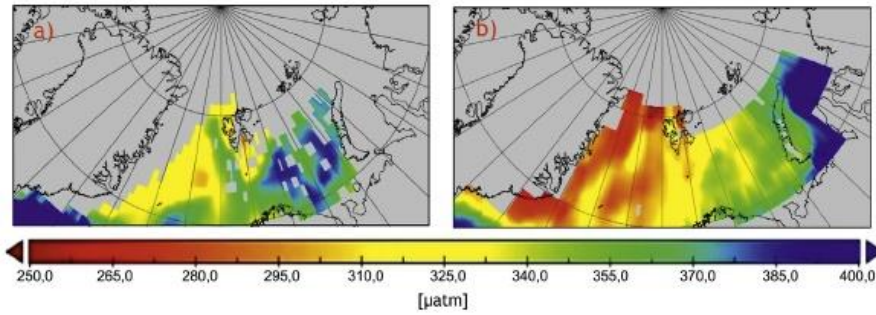


Figure 4 Monthly mean values for $p\text{CO}_2$ in seawater [μatm] in February (a) and August (b).

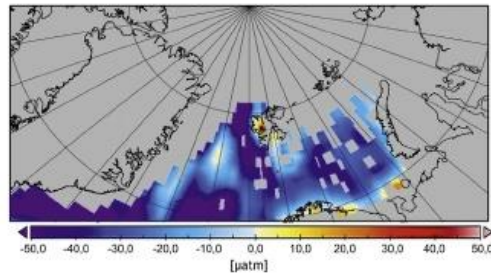


Figure 5 Difference maps for surface water $p\text{CO}_2$ [μatm] values for August–February.

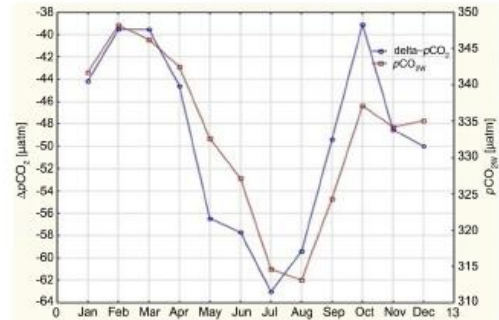


Figure 6 Monthly variability of differences in partial pressure of CO_2 $\Delta p\text{CO}_2$ [μatm] and $p\text{CO}_2$ in seawater [μatm].

Table 3 The Pearson linear correlation between datasets in the Arctic Ocean. Descriptions in rows and columns: k – gas transfer coefficient, U_{10} – 10-m wind speed, $p\text{CO}_{2W}$ and $p\text{CO}_{2A}$ – atmospheric and seawater partial pressure of CO_2 , respectively, $\Delta p\text{CO}_2$ – difference in partial pressure, SST – sea surface temperature.

	F [$\text{mgC m}^{-2} \text{ day}^{-1}$]	k [cm h^{-1}]	U_{10} [m s^{-1}]	$p\text{CO}_{2W}$ [μatm]	$\Delta p\text{CO}_2$ [μatm]	$p\text{CO}_{2A}$ [μatm]	SST [$^{\circ}\text{C}$]
F [$\text{mgC m}^{-2} \text{ day}^{-1}$]	1.000	0.185	0.042	0.757	0.759	−0.664	0.628
k [cm h^{-1}]	0.185	1.000	0.930	0.636	0.643	−0.663	0.655
U_{10} [m s^{-1}]	0.042	0.930	1.000	0.567	0.570	−0.540	0.457
$p\text{CO}_{2W}$ [μatm]	0.757	0.636	0.567	1.000	1.000	−0.833	0.732
$\Delta p\text{CO}_2$ [μatm]	0.759	0.643	0.570	1.000	1.000	−0.849	0.745
$p\text{CO}_{2A}$ [μatm]	−0.664	−0.663	−0.540	−0.833	−0.849	1.000	−0.878
SST [$^{\circ}\text{C}$]	0.628	0.655	0.457	0.732	0.745	−0.878	1.000

Table 4 The Pearson linear correlation coefficient between datasets in 2010. Descriptions in columns and rows: k – gas transfer coefficient, U_{10} – 10-m wind speed, $p\text{CO}_{2W}$ and $p\text{CO}_{2A}$ – seawater and atmospheric partial pressure of CO_2 , respectively, $\Delta p\text{CO}_2$ – difference in partial pressure, SST – sea surface temperature.

	F [$\text{mgC m}^{-2} \text{ day}^{-1}$]	k [cm h^{-1}]	U_{10} [m s^{-1}]	$p\text{CO}_{2W}$ [μatm]	$\Delta p\text{CO}_2$ [μatm]	$p\text{CO}_{2A}$ [μatm]	SST [$^{\circ}\text{C}$]
F [$\text{mgC m}^{-2} \text{ day}^{-1}$]	1.000	−0.934	−0.928	−0.640	−0.559	−0.475	0.606
k [cm h^{-1}]	−0.934	1.000	0.992	0.761	0.788	0.382	−0.568
U_{10} [m s^{-1}]	−0.928	0.992	1.000	0.826	0.815	0.472	−0.661
$p\text{CO}_{2W}$ [μatm]	−0.640	0.761	0.826	1.000	0.877	0.718	−0.858
$\Delta p\text{CO}_2$ [μatm]	−0.559	0.788	0.815	0.877	1.000	0.295	−0.562
$p\text{CO}_{2A}$ [μatm]	−0.475	0.382	0.472	0.718	0.295	1.000	−0.888
SST [$^{\circ}\text{C}$]	0.606	−0.568	−0.661	−0.858	−0.562	−0.888	1.000

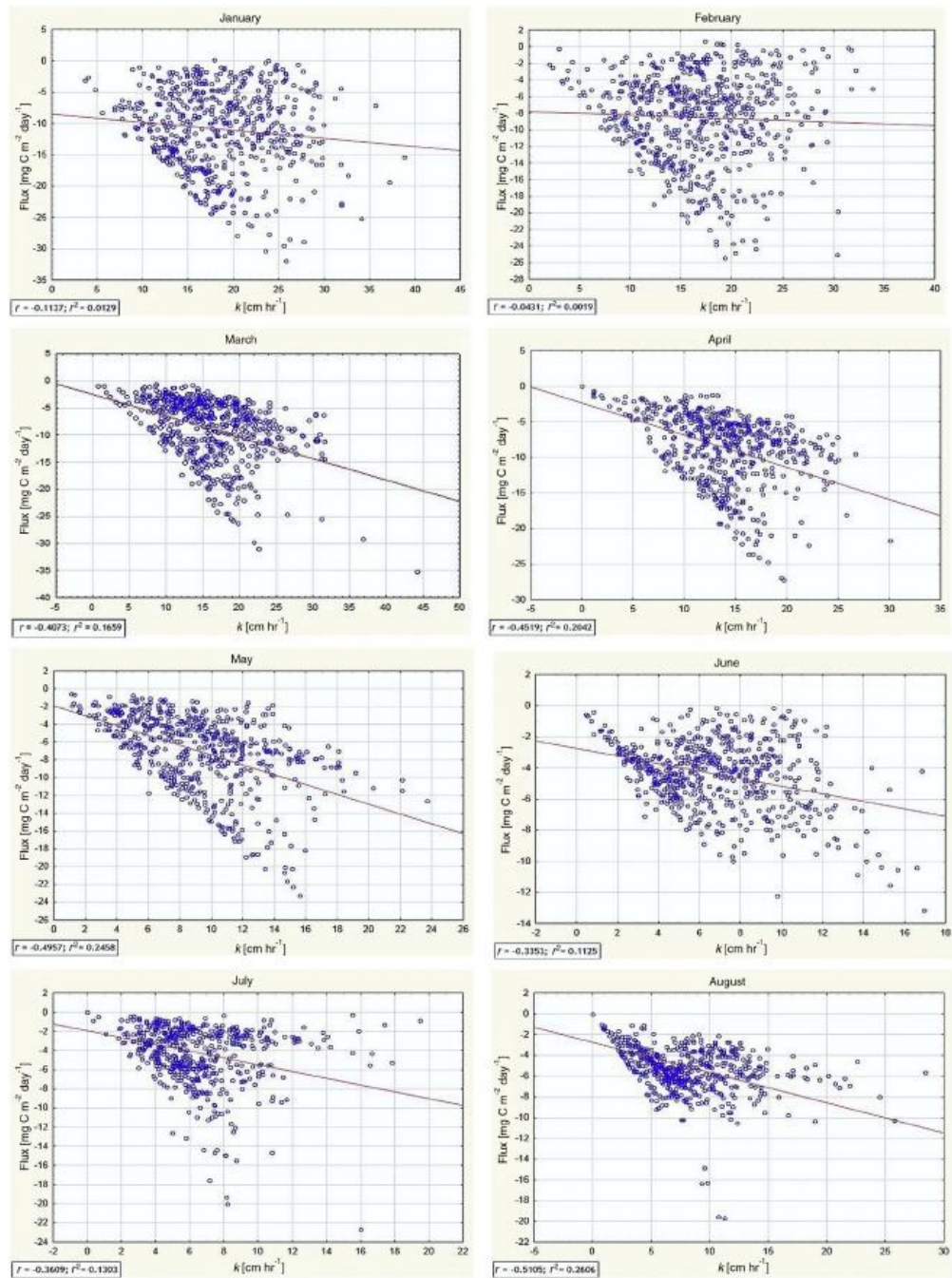


Figure 7 Monthly variations of air-sea CO₂ fluxes [$\text{mg C m}^{-2} \text{ day}^{-1}$] as a function of gas transfer velocity [cm h^{-1}].

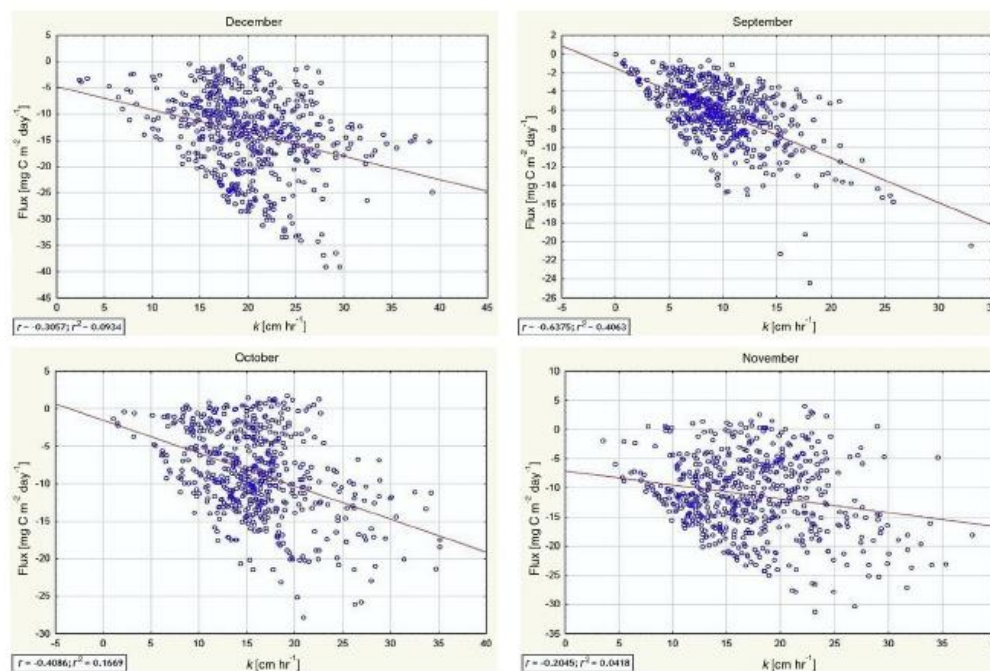


Figure 7. (Continued).

are shallow coastal areas where it is a source of CO₂ to the atmosphere, caused by river outputs and sea ice melting (Bates and Mathis, 2009). Seasonal changes in biological activity (phytoplankton primary production, PP), sea water warming and cooling, and the volume of CO₂ exchange caused seasonal changes in surface pCO₂. In wintertime, during the study, when the temperature of sea water was lower than in summer, pCO_{2w} levels were higher in the open water of the GS and BS in February (310–370 and 355–400 μatm, respectively) than in August (250–325 and 325–370 μatm, respectively) (Fig. 4). Additionally, in the GS, in both February and August, the concentration of pCO_{2w} was lower (Fig. 4) with differences in absolute values higher than in the BS (Fig. 5). This observation agrees well with earlier results obtained by Takahashi et al. (2002), Olsen et al. (2003), and Nakaoko et al. (2006). During summertime, surface pCO_{2w} values decreased, in spite of seasonal warming and oceanic CO₂ uptake increased thanks to high CO₂ exchange (Bates and Mathis, 2009). These processes were counterbalanced by the uptake of CO₂ in summertime by phytoplankton that decreased pCO₂.

Fig. 5 shows that inside the Arctic fjord the difference between pCO₂ in the summer and the winter was caused by lower surface-water pCO₂ levels resulting from sea ice melt, dissolution of CaCO₃, primary production, and strong stratification of the water column inside the fjord. Melting sea ice in the summer caused low pCO₂ levels, but melt water ponds were also pCO_{2A} sinks (Sejr et al., 2011; Semiletov et al., 2004). The results from estimations contrast with those

gathered by Omar et al. (2007) and Sejr et al. (2011), and they show that fjords and nearby lands in the AO are places where physical process do not exceed biological CO₂ uptake because of runoff from lands, but in the open water area of the AO the opposite was found. This could stem from the fjords not being well represented in the data, and it could imply some underestimation of ΔpCO₂ rates. It does indicate, though, that more study of the shallow and marginal areas is required.

Fig. 6 shows the monthly values of pCO_{2w} and ΔpCO₂. Over the temporal scale, of the study period, all surface pCO₂ levels were below atmospheric levels (average 380 μatm) resulting in negative ΔpCO₂. The calculated pCO_{2w} and ΔpCO₂ values show seasonal variation of about 39 and 24 μatm, respectively, with two maxima for pCO_{2w} in February and October and one minima in August, and two minima for ΔpCO₂ in March and October and one maxima in July. These observations agree well with the previous studies (Nakaoko et al., 2006; Takahashi et al., 2009). The ΔpCO₂ values increased (at a rate of 5 μatm) compared to previous results obtained by Takahashi et al. (2009). The seasonal difference in ΔpCO₂ (strong negative values in the summertime) resulted from the biological drawdown of CO₂. Differences in the partial pressure of CO₂ were very strongly correlated with changes in the partial pressure of CO_{2w}, especially in wintertime, when the average water temperature was higher than the air temperature (see also the discussion in Table 2).

Figs. 7 and 8 show regression lines, correlations, and determination coefficients between air-sea CO₂ fluxes,

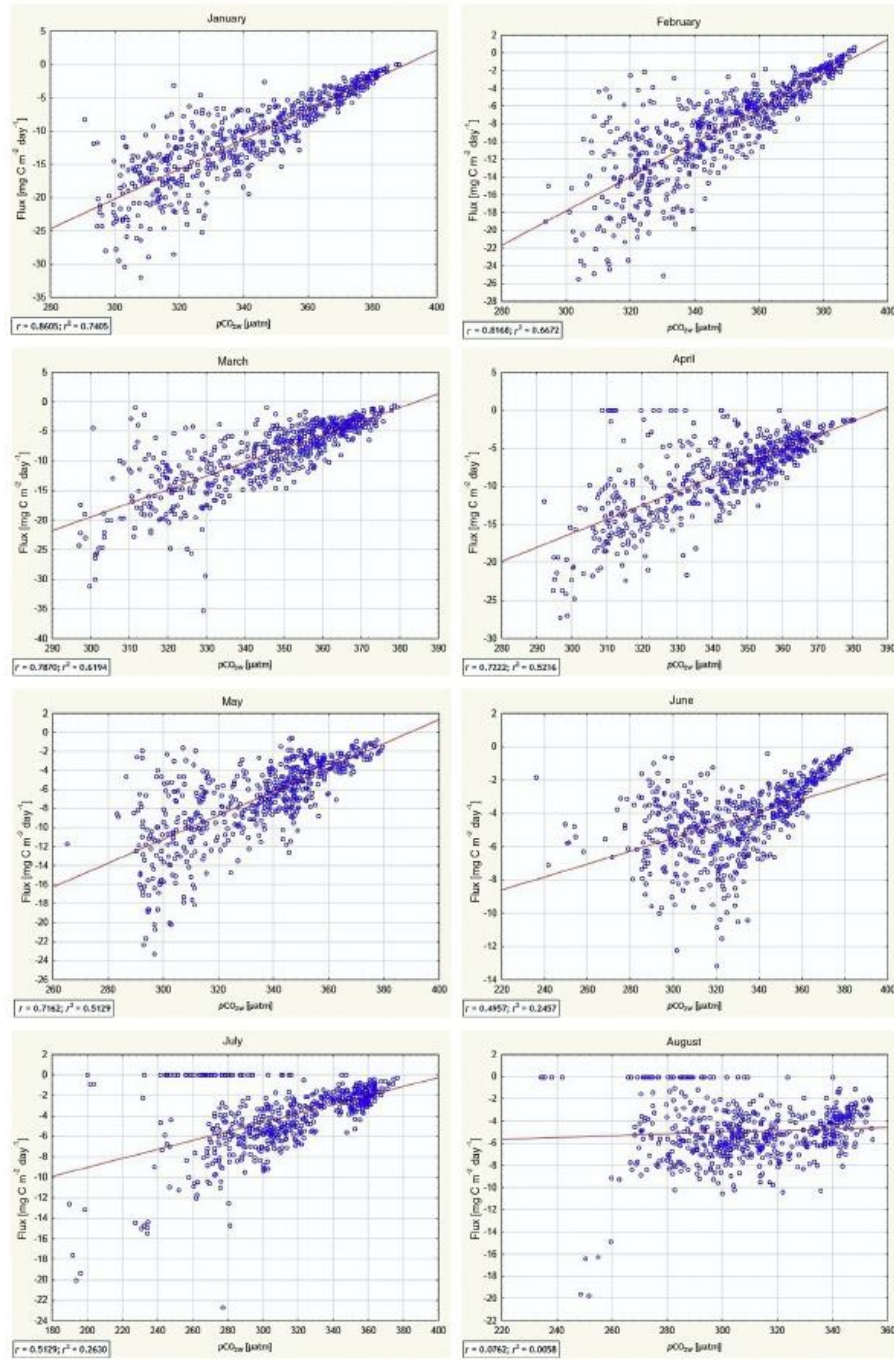


Figure 8 Monthly dynamics of air-sea CO₂ flux [mg C m⁻² day⁻¹] as a function of pCO₂ in seawater [µatm].

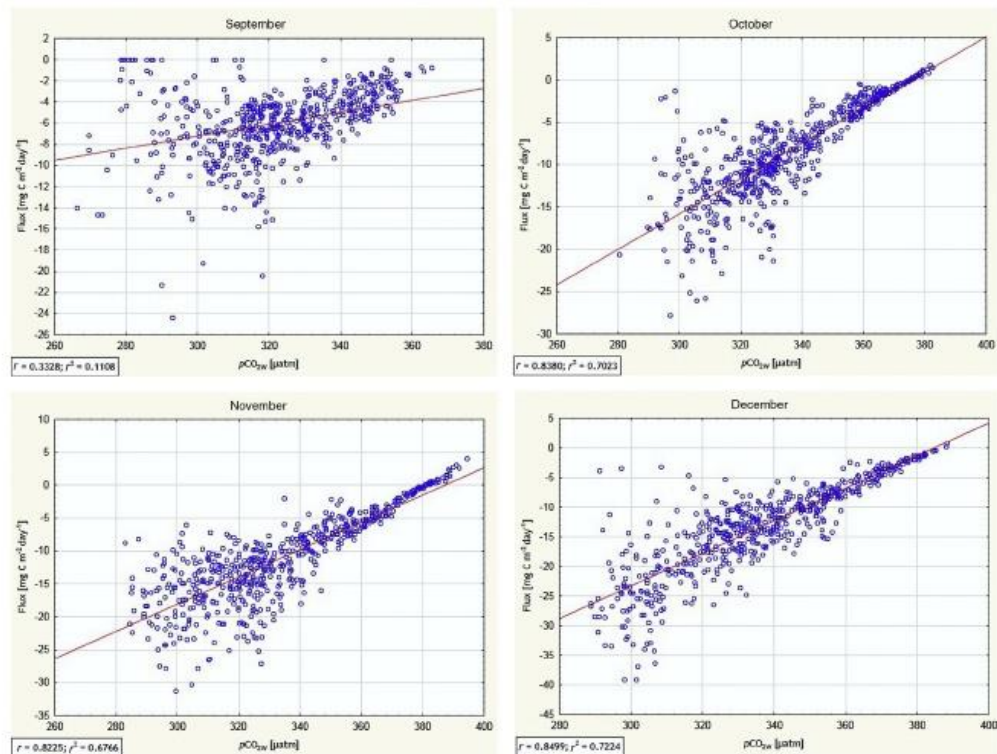


Figure 8. (Continued).

pCO_{2w}, and k for individual months. The correlation coefficient (r) represents the linear relationship between two variables and the determination coefficient (r^2) represents the proportion of common variation between the two variables (StatSoft Inc., 2013). Over spatial scales, fluxes were better correlated with pCO_{2w} than with gas transfer velocity during each month. In the relationship between air-sea fluxes and k , in May, August, and September more than 20% of variability in fluxes was explained by k (typically less than 20%; Fig. 7). More than 50% of variability in fluxes was explained by pCO_{2w} (except from June to September, when it was less than 20%; Fig. 8). In summertime, CO₂ flux variability was controlled by k , as a function of sea ice cover. The results reflect those obtained by Doney et al. (2009) and Couldrey et al. (2016). They demonstrated that variability in k contributes to only approximately 35% of the global interannual flux variability, while Δ pCO₂ contributes 60% of total variability.

Fig. 9 shows spatiotemporal mean air-sea CO₂ fluxes in the GS and BS during study period using the Nightingale et al. (2000) k parameterization. Cai et al. (2006) estimated that the continental shelves of the AO were responsible for the total uptake of atmospheric CO₂ of 52 TgC a⁻¹, equivalent to an average air-sea CO₂ flux of -12 gC m⁻² a⁻¹. The total

uptake for the BS was estimated to be about 3.2 TgC a⁻¹ or a flux of -4.38 gC m⁻² a⁻¹. Following the methods described in Table S1 in Cai et al. (2006), the total uptake of atmospheric CO₂ on the continental shelves of the GS and BS was estimated as 3.6 TgC a⁻¹ and the average air-sea CO₂ fluxes were estimated about -3.62 gC m⁻² a⁻¹. As can be seen, the GS was a stronger net sink of CO₂ in winter (approximately -12 mgC m⁻² day⁻¹), while the BS was a very weak sink for CO₂ that was close to equilibrium. There were seasonal changes throughout the year. The annual mean air-sea CO₂ flux for the whole study area was -8.0 mgC m⁻² day⁻¹ (see Table 1). This is because the BS had higher SST than the GS because of the inflow of warm water via the North Atlantic Current (Land et al., 2013). Additionally, as is shown in Fig. 3, air-sea CO₂ fluxes are strongly positively correlated with pCO_{2w} over spatial scales. Estimates for the central GS are similar to previous results: 52 gC m⁻² a⁻¹ for the 1992–2001 period (Nakaoko et al., 2006), 25 gC m⁻² a⁻¹ for 2006, and 42 gC m⁻² a⁻¹ for 2009 (Sejr et al., 2011). Most areas of the BS became CO₂ sources in summer and fall, which is likely to be from the effect of sea–water temperature changes. During spring, no upward CO₂ flux was observed in the Arctic sector of the Atlantic Ocean. The air-sea CO₂ flux from the atmosphere decreased slightly

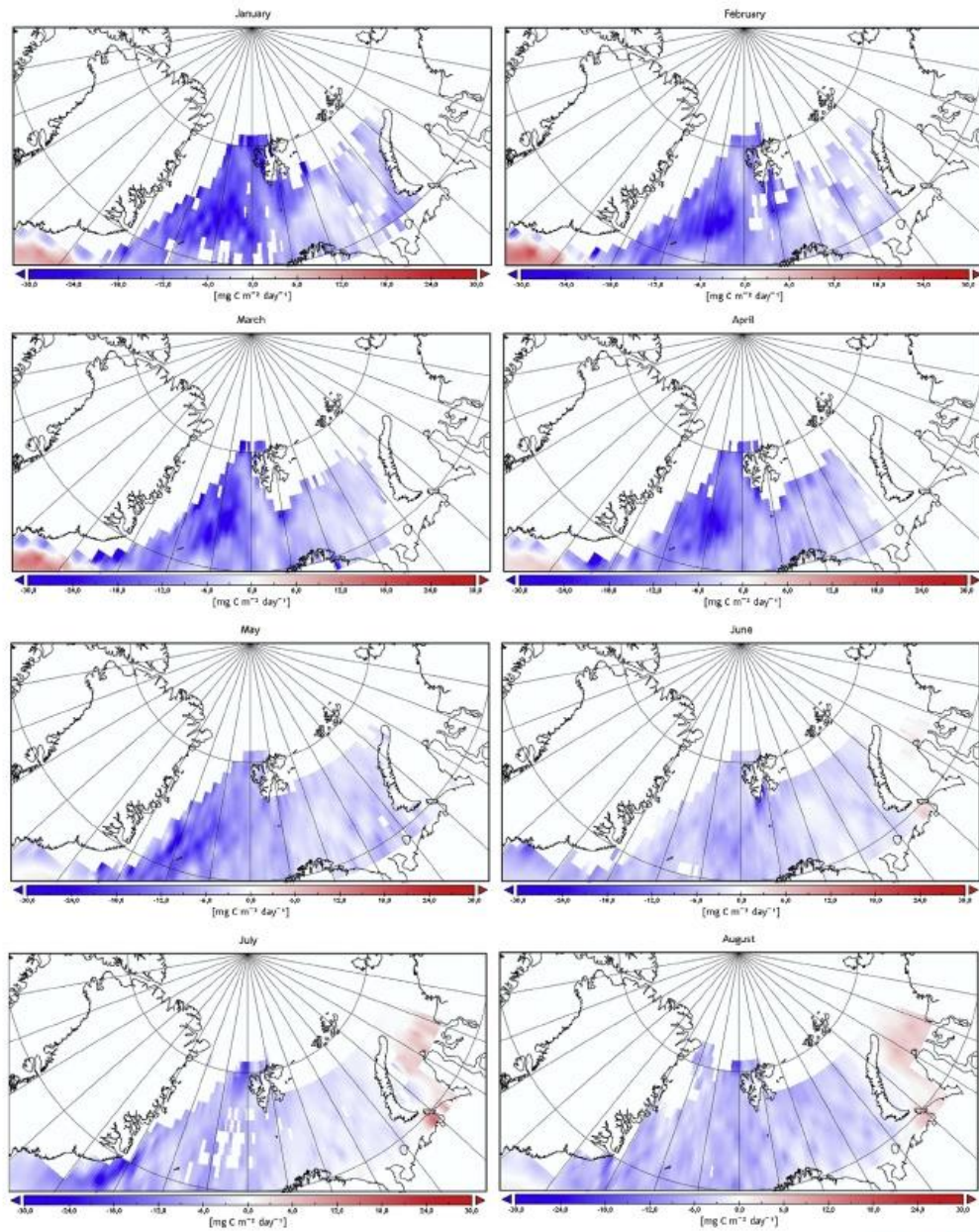


Figure 9 Monthly mean values for air–sea CO₂ fluxes [$\text{mg C m}^{-2} \text{ day}^{-1}$] combined using k parameterization by Nightingale et al. (2000). Blue is absorbing, red is emitting. (For interpretation of the references to color in this figure legend, the reader is referred to the web version of the article.)

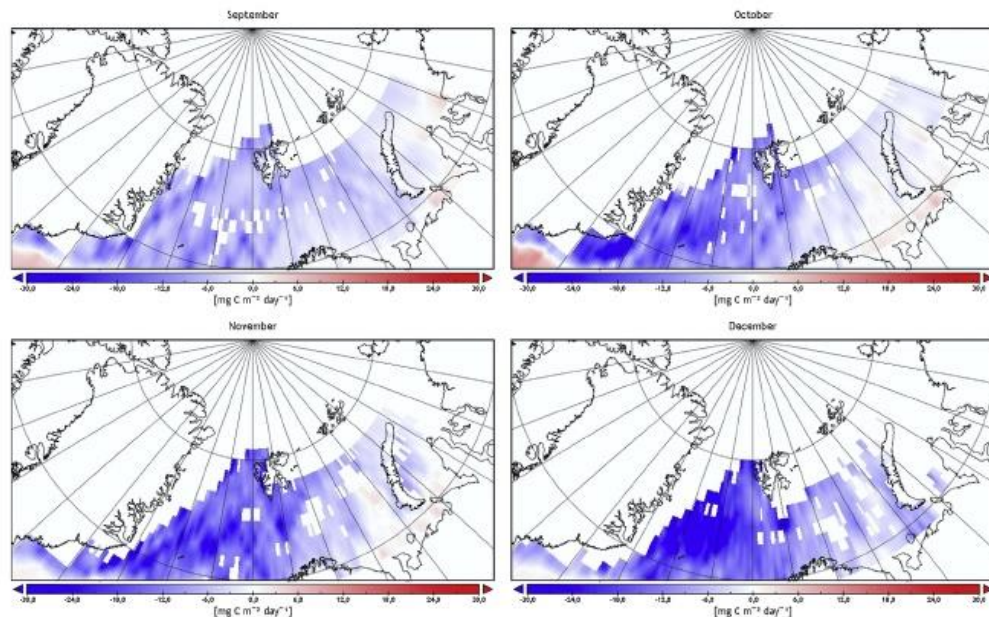


Figure 9. (Continued).

during June and July (Fig. 9), which was because of a steep decrease in average wind speed and low $p\text{CO}_2$; these values were in good agreement with results reported by Arrigo et al. (2010).

The relationships among the variables influencing gas fluxes on spatial and temporal scales are shown in Tables 3 and 4. In general, there were very few positive correlations between air–sea CO_2 fluxes and k over spatial scales ($r = 0.185$, $p < 0.05$), and very strong negative correlations over temporal scales ($r = -0.935$, $p < 0.05$) with moderate negative correlations in individual months (Fig. 7). In wintertime, when the wind was stronger (hence higher k), than in summertime, the rates of air–sea CO_2 fluxes were up to $-10 \text{ mg C m}^{-2} \text{ day}^{-1}$. In June and July, the rates of air–sea CO_2 exchange were small ($< 5 \text{ mg C m}^{-2} \text{ day}^{-1}$) when compared to the annual average (Table 1). These results match those derived by Nakaoko et al. (2006) for the GS and BS. In summertime, the majority of measurements were much less scattered around the trend line than in wintertime when the values were more scattered (Fig. 7). The fluxes across the air–sea interface were controlled by SST, wave breaking, friction velocity, sea state, turbulence, etc. (Goddijn-Murphy et al., 2016; Nightingale et al., 2000). The rate of transfer across the sea surface is usually a parameter that is a function of wind speed at 10 m. a.s.l. However, there were also other factors that influence air–sea CO_2 fluxes, such as surface films, fetch, and chemical enhancement (McGillis et al., 2001; Wanninkhof et al., 2009). Strong positive correlations between $p\text{CO}_2$ and air–sea fluxes ($r = 0.757$, $p < 0.05$) over spatial scales and quite strong negative correlations over temporal scales ($r = -0.640$,

$p < 0.05$) were noted (Fig. 8). In the AO, the spatial variability in $p\text{CO}_{2w}$ showed quite strong positive correlations with SST ($r = 0.732$, $p > 0.05$), while temporal variability showed even stronger negative correlations with SST ($r = -0.858$, $p > 0.05$; Tables 3 and 4).

4. Conclusions

This study examined the effect of monthly changes in gas transfer velocity and $\Delta p\text{CO}_2$ in controlling air–sea CO_2 fluxes in the Greenland Sea and the Barents Sea, during a one year period. It also examined the following testable hypothesis: air–sea CO_2 fluxes over one year are dependent on both $\Delta p\text{CO}_2$ and k . Results from FluxEngine showed that air–sea CO_2 fluxes had fewer positive correlations with gas transfer velocity (k) over spatial scales (Table 3), and almost perfect negative correlations over temporal scales (Table 4) with moderate negative correlations within individual months (Fig. 7). Additionally, there were strong positive correlations between $p\text{CO}_2$ and air–sea fluxes over spatial scales (Table 3) and quite strong negative correlations over temporal scales (Table 4), with strong positive correlations within individual months (Fig. 8). In the relationships between air–sea fluxes and gas transfer velocity in May, August, and September, more than 20% of the variability in fluxes was explained by k (typically it was less than 20%; Fig. 7). More than 50% of variability in fluxes was explained by $p\text{CO}_{2w}$ (except from June to September, where it was less than 20%; Fig. 8). The results indicate that the variability in wind speed, and, hence, gas transfer velocity, plays a major role over temporal

scales, while $\Delta p\text{CO}_2$, and hence $p\text{CO}_{2w}$, plays a major role over spatial scales in determining the monthly variation of CO_2 uptake in this area. On these timescales it is critical to obtain estimates of $p\text{CO}_2$ and k for accurate flux variability to be derived. We can predict the future state of the global carbon cycle only if we improve understanding the carbon cycle mechanisms of this area by using our ability to diagnose past change and analyze present variability.

As can be seen, even using satellite data is insufficient for specifying the mechanisms controlling carbon uptake in the Arctic Ocean. There are many gaps in the data from this region, and many uncertainties in approaches to estimating air–sea fluxes. We still do not know exactly how sea ice melting influences carbon uptake or how each component of the biological and physical carbon dioxide pumps influence air–sea flux values. Two relatively simple improvements may prevent the data gaps in projecting and evaluating carbon fluxes in this region in the future – a use of new techniques for interpolating data as well as a use of commercial ships for transporting and deploying sampling equipment in the winter.

Acknowledgements

The publication was financed with funds from Leading National Research Centre (KNOW) received by the Centre for Polar Studies for the period 2014–2018; OceanFlux Greenhouse Gases Evolution, a project funded by the European Space Agency, ESRIN Contract No. 4000112091/14/I-LG; and GAME project of National Science Centre No. DEC-2012/04/A/NZ8/00661. I would also like to thank Jacek Piskozub for significant corrections and comments.

References

- Arrigo, K.R., van Dijken, G.L., Pabi, S., 2008. Impact of a shrinking Arctic ice cover on marine primary production. *Geophys. Res. Lett.* 35 (19), L19603, 6 pp., <http://dx.doi.org/10.1029/2008GL035028>.
- Arrigo, K.R., Pabi, S., van Dijken, G.L., Maslowski, W., 2010. Air–sea flux of CO_2 in the Arctic Ocean, 1998–2003. *J. Geophys. Res. Biogeosci.* 115 (G4), 15 pp., <http://dx.doi.org/10.1029/2009JG001224>.
- Ashton, I.G., Shutler, J.D., Land, P.E., Woolf, D.K., Quartly, G.D., 2016. A sensitivity analysis of the impact of rain on regional and global sea–air fluxes of CO_2 . *PLOS ONE* 11 (9), e0161105, 18 pp., <http://dx.doi.org/10.1371/journal.pone.0161105>.
- Bates, N.R., 2012. Multi-decadal uptake of carbon dioxide into subtropical mode water of the North Atlantic Ocean. *Biogeosciences* 9 (7), 2649–2659, <http://dx.doi.org/10.5194/bg-9-2649-2012>.
- Bates, N.R., Mathis, J.T., 2009. The Arctic Ocean marine carbon cycle: evaluation of air–sea CO_2 exchanges, ocean acidification impacts and potential feedbacks. *Biogeosciences* 6 (11), 2433–2459, <http://dx.doi.org/10.5194/bg-6-2433-2009>.
- Boutin, J., Etcheto, J., Merlivat, L., Rangama, Y., 2002. Influence of gas exchange coefficient parameterization on seasonal and regional variability of CO_2 air–sea fluxes. *Geophys. Res. Lett.* 29 (8), 23–1–23–4, <http://dx.doi.org/10.1029/2001GL013872>.
- Cai, W.-J., Dai, M., Wang, Y., 2006. Air–sea exchange of carbon dioxide in ocean margins: a province-based synthesis. *Geophys. Res. Lett.* 33 (12), L12603, <http://dx.doi.org/10.1029/2006GL026219>.
- Couldrey, M.P., Oliver, K.I.C., Yool, A., Halloran, P.R., 2016. On which timescales do gas transfer velocities control North Atlantic CO_2 flux variability? *Global Biogeochem. Cycl.* 30 (5), 787–802, <http://dx.doi.org/10.1002/2015GB005267>.
- Dai, A., Qian, T., Trenberth, K.E., Milliman, J.D., 2009. Changes in continental freshwater discharge from 1948 to 2004. *J. Climate* 22 (10), 2773–2792, <http://dx.doi.org/10.1175/2008JCLI2592.1>.
- Doney, S.C., Lima, I., Feely, R.A., Glover, D.M., Lindsey, K., Mahowald, N., Moore, J.K., Wanninkhof, R., 2009. Mechanisms governing interannual variability in upper-ocean inorganic carbon system and air–sea CO_2 fluxes: physical climate and atmospheric dust. *Deep-Sea Res. Pt. II* 56 (8–10), 640–655, <http://dx.doi.org/10.1016/j.dsr2.2008.12.006>.
- Else, B.G.T., Papakyriakou, T.N., Galley, R.J., Drennan, W.M., Miller, L.A., Thomas, H., 2011. Wintertime CO_2 fluxes in an Arctic polynya using eddy covariance: evidence for enhanced air–sea gas transfer during ice formation. *J. Geophys. Res.* 116 (C9), C00G03, 15 pp., <http://dx.doi.org/10.1029/2010JC006760>.
- Garbe, C.S., Rutgersson, A., Boutin, J., de Leeuw, G., Delille, B., Fairall, C.W., Gruber, N., Hare, J., Ho, D.T., Johnson, M.T., Nightingale, P.D., Pettersson, H., Piskozub, J., Sahlee, E., Tsai, W., Ward, B., Woolf, D.K., Zappa, C.J., 2014. Transfer across the air–sea interface. In: Liss, P.S., Johnson, M.T. (Eds.), *Ocean–Atmosphere Interactions of Gases and Particles*. Springer-Earth Sys. Sciences, Berlin, Heidelberg, 55–111.
- Goddijn-Murphy, L., Woolf, D.K., Land, P.E., Shutler, J.D., Donlon, C., 2015. The OceanFlux Greenhouse Gases methodology for deriving a sea surface climatology of CO_2 fugacity in support of air–sea gas flux studies. *Ocean Sci.* 11 (4), 519–541, <http://dx.doi.org/10.5194/os-11-519-2015>.
- Goddijn-Murphy, L., Woolf, D.K., Callaghan, A.H., Nightingale, P.D., Shutler, J.D., 2016. A reconciliation of empirical and mechanistic models of the air–sea gas transfer velocity. *J. Geophys. Res.* 121 (1), 818–835, <http://dx.doi.org/10.1002/2015JC010996>.
- Gruber, N., 2009. Carbon cycle: fickle trends in the ocean. *Nature* 458 (7235), 155–156, <http://dx.doi.org/10.1038/458155a>.
- Gruber, N., Keeling, C.D., Bates, N.P., 2003. Interannual variability in the North Atlantic Ocean carbon sink. *Science* 298 (5602), 2374–2378, <http://dx.doi.org/10.1126/science.1077077>.
- Gurgul, H., 2002. *Białe Pustynie – Arktyka*. Wyd. Kurpisz. Poznań, 4–30.
- Ho, D.T., Law, C.S., Smith, M.J., Schlosser, P., Harvey, M., Hill, P., 2006. Measurements of air–sea gas exchange at high wind speeds in the Southern Ocean: implications for global parameterizations. *Geophys. Res. Lett.* 33 (16), L16611, <http://dx.doi.org/10.1029/2006GL026817>.
- IPCC, 2013. Carbon and other biogeochemical cycles. In: Stocker, T. F., Qin, D., Plattner, G.-K., Tignor, W., Allen, S.K., Boschung, J., Nauels, A., Xia, Y., Bex, V., Midgley, P.M. (Eds.), *Climate Change 2013: The Physical Science Basis. Contribution of Working Group I to the Fifth Assessment Report of the Intergovernmental Panel on Climate Change*. Cambridge Univ. Press, Cambridge, 470–516.
- Kondo, F., Tsukamoto, O., 2012. Comparative CO_2 flux measurements by eddy covariance technique using open- and closed-path gas analysers over the Equatorial Pacific Ocean. *Tellus B* 64 (17511), 1–12, <http://dx.doi.org/10.3402/tellusb.v64i0.17511>.
- Kulinski, K., She, J., Pempkowiak, J., 2011. Short and medium term dynamics of the carbon exchange between the Baltic Sea and the North Sea. *Cont. Shelf Res.* 31 (15), 1611–1619, <http://dx.doi.org/10.1016/j.csr.2011.07.001>.
- Land, P.E., Shutler, J.D., Cowling, R.D., Woolf, D.K., Walker, P., Findlay, H.S., Upstill-Goddard, R.C., Donlon, C.J., 2013. Climate change impacts on sea–air fluxes of CO_2 in three Arctic seas: a sensitivity study using Earth observation. *Biogeosciences* 10 (12), 8109–8128, <http://dx.doi.org/10.5194/bg-10-8109-2013>.
- Landschützer, P., Gruber, N., Bakker, D.C.E., Schuster, U., 2014. Recent variability of the global ocean carbon sink. *Global*

- Biogeochem. Cycl. 28 (9), 927–949, <http://dx.doi.org/10.1002/2014GB004853>.
- Le Quéré, C., Andres, R.J., Boden, T., Conway, T., Houghton, R.A., House, J.I., Marland, G., Peters, G.P., van der Werf, G.R., Ahlström, A., Andrew, R.M., Bopp, L., Canadell, J.G., Ciais, P., Doney, S.C., Enright, C., Friedlingstein, P., Huntingford, C., Jain, A.K., Jourdain, C., Kato, E., Keeling, R.F., Klein Goldewijk, K., Levis, S., Levy, P., Lomas, M., Poulter, B., Raupach, M.R., Schwinger, J., Sitch, S., Stocker, B.D., Viovy, N., Zaehle, S., Zeng, N., 2013. The global carbon budget 1959–2011. *Earth Syst. Sci. Data* 5, 165–185, <http://dx.doi.org/10.5194/essd-5-165-2013>.
- Le Quéré, C., Andrew, R.M., Canadell, J.G., Sitch, S., Korsbakken, J.I., Peters, G.P., Manning, A.C., Boden, T.A., Tans, P.P., Houghton, R.A., Kelling, R.F., Alin, S., Andrews, O.D., Anthoni, P., Barbero, L., Bopp, L., Chevallier, F., Chini, L.P., Ciais, P., Currie, K., Delire, C., Doney, S.C., Friedlingstein, P., Gkritzalis, T., Harris, I., Hauck, J., Haverd, V., Hoppema, M., Goldewijk, K., Jain, A.K., Kato, E., Körtzinger, A., Landschützer, P., Lefèvre, N., Lenton, A., Lienert, S., Lombardozzi, D., Melton, J.R., Metzl, N., Millero, F., Monteiro, P.M.S., Munro, D.R., Nabel, J.E.M.S., Nakaoko, S.I., O'Brien, K., Olsen, A., Omar, A.M., Ono, T., Pierrot, D., Poulter, B., Rödenbeck, C., Salisbury, J., Schuster, U., Schwinger, J., Séférian, R., Skjelvan, I., Stocker, B.D., Sutton, A.J., Takahashi, T., Hanqin, T., Tilbrook, B., van der Laan-Luijckx, I.T., van der Werf, G.R., Viovy, N., Walker, A.P., Wiltshire, A.J., Zaehle, S., 2016. Global Carbon budget 2016. *Earth Syst. Sci. Data* 8 (2), 605–649, <http://dx.doi.org/10.5194/essd-8-605-2016>.
- Le Quéré, C., Orr, J.C., Monfray, P., Aumont, O., Madec, G., 2000. Interannual variability of the oceanic sink of CO₂ from 1979 through 1997. *Global Biogeochem. Cycl.* 14 (4), 1247–1265, <http://dx.doi.org/10.1029/1999GB000049>.
- Le Quéré, C., Takahashi, T., Buitenhuis, E.T., Rödenbeck, C., Sutherland, S.C., 2010. Impact of climate change and variability on the global oceanic sink of CO₂. *Global Biogeochem. Cycl.* 24 (4), GB4007, <http://dx.doi.org/10.1029/2009GB003599>.
- Lefèvre, N., Watson, A.J., Olsen, A., Rios, A.F., Perez, F.F., Johannessen, T., 2004. A decrease in the sink for atmospheric CO₂ in the North Atlantic. *Geophys. Res. Lett.* 31 (7), L07306, <http://dx.doi.org/10.1029/2003GL018957>.
- Lefèvre, N., Watson, A.J., Watson, A.R., 2005. A comparison of multiple regression and neural network techniques for mapping in situ pCO₂ data. *Tellus B* 57 (5), 375–384, <http://dx.doi.org/10.1111/j.1600-0889.2005.00164.x>.
- MacGilchrist, G.A., Naveira Garabato, A.C., Tsubouchi, T., Bacon, S., Torres-Valdés, S., Azetsu-Scott, K., 2014. The Arctic Ocean carbon sink. *Deep-Sea Res. Pt. I* 86, 39–55, <http://dx.doi.org/10.1016/j.dsr.2014.01.002>.
- McGillis, W.R., Edson, J.B., Hare, J.E., Fairall, C.W., 2001. Direct covariance air–sea CO₂ fluxes. *J. Geophys. Res.* 106 (C8), 16729–16745, <http://dx.doi.org/10.1029/2000JC000506>.
- Merchant, C.J., Embury, O., Rayner, N.A., Berry, D.I., Corlett, G.K., Lean, K., Veal, K.L., Kent, E.C., Llewellyn-Jones, D.T., Remedios, J.J., Saunders, R., 2012. A 20 year independent record of sea surface temperature for climate from Along-Track Scanning Radiometers. *J. Geophys. Res.* 117 (C12), C12013, 18 pp., <http://dx.doi.org/10.1029/2012JC008400>.
- Minnett, P., Kaiser-Weiss, A., 2012. Discussion Document: Near-surface Oceanic Temperature Gradients, <https://www.ghrsst.org/wp-content/uploads/2016/10/SSTDefinitionsDiscussion.pdf>.
- Nakaoko, S.I., Aoki, A., Nakazawa, T., Hashida, G., Morimoto, S., Yamanouchi, T., Yoshikawa-Inoue, H., 2006. Temporal and spatial variations of oceanic pCO₂ and air–sea CO₂ flux in Greenland Sea and Barents Sea. *Tellus B* 58 (2), 148–166, <http://dx.doi.org/10.1111/j.1600-0889.2006.00178>.
- Nightingale, P.D., Malin, G., Law, C.S., Watson, A.J., Liss, P.S., Liddicoat, M.I., Boutin, J., Upstill-Goddard, R.C., 2000. In situ evaluation of air–sea gas exchange parameterizations using novel conservative and volatile tracers. *Global Biogeochem. Cycl.* 14 (1), 373–387, <http://dx.doi.org/10.1029/1999GB000091>.
- Olsen, A., Bellerby, R.G.J., Johannessen, T., Omar, A.M., Skjelvan, I., 2003. Interannual variability in the wintertime air–sea flux of carbon dioxide in the northern North Atlantic 1981–2001. *Deep-Sea Res. Pt. I* 50 (11), 1323–1338, [http://dx.doi.org/10.1016/S0967-0637\(03\)00144-4](http://dx.doi.org/10.1016/S0967-0637(03)00144-4).
- Omar, A.M., Johannessen, T., Kaltin, S., Olsen, A., 2003. Anthropogenic increase of oceanic pCO₂ in the Barents Sea surface water. *J. Geophys. Res.* 108 (C12), 18-1–18-8, <http://dx.doi.org/10.1029/2002JC001628>.
- Omar, A.M., Johannessen, T., Olsen, A., Kaltin, S., Rey, F., 2007. Seasonal and interannual variability of the air–sea CO₂ flux in the Atlantic sector of the Barents Sea. *Mar. Chem.* 104 (3), 203–213, <http://dx.doi.org/10.1016/j.marchem.2006.11.002>.
- Piechura, J., Walczowski, W., 2009. Warming of the West Spitsbergen Current and sea ice north of Svalbard. *Oceanologia* 51 (2), 147–164, <http://dx.doi.org/10.5697/oc.51-2.147>.
- Polyakov, I.V., Alekseev, G.V., Timokhov, L.A., Bhatt, U.S., Colony, R.L., Simmons, H.L., Walsh, D., Walsh, J.E., Zakharov, V.F., 2004. Variability of the Intermediate Atlantic Water of the Arctic Ocean over the last 100 years. *J. Climate* 17 (23), 4485–4497, <http://dx.doi.org/10.1175/JCLI-3224.1>.
- Repina, I.A., Semiletov, I.P., Smirnov, A.S., 2007. Eddy correlation measurements of air–sea CO₂ fluxes in the Laptev Sea in the summer period. *Doklady Earth Sci.* 413 (2), 452–456, <http://dx.doi.org/10.1134/S1028334X07030300>.
- Rödenbeck, C., 2005. Estimating CO₂ Sources and Sinks From Atmospheric Mixing Ratio Measurements Using a Global Inversion of Atmospheric Transport. Max-Planck Institute for Biogeochemistry, Jena, 53 pp.
- Sabine, C.L., Feely, R.A., Gruber, N., Key, R.M., Lee, K., Bullister, J.L., Wanninkhof, R., Wong, C.S., Wallace, D.W.R., Tilbrook, B., Millero, F.J., Peng, T.-H., Kozyr, A., Ono, T., Rios, A.F., 2004. The oceanic sink for anthropogenic CO₂. *Science* 305 (5682), 367–371, <http://dx.doi.org/10.1126/science.1097403>.
- Schuster, U., McKinley, G.A., Bates, N., Chevallier, F., Doney, S.C., Fay, A.R., González-Dávila, M., Gruber, N., Jones, S., Krijnen, J., Landschützer, P., Lefèvre, N., Manizza, M., Mathis, J., Metzl, N., Olsen, A., Rios, A.F., Rödenbeck, C., Santana-Casiano, J.M., Takahashi, T., Wanninkhof, R., Watson, A.J., 2013. An assessment of the Atlantic and Arctic sea–air CO₂ fluxes, 1990–2009. *Biogeochemistry* 10 (1), 607–627, <http://dx.doi.org/10.5194/bg-10-607-2013>.
- Sejr, M.K., Krause-Jensen, D., Rysgaard, R., Sørensen, L.L., Christensen, P.B., Glud, R.N., 2011. Air–sea flux of CO₂ in arctic coastal waters influenced by glacial melt water and sea ice. *Tellus B* 63 (5), 815–822.
- Semiletov, I.P., Makshtas, A., Akasofu, S.-I., Andreas, L.A., 2004. Atmospheric CO₂ balance: the role of the Arctic sea ice. *Geophys. Res. Lett.* 31 (5), L05121, 4 pp., <http://dx.doi.org/10.1029/2003GL017996>.
- Shutler, J.D., Piolle, J.-F., Land, P.E., Woolf, D.K., Goddijn-Murphy, L., Paul, F., Girard-Arduin, F., Chapron, B., Donlon, C.J., 2016. FluxEngine: a flexible processing system for calculating atmosphere–ocean carbon dioxide gas fluxes and climatologies. *J. Atmos. Ocean. Technol.* 33 (4), 741–756, <http://dx.doi.org/10.1175/JTECH-D-14-00204.1>.
- StatSoft Inc., 2013. Electronic Statistical Textbook. StatSoft. WEB, Tulsa, OK, <http://www.statsoft.com/textbook/>.
- Takahashi, T., Sutherland, S.C., Sweeney, C., Poisson, A., Metzl, N., Tilbrook, B., Bates, N., Wanninkhof, R., Feely, R.A., Sabine, C., Olafsson, J., Nojiri, Y., 2002. Global sea–air CO₂ flux based on climatological surface ocean pCO₂, and seasonal biological and temperature effects. *Deep-Sea Res. Pt. II* 49 (9–10), 1601–1622, [http://dx.doi.org/10.1016/S0967-0645\(02\)00003-6](http://dx.doi.org/10.1016/S0967-0645(02)00003-6).
- Takahashi, T., Sutherland, S.C., Kozyr, A., 2008. Global Ocean Surface Water Partial Pressure of CO₂ Database: Measurements

- Performed during 1968–2006 (Version 1.0). ORNL/CDIAC-152, NDP-088, Carbon Dioxide Information Analysis Center, Oak Ridge National Laboratory. U.S. Department of Energy, Oak Ridge, TN, p. 37831.
- Takahashi, T., Sutherland, S.C., Wanninkhof, R., Sweeney, C., Feely, R.A., Chipman, D.W., Hales, B., Friederich, G., Chavez, F., Sabine, C., Watson, A., Bakker, D.C.E., Schuster, U., Metzl, N., Yoshikawa-Inoue, H.Y., Ishii, M., Midorikawa, T., Nojiri, Y., Körtzinger, A., Steinhoff, T., Hoppema, M., Olafsson, J., Arnarson, T. S., Tilbrook, B., Johannessen, T., Olsen, A., Bellerby, R., Wong, C. S., Delille, B., Bates, N.R., de Baar, H.J.W., 2009. Climatological mean and decadal change in surface ocean pCO₂ and net sea–air CO₂ flux over the global oceans. *Deep-Sea Res. II* 56 (8–10), 554–577, <http://dx.doi.org/10.1016/j.dsr2.2008.12.009>.
- Telszewski, M., Chazottes, A., Schuster, U., Watson, A.J., Moulin, C., Bakker, D.C.E., González-Dávila, M., Johannessen, T., Körtzinger, A., Lüger, H., Olsen, A., Omar, A., Padin, X.A., Ríos, A.F., Steinhoff, T., Santana-Casiano, M., Wallace, D.W.R., Wanninkhof, R., 2009. Estimating the monthly pCO₂ distribution in the North Atlantic using a self-organizing neural network. *Biogeosciences* 6 (10), 1405–1421, <http://dx.doi.org/10.5194/bg-6-1405-2009>.
- Thomas, H., Bozec, Y., Elkalay, K., de Baar, H.J.W., 2004. Enhanced open ocean storage of CO₂ from Shelf Sea pumping. *Science* 304 (5673), 1005–1008, <http://dx.doi.org/10.1126/science.1095491>.
- Wanninkhof, R., McGillis, W.R., 1999. A cubic relationship between air–sea CO₂ exchange and wind speed. *Geophys. Res. Lett.* 26 (13), 1889–1892.
- Wanninkhof, R., Asher, W.E., Ho, D.T., Sweeney, C.S., McGillis, W.R., 2009. Advances in quantifying air–sea gas exchange and environmental forcing. *Ann. Rev. Mar. Sci.* 1, 213–244, <http://dx.doi.org/10.1146/annurev.marine.010908.163742>.
- Wanninkhof, R., Park, G.-H., Takahashi, T., Sweeney, C., Feely, R., Nojiri, Y., Gruber, N., Doney, S.C., McKinley, G.A., Lenton, A., Le Quéré, C., Heinze, C., Schwinger, J., Graven, H., Khaliwala, S., 2013. Global ocean carbon uptake: magnitude, variability and trends. *Biogeosciences* 10 (3), 1983–2000, <http://dx.doi.org/10.5194/bg-10-1983-2013>.
- Weiss, R.F., Van Woy, F.A., Salameh, P.K., 1992. Surface Water and Atmospheric Gas Chromatography: Results From Expeditions Between 1977 and 1990. Scripps Institute of Oceanography. Carbon Dioxide Information Analysis, Centre Oak Ridge National Laboratory, NDP-044.
- Woolf, D.K., Goddijn-Murphy, L.M., Prytherch, J., Yelland, M.J., Nightingale, P.D., Shutler, J.D., Piolle, J.-F., Hanafin, J., Chapron, B., 2013. Appropriate treatment of uncertainty and ambiguity; a flexible system for climatological calculations in response to an on-going debate on the transfer velocity. *Proc. ESA Living Planet Symposium 2013*, Edinburgh, 9–13 September 2013, 8 pp., http://www.oceanflux-ghg.org/content/download/75643/973537/file/Woolf_et_al_LivingPlanet_2013.pdf.
- Wrobel, I., Piskozub, J., 2016. Effect of gas-transfer-velocity parameterizations choice on air–sea CO₂ fluxes in the North Atlantic and the European Arctic. *Ocean Sci.* 12 (5), 1091–1103, <http://dx.doi.org/10.5194/os-12-1091-2016>.
- Yasunaka, S., Murata, A., Watanabe, E., Chierici, M., Fransson, A., van Heuven, S., Hoppema, M., Ishii, M., Johannessen, T., Kosugi, N., Lauvset, S.V., Mathis, J.T., Nishino, S., Omar, A.M., Olsen, A., Sasano, D., Takahashi, T., Wanninkhof, R., 2016. Mapping of the air–sea CO₂ flux in the Arctic Ocean and its adjacent seas: basin-wide distribution and seasonal to interannual variability. *Polar Sci.* 10 (3), 323–334, <http://dx.doi.org/10.1016/j.polar.2016.03.006>.

3. Research paper no 3

Wróbel-Niedźwiecka, I., Drozdowska, V., Piskozub, J. 2019. *Effect of drag coefficient formula choice on wind stress climatology in the North Atlantic and the European Arctic*. Oceanologia, 61, 291-299, doi:10.1016/j.oceano.2019.02.002.



ORIGINAL RESEARCH ARTICLE

Effect of drag coefficient formula choice on wind stress climatology in the North Atlantic and the European Arctic

Iwona Wróbel-Niedźwiecka^{*}, Violetta Drozdowska, Jacek Piskozub

Institute of Oceanology, Polish Academy of Sciences, Sopot, Poland

Received 13 December 2018; accepted 26 February 2019
Available online 9 March 2019

KEYWORDS

Drag coefficient;
European Arctic;
North Atlantic;
Parameterizations

Summary Interactions between the atmosphere and the ocean determine boundary conditions for physical and biogeochemical processes in adjacent boundary layers, and the ocean surface is a complex interface where all air-sea fluxes take place and is a crucial valuable for ocean circulation and the ecosystem. We have chosen to study the differences between the relevant or most commonly used parameterizations for drag coefficient (C_D) for the momentum transfer values, especially in the North Atlantic (NA) and the European Arctic (EA), using them together with realistic wind field. We studied monthly mean values of air-sea momentum flux resulting from the choice of different drag coefficient parameterizations, adapted them to momentum flux (wind stress) calculations using wind fields, sea-ice masks, as well as integrating procedures. We compared the resulting spreads in momentum flux to global values and values in the tropics, an area of prevailing low winds. We found that the spread of results stemming from the choice of drag coefficient parameterization was 14% in the Arctic, the NA and globally, but it was higher (19%) in the tropics. On monthly time scales, the differences were larger at up to 29% in the NA and 36% in the EA (in months of low winds) and even 50% locally (the area west of Spitsbergen). Comparing the values of drag coefficient from chosen parameterizations, it showed that momentum fluxes were largest for all months, in both regions with low and high winds, when the C_D values increased linearly with wind speed.

© 2019 Institute of Oceanology of the Polish Academy of Sciences. Production and hosting by Elsevier Sp. z o.o. This is an open access article under the CC BY-NC-ND license (<http://creativecommons.org/licenses/by-nc-nd/4.0/>).

^{*} Corresponding author at: Institute of Oceanology, Polish Academy of Sciences, ul. Powstańców Warszawy 55, 81-712 Sopot, Poland.
Tel.: +48 587311801; fax: (+48 58) 551 21 30.

E-mail address: iwrobel@iopan.gda.pl (I. Wróbel-Niedźwiecka).

Peer review under the responsibility of Institute of Oceanology of the Polish Academy of Sciences.



Production and hosting by Elsevier

<https://doi.org/10.1016/j.oceano.2019.02.002>

0078-3234/© 2019 Institute of Oceanology of the Polish Academy of Sciences. Production and hosting by Elsevier Sp. z o.o. This is an open access article under the CC BY-NC-ND license (<http://creativecommons.org/licenses/by-nc-nd/4.0/>).

1. Introduction

The surface of the ocean is a complex boundary layer through which all air-sea fluxes of mass, momentum and energy take place. Determining the nature and consequences of exchanges between the atmosphere and the ocean is one of the greatest challenges in climate and sea studies, as well as ocean modelling and prediction. In this article we focus mainly on the surface momentum flux by which the atmospheric winds drive oceanic currents (so that the ocean acts as a sink for atmospheric momentum), which determine current system and sea state conditions and are most commonly parameterized using bulk aerodynamic formulae. Our goal is to evaluate how much the average monthly and annual momentum transfer values depend on the choice of non-dimensional drag coefficient (C_D), using the actual wind field from the North Atlantic (NA) and the European Arctic (EA), and demonstrate existing differences as a result of the formula used.

The ocean surface mixed layer is a region where kinematic forcing affects the exchange of horizontal momentum and controls transport from the surface to depths (Bigdeli et al., 2017; Gerbi et al., 2008). Any attempt to properly model the momentum flux from one fluid to another as the drag force per unit area at the sea surface (surface shear stress, τ) takes into account other physical processes responsible for generating turbulence such as boundary stress, boundary buoyancy flux, and wave breaking (Rieder et al., 1994; Toba et al., 2001). Fluxes across the sea surface usually depend nonlinearly on the relevant atmospheric or oceanic parameters. Over the past fifty years, as the collection of flux data has increased, many empirical formulas have been developed to express the ocean surface momentum flux as a relationship between C_D , wind speed (U_{10}), and surface roughness (z_0) (Andreas et al., 2012; Bunker, 1976; Donelan et al., 1997; Garratt, 1977; Kukulka et al., 2007; Large and Pond, 1981; Trenberth et al., 1989; Wu, 1969, 1982; Yelland and Taylor, 1996). These formulas can be divided into two groups. One group of theories gives the C_D at level z in terms of wind speed and possibly one or more sea-state parameters (for example, Enriquez and Friehe, 1997; Geernaert et al., 1987; Yelland and Taylor, 1996), while the second group provides formulas for roughness length z_0 in terms of atmospheric and sea-state parameters (for example, Andreas et al., 2012 (further referred to as A12), Donelan et al., 1997; Wu, 1969).

As the exchange of air-sea momentum is difficult to measure directly over the ocean, meteorologist and oceanographers often rely on bulk formulas first parameterized by Taylor (1916), that relate the fluxes to averaged wind speed through transfer coefficients:

$$\tau = \rho C_{Dz} U_z^2, \quad (1)$$

where τ is the momentum flux of surface stress, ρ is air density, C_{Dz} is the non-dimensional drag coefficient appropriate for z height, and U_z is the average wind speed at some reference height z above the sea. C_{Dz} is commonly identified as C_{DN10} or C_{D10} which is neutral-stability, 10-m drag coefficient (Toba et al., 2001), defined as:

$$C_{DN10} = \frac{\tau}{\rho U_{10}^2} = \left(\frac{u_*}{U_{10}} \right)^2, \quad (2)$$

where u_* is friction velocity. Alternatively, the neutrally stratified momentum flux can be determined from the logarithmic profile, thus Eq. (1) can be expressed as:

$$C_{DN10} = \left[\frac{\kappa}{\ln(10/z_0)} \right]^2, \quad (3)$$

where z_0 [m] is the aerodynamic roughness length, which is the height, above the surface to define the measure of drag at which wind speed extrapolates to 0 on the logarithmic wind profile (Andreas et al., 2012), and κ is von Kármán constant ($\kappa = 0.4$).

At the same time, we can define the value of friction velocity by the following equation:

$$\tau = \rho u_*^2. \quad (4)$$

Comparison with bulk formula (1) leads to the equation:

$$u_*^2 = C_{D10} U_{10}^2. \quad (5)$$

Some of the first studies (Garratt, 1977; Wu, 1969, 1982) focused on the relationship between wind stress and sea surface roughness, as proposed by Charnock (1955), and they formulated (for winds below 15 m s^{-1}) the logarithmic dependence of the stress coefficient on wind velocity (measured at a certain height) and the von Kármán constant. Currently common parameterizations of the drag coefficient are a linear function of 10 m wind speed (U_{10}), and the parameters in the equation are determined empirically by fitting observational data to a curve. The general form is expressed as (Guan and Xie, 2004):

$$C_D 10^3 = (a + b U_{10}). \quad (6)$$

In this work our focus is on the average flux values using seven different drag coefficient parameterizations (Table 1), chosen for their importance for the history of the field out of many published within the last half century (Bryant and Akbar, 2016).

All of the parameterizations are generated from the vertical wind profile, but they differ in the formulas used. Two of the parameterizations which we chosen are formulated as power-law of the relationship between C_D and U_{10} (Eq. (7) and (13) in Table 1), three are formulated as linear-law (Eqs. (8)–(10) and (12) in Table 1), and one as constant value of the relationship (Eq. (11) in Table 1). All the above studies propose different parameterizations (see Fig. 1) for the drag coefficient and the function of wind speed, which reflects the difficulties in simultaneously measuring at high sea stress (or friction velocity) and wind speed.

Wu (1969) compiled data from 12 laboratory studies and 30 oceanic observations, formulated power-law (for breezes and light winds) and linear-law (for strong winds) relationships between the wind-stress coefficient (C_z) and wind velocity (U_{10}) at a certain height z at various sea states. In his study, he used roughness Reynolds numbers to characterize the boundary layer flow conditions, and he assumed that the sea surface is aerodynamically smooth in the range of $U_{10} < 3 \text{ m s}^{-1}$, transient at wind speed $3 \text{ m s}^{-1} < U_{10} < 7 \text{ m s}^{-1}$, and aerodynamically rough at strong winds $U_{10} > 7 \text{ m s}^{-1}$. He also showed that the wind-stress coefficient and surface roughness increase with wind speed at light winds ($U_{10} < 15 \text{ m s}^{-1}$) and is constant at high winds ($U_{10} > 15 \text{ m s}^{-1}$) with aerodynamically rough flow.

Table 1 Neutral drag coefficient values over the ocean taken from the recent literature for a reference height of 10 m: C_{D10} is the drag coefficient dependent on surface roughness, C_{DN10} is the expression of neutral-stability (10-m drag coefficient), U_{10} is the mean wind speed measured at 10 m above the mean sea surface, U_{10N} is the 10-m neutral-stability wind speed, and a and b are proportionality constant.

Eq. no.	Source	Wind speed range [m s^{-1}]	$C_{DN(10)} (\times 10^3)$
7	Wu (1969)	1–15	$0.5U_{10}^{0.5}$
8	Garratt (1977)	4–21	$0.75 + 0.067U_{10}$
9	Wu (1982)	>1	$0.8 + 0.065U_{10}$
10	Yelland and Taylor (1996)	3–6	$0.29 + \frac{3.1}{U} + \frac{7.7}{U_{10N}^2}$
		6–26	$0.60 + 0.070U_{10N}$
11	NCEP/NCAR	Everywhere	1.3
12	Large and Yeager (2004)	Everywhere	$\frac{2.7}{U_{10N}} + 0.142 + 0.076U_{10N}$
13	Andreas et al. (2012)	Everywhere	$\left(\frac{u_*}{U_{10N}}\right)^2 = a^2 \left(1 + \frac{b}{a}U_{10N}\right)^2$ $a = 0.0583, b = -0.243$

Garratt (1977), who assessed the 10 m neutral drag coefficient (C_{DN10}) based on 17 publications, confirmed the previous relationship and simultaneously suggested a linear form of this relationship for light wind. Wu (1980) proposed the linear-law formula for all wind velocities and later (Wu, 1982) extended this even to hurricane wind speeds. Yelland and Taylor (1996) presented results obtained from three cruises using the inertial dissipation method in the Southern Ocean and indicate that using the linear-law relationship between the drag coefficient and wind speed (for $U_{10} > 6 \text{ m s}^{-1}$) is better than using u_* with U_{10} . The NCEP/NCAR reanalysis (Kalnay et al., 1996) uses a constant drag coefficient of 1.3×10^{-3} while, for example, the Community Climate System Model version 3 (Collins et al., 2006) uses a single mathematical formula proposed by Large and Yeager (2004)

for all wind speeds. Andreas et al. (2012) based on available datasets, friction velocity coefficient versus neutral-stability wind speed at 10 m, and sea surface roughness tested the approach proposed by Foreman and Emeis (2010) for friction velocity in order to find the best fit for parameters $a = 0.0583$ and $b = -0.243$. They justify their choice by demonstrating that u_* vs. U_{10N} has smaller experimental uncertainty than C_{DN10} , and that one expression of C_{DN10} for all wind speeds overstates and overestimates results in low and high winds (Figs. 7 and 8 in A12).

In this paper we investigate how the relevant or most commonly used parameterizations for drag coefficient (C_D) affect value of momentum transfer values, especially in the North Atlantic and the European Arctic. Our task was to demonstrate how big differences can be as a result of the

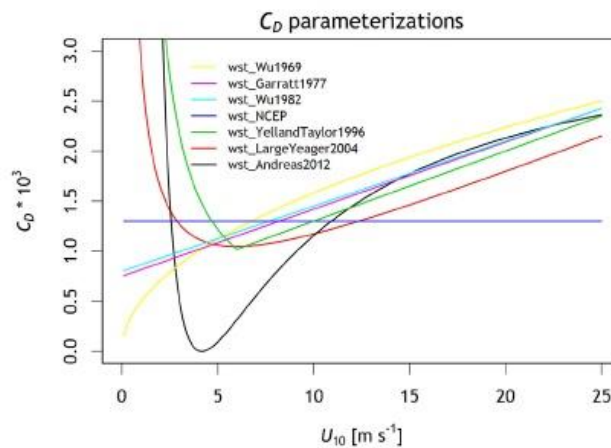


Figure 1 The drag coefficient parameterization used in the study (Eqs. (7)–(13) in Table 1) as a function of wind speed U_{10} [m s^{-1}].

formula used. As is widely known, the exact equation that describes the connection between the drag coefficient and wind speed depends on the author (Geernaert, 1990). Our intention here is not to re-invent or formulate a new drag parameterization for the NA or the EA, but to revisit the existing definition of drag parameterization, and, using satellite data, to investigate how existing formulas represent the environment in the North Atlantic Ocean. We concentrated on wind speed parameterizations, because wind speed is a parameter that is available in every atmospheric circulation model. Therefore, it is used in all air-sea flux parameterizations, and presently it is used even when sea state provides a closer physical coupling to the drag coefficient (for review see Geernaert et al., 1986).

2. Material and methods

We calculated monthly and annual mean momentum fluxes using a set of software processing tools called the FluxEngine (Shutler et al., 2016), which was created as part of the OceanFlux Greenhouse Gases project funded by the European Space Agency (ESA). Since the toolbox, for now, is designed to calculate only air-sea gas fluxes but it does contain the necessary datasets for other fluxes, we made minor changes in the source code by adding parameterizations for the air-sea drag relationship. For the calculations, we used Earth Observation (EO) U_{10} for 1992–2010 from the GlobWave project (<http://globwave.ifremer.fr/>). GlobWave produced a 20-year time series of global coverage multi-sensor cross-calibrated wave and wind data, which are publicly available via the Ifremer/CERSAT cloud. Satellite scatterometer derived wind fields are at present believed to be at least equally as good as wind products from reanalyses (see, for

example, Dukhovskoy et al., 2017) for the area of our interest in the present study. The scatterometer derived wind values are calibrated to the U_{10N} , and, therefore, are fit for use with the neutral-stability drag coefficient (Chelton and Freilich, 2005). All data came in netCDF-4 format. The output data is a compilation file that contains data layers, and process indicator layers. The data layers within each output file, which are part of the FluxEngine, include statistics of the input datasets (e.g., variance of wind speed, percentage of ice cover), while the process indicator layers include fixed masks as land, open ocean, coastal classification, and ice.

All analyses using the global data contained in the FluxEngine software create a gridded ($1^\circ \times 1^\circ$) product. The NA was defined as all sea areas in the Atlantic sector north of 30°N , and the EA subset was those sea areas north of 64°N (Fig. 2). We also defined the subset of the EA east of Svalbard (“West Svalbard” between 76° and 80°N and 10° to 16°E), because it is a region that is studied intensively by multiple, annual oceanographic ship deployments (including that of the *r/v Oceania*, the ship of the institution the authors are affiliated with). FluxEngine treats areas with sea-ice presence in a way that is compatible with Lüpkes et al. (2012) multiplying the water drag coefficient by the ice-free fraction of each grid element. We also define “tropical ocean” as all areas within the Tropics (23°S to 23°N) in order to test the hypothesis that the new A12 parameterization will produce significantly lower wind stress values in the region.

3. Results and discussion

Some of the parameterizations used were limited to a restricted wind speed domain. We used them for all the global wind speed data to avoid data gaps for winds that

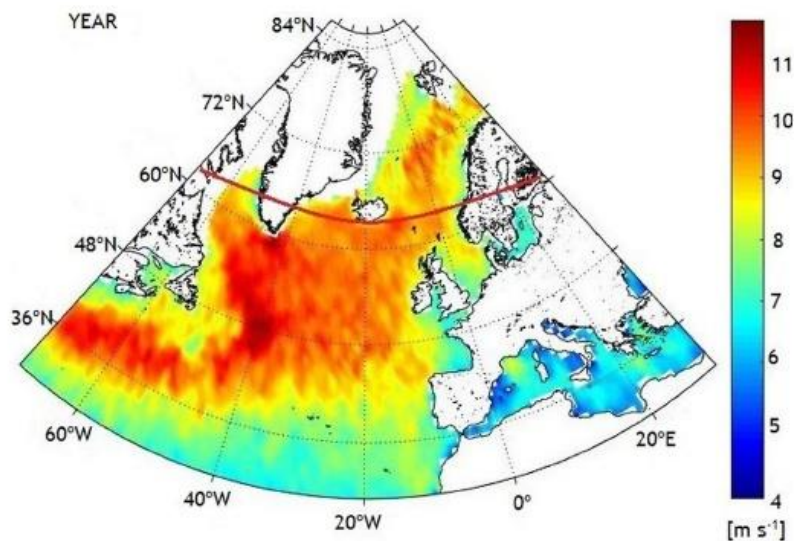


Figure 2 Annual mean wind speed U_{10} [m s^{-1}] in the study area – the North Atlantic and the European Arctic (north of the red line). (For interpretation of the references to color in this figure legend, the reader is referred to the web version of this article.)

were too high or too low for a given parameterization (Fig. 1). Results from those calculation are available online under the link in Ocean Science Discussion <https://www.ocean-sci-discuss.net/os-2018-61/>.

Since wind velocity was used to estimate C_D , Fig. 1 shows a wide range of empirical formulas and Fig. 2 shows annual mean wind speed U_{10} [m s^{-1}] in the NA and the EA. The differences between the parameterizations are distinct (Fig. 1). The C_D values from the parameterizations 7–9 (Table 1) increased linearly with wind speed while the results from the parameterizations 10, 12, 13 (Table 1) decreased at low winds speed (for $U_{10} < 10 \text{ m s}^{-1}$). Despite many measurements, the drag coefficient still has wide variability at low and moderate wind speeds. Our results showed that at lower wind values ($< 10 \text{ m s}^{-1}$) the differences between the drag coefficient parameterizations are greater than at higher speeds ($> 10 \text{ m s}^{-1}$) and the most outlier results are those obtained from the power law parameterization of A12. The lower the wind speed, the higher the uncertainty are, and at low winds it is uncertainty by a factor of 0.5–1.5 depending on the formula used, while at moderate winds it is uncertainty by a factor of 1.5–2.0 (Fig. 1). At a wind value of about 15 m s^{-1} , the results from Eqs. (8), (9) and (13) (Table 1) overlapped providing the same values for the drag coefficient parameterizations. Additionally, we compared directly the results of the two parameterizations for the drag air-sea relation that uses different dependencies (Fig. 1). For this estimation we chose the two most-recent parameterizations (Eqs. (12) and (13) in Table 1) that showed the lowest values

and change seasonally depending on the area used. As a result, these months with weak winds have significantly lower momentum flux values, which could be the effect of statistically weaker wind in ocean areas having stable winds with waves travelling in the same direction as the wind at similar speeds. Comparison showed that the A12 parameterization demonstrates almost zero sea surface drag for winds in the range of $3\text{--}5 \text{ m s}^{-1}$, which is compensated for by a certain surplus value for strong winds. The small drag coefficient values facilitate what Grachev and Fairall (2001) describe as the transfer of momentum from the ocean to the atmosphere at wind speeds of $2\text{--}4 \text{ m s}^{-1}$, which correspond to the negative drag coefficient value. Such events require specific meteorologist conditions, but this strongly suggests that the average C_D value for similar wind speeds could be close to zero. The annual mean wind speed in the NA is 10 m s^{-1} , and in the EA it is 8.5 m s^{-1} (Fig. 2).

Fig. 3 presents maps of the mean boreal winter DJF and summer JJA momentum fluxes for the chosen C_D parameterizations (Wu, 1969 and A12 – the ones with the largest and smallest C_D values). The supplementary materials contain complete maps of annual and seasonal means for all the parameterizations. The zones of the strongest winds are in the extra-tropics in the winter hemisphere (southern for JJA and northern for DJF). The older Wu (1969) parameterization produces higher wind stress values than A12 in both regions with high and low winds and C_D values are consistently higher for all wind speeds except the lowest ones (which, after multiplying by U^2 , produced negligible differences in wind

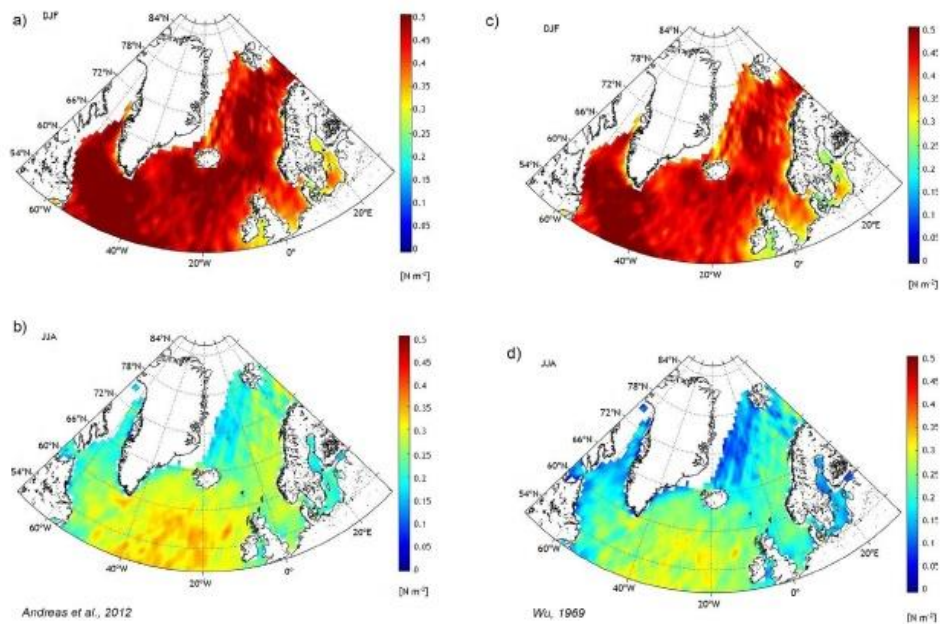


Figure 3 Maps of momentum flux [N m^{-2}] across the sea surface (wind stress) for boreal winters (a and c) and summers (b and d) for Wu (1969) and A12 drag coefficient parameterizations (the two parameterizations with the highest and lowest average values, respectively).

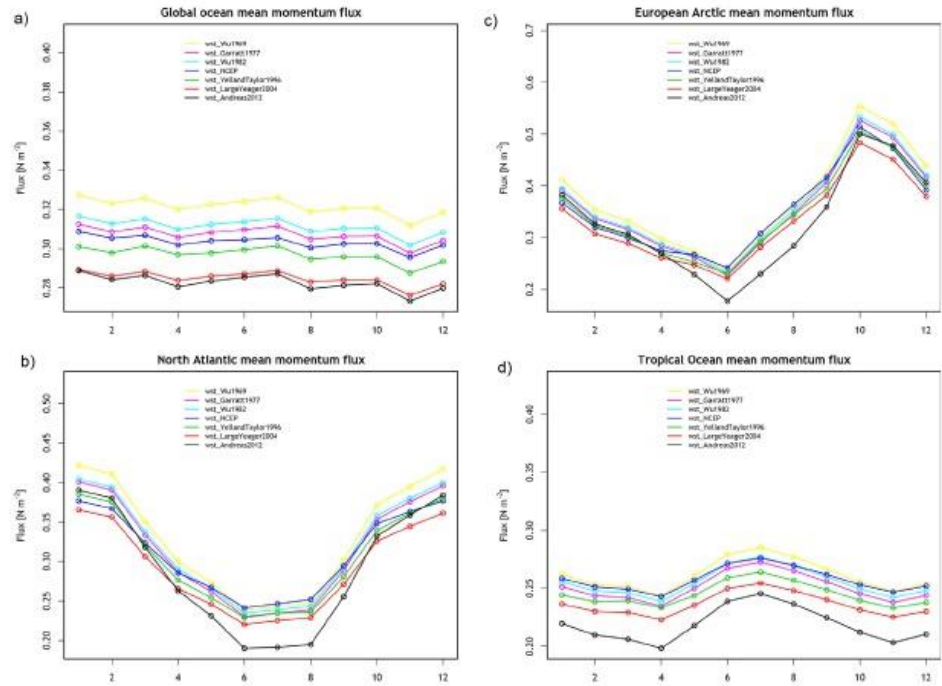


Figure 4 Monthly average momentum flux values [N m^{-2}] for (a) global ocean, (b) North Atlantic, (c) European Arctic, and (d) tropical ocean. The regions are defined in the text.

stress for the lowest winds). The average monthly values for each of the studied areas are shown in Fig. 4. For global data (Fig. 4a), not much seasonal change is noted, because the strongest winds are in fall and winter, but these seasons are

the opposite in the northern and southern hemispheres. The parameterization with the largest momentum flux values for all months is that of Wu (1969), the linear one, while the two parameterizations with the lowest values are the sinusoidal

	Global	North Atlantic	Arctic	W. Spitsbergen	Tropics
Wu (1969)	0.322 (114%)	0.330 (114%)	0.375 (114%)	0.360 (114%)	0.261 (119%)
Garratt (1977)	0.307 (109%)	0.316 (109%)	0.358 (109%)	0.344 (110%)	0.251 (115%)
Wu (1982)	0.311 (110%)	0.320 (110%)	0.363 (110%)	0.349 (111%)	0.255 (117%)
NCEP/NCAR	0.303 (107%)	0.312 (107%)	0.353 (107%)	0.341 (108%)	0.258 (118%)
Yelland and Taylor (1996)	0.297 (105%)	0.306 (105%)	0.348 (106%)	0.335 (107%)	0.245 (112%)
Large and Yeager (2004)	0.285 (101%)	0.293 (101%)	0.333 (101%)	0.320 (102%)	0.236 (108%)
Andreas et al. (2012)	0.283 (100%)	0.290 (100%)	0.329 (100%)	0.314 (100%)	0.219 (100%)

ones (A12; Large and Yeager, 2004). For the NA (Fig. 4b), much more pronounced seasonal wind changes, the situation is more complicated. With high winter winds, the A12 parameterization is no longer the one that produces the smallest wind stress (it is actually in the middle of the seven). However, for low summer winds, it is the lowermost outlier. Actually, in summer, the constant C_D value used by the NCEP/NCAR reanalysis produces the highest wind stress values in the NA. The situation is similar for the EA (a subset of the NA), the wind stress values of which are shown in Fig. 4c, and for the WS area (not shown). In the Arctic summer, A12 produces the least wind stresses, while all the other parameterizations

look very similar qualitatively (even more so in the Arctic than in the whole NA). Because the A12 parameterization behaves so distinctly differently with low winds, we also show seasonal results for the tropical ocean (Fig. 4d). The seasonal changes are subdued for the whole tropical ocean with the slight domination of the Southern Hemisphere (the strongest winds are during the boreal summer) with generally lower momentum transfer values (monthly averages in the range of $0.2\text{--}0.3\text{ N m}^{-2}$ compared to $0.2\text{--}0.4\text{ N m}^{-2}$ for the NA and $0.2\text{--}0.5\text{ N m}^{-2}$ for the Arctic). The sequence of values for the parameterization is similar to that of the global ocean, but there are differences. Here the NCEP/NCAR constant

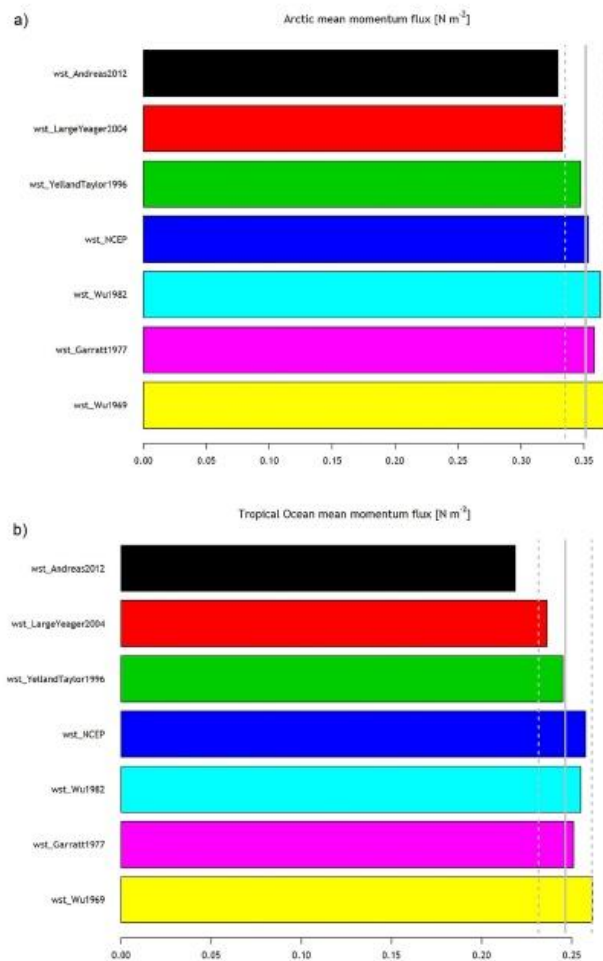


Figure 5 Area annual average momentum flux values for (a) European Arctic and (b) Tropical ocean. The vertical solid line is the average of all seven parameterization and the dashed lines are standard deviations for the presented values. Global and the North Atlantic results are not shown because the relative values for different parameterizations are very similar (see Table 2), scaling almost identically between the basins.

parameterization is the second highest (instead of Wu, 1982 for the global ocean) while, unlike in the case of the global ocean, A12 produces visibly lower values than does the Large and Yeager (2004) parameterization.

Table 2 and Fig. 5 present the annual average air-sea momentum flux values (in N m^{-2}) for all the regions studied and all the parameterizations. The results show that the annual North Atlantic momentum fluxes, depending on the formula used, varies from -0.290 N m^{-2} for A12 to 0.333 N m^{-2} for Wu (1969). In the case of global annual average, the values are -0.283 and 0.322 , respectively. Table 2 shows also the same data “normalized” to the A12 data (presented as percentages of A12, which produced the lowest values for each region), which allows us to visualize the relative differences. A surprising result is the annual ratios of the parameterizations values for the global, the NA, and the Arctic regions (Fig. 4 shows that this is not true on monthly scales). The spread of the momentum flux results is 14% in all three regions, and even flux values themselves are larger in the NA than globally and larger in the Arctic than in the whole of the NA basin. In the NA region with winds stronger than average for world ocean, the formula giving highest momentum transfer results are the ones with highest values for strong winds, with exception of Andreas et al. (2012) which is lower due to its low values for lower winds speeds. The smaller WS region, with winds that are, on average, weaker than those of the whole Arctic (but stronger than those of the whole NA), had slightly different ratios of the resultant fluxes. For the tropical ocean, which is included for comparison because of its weaker winds, the spread in momentum flux values on an annual scale is 19%. The spreads are even larger on monthly scales (not shown). The difference between A12 and Wu (1969) and NCEP/NCAR (the two parameterizations producing the largest fluxes on monthly scales) are 27% and 29% for the NA (in July), 31% and 36% for the Arctic (in June), 42% and 51% for the WS region (in July), and 23% and 22% for the tropical ocean (in April), respectively. Seasonality in the tropics is weak, therefore, the smallest monthly difference of 16% (July) is larger than the difference for the global data in any month (the global differences between the parameterizations have practically no seasonality). On the other hand, the smallest monthly differences between the parameterizations in the NA, the Arctic, and the WS regions are all 7%, in the month of the strongest winds (January).

Because the value of momentum flux is important for ocean circulation, its correct calculation in coupled models is very important, especially in the Arctic, where cold halocline stratification depends on the amount of mixing (Fer, 2009). We show that with the parameterization used in modelling, such as the NCEP/NCAR constant parameterization and Large and Yeager (2004), production stress results differ by about 5%, on average (both in the Arctic and globally), and the whole range of parameterizations leads to results that differ, on average, by 14% (more in low wind areas) and much more on monthly scales. One aspect that needs more research is the fact that the newest parameterization, A12, produces less momentum flux than all the previous ones, especially in lower winds (which, by the way, continues the trend of decreasing values throughout the history of the formulas discussed). The A12 parameterization is based on the largest set of measurements of friction

velocity as a function of wind speed and utilizes the recently discovered fact that b in equation (6) is not negligible. It also fits the observations that developed swell at low wind velocity has celerity which leads to zero or even negative momentum transfer (Grachev and Fairall, 2001). Therefore, the significantly lower A12 results for the tropical ocean (the trade wind region) and months of low winds elsewhere could mean that most momentum transfer calculations are overestimated. This matter needs further study, preferably with new empirical datasets. Based on our results, we still do not know which one of the parameterizations can be recommended as the most suitable for the NA and the EU study. Further investigation of the differences in the parameterization of the exchange coefficient in the various algorithm would help in resolving this problem.

4. Conclusions

In the present work, we assessed how the choice of parameterization affects the momentum fluxes when calculated on an ocean. This allows constraining of the uncertainty caused by the parameterization choice.

Despite many measurements, the drag coefficient still has wide variability at low and moderate wind speeds. The lower the wind speed, the higher the uncertainty are, and at low winds it is uncertainty by a factor of 0.5–1.5 depending on the formula used, while at moderate winds it is uncertainty by a factor of 1.5–2.0 (Fig. 1). The annual mean wind speed in the NA is 10 m s^{-1} , and in the EU it is 8.5 m s^{-1} .

We showed that the choice of drag coefficient parameterization can lead to significant differences in resultant momentum flux (or wind stress) values. Comparing the values of momentum flux across the sea surface from the power law parameterization, it showed that in both regions with low and high winds, the parameterizations specified for all wind speeds (Eq. (13) in Table 1) has lower values of wind stress than the parameterizations specified for light winds (Eq. (7) in Table 1). In the Arctic, the NA, and globally the differences between the wind stress, depending on formula used, are 14% and they are higher in low winds areas and can be much larger on monthly scales, up to 29% in the NA and 36% in the EA (in months of low winds), and even 50% locally in the area west of Spitsbergen. For months that have the highest average winds, the percentage differences are smaller (about 7% everywhere), but because the absolute value of the flux are largest for high winds, this 7% discrepancy is also important for air-sea momentum flux values.

Acknowledgements

We would like to express our gratitude to Ed Andreas for inspiring us. His untimely departure is an irreplaceable loss to the air-sea exchange community. We would also like to thank the entire OceanFlux team. This publication was financed with funds from the Centre for Polar Studies for the period 2014–2018, KNOW-Leading National Research Centre, Sosnowiec, Poland and from OceanFlux Greenhouse Gases Evolution, a project funded by the European Space Agency, ESRIN Contract No. 4000112091/14/I-LG with the help from National Science Centre funds, contract no. UMO-2016/21/N/ST10/00387.

Appendix A. Supplementary data

Supplementary data associated with this article can be found, in the online version, at [doi:10.1016/j.oceano.2019.02.002](https://doi.org/10.1016/j.oceano.2019.02.002).

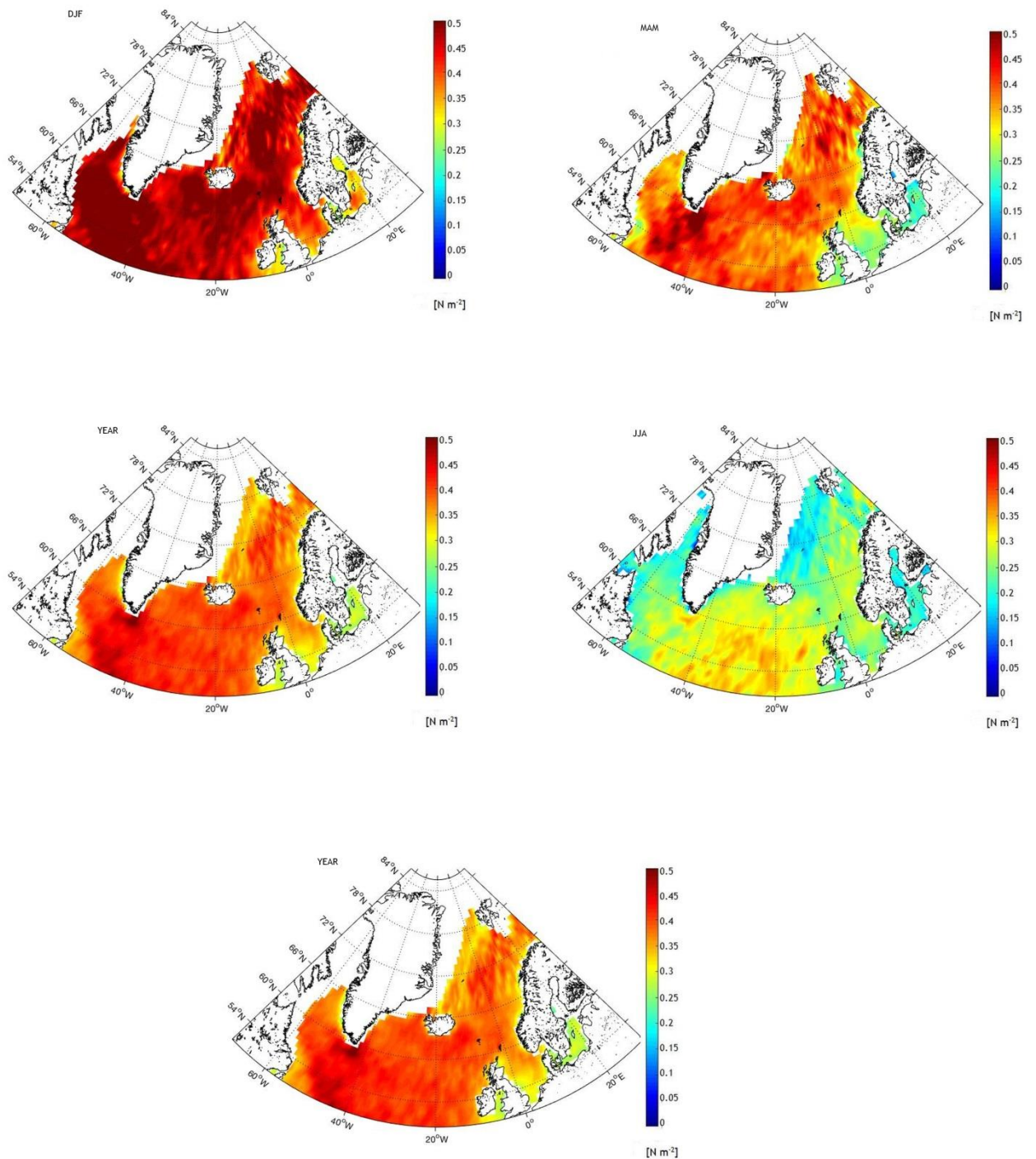
References

- Andreas, E.L., Mahrt, L., Vickers, D., 2012. A new drag relation for aerodynamically rough flow over the Ocean. *J. Atmos. Sci.* 69 (8), 2520–2539, [http://dx.doi.org/10.1175/JAS-D-11-0312.1](https://dx.doi.org/10.1175/JAS-D-11-0312.1).
- Bigdeli, A., Loose, B., Nguyen, A.T., Cole, S.T., 2017. Numerical investigation of the Arctic ice-ocean boundary layer and implications for air-sea gas fluxes. *Ocean Sci.* 13 (1), 61–75, [http://dx.doi.org/10.5194/os-13-61-2017](https://dx.doi.org/10.5194/os-13-61-2017).
- Bryant, K.M., Akbar, M., 2016. An exploration of wind stress calculation techniques in hurricane storm surge modeling. *J. Mar. Sci. Eng.* 4 (3), 58–83, [http://dx.doi.org/10.3390/jmse4030058](https://dx.doi.org/10.3390/jmse4030058).
- Bunker, A.F., 1976. Computations of surface energy flux and annual air-sea interaction cycles of the North Atlantic. *Ocean Mon. Weather Rev.* 104 (9), 1122–1140, [http://dx.doi.org/10.1175/1520-0493\(1976\)104<1122:COSEFA>2.0.CO;2](https://dx.doi.org/10.1175/1520-0493(1976)104<1122:COSEFA>2.0.CO;2).
- Charnock, H., 1955. Wind stress on a water surface. *Q. J. Roy. Meteorol. Soc.* 81, 639–640, [http://dx.doi.org/10.1002/qj.49708135027](https://dx.doi.org/10.1002/qj.49708135027).
- Chelton, D.B., Freilich, M.H., 2005. Scatterometer-based assessment of 10-m wind analyses from the operational ECMWF and NCEP numerical weather prediction models. *MWR Mon. Weather Rev.* 133, 409–429.
- Collins, W.D., Bitz, C.M., Blackmon, M.L., Bonan, G.B., Bretherton, S.C., Carton, A.J., Chang, P., Doney, S.C., Hack, J., Henderson, T.B., Kiehl, J.T., Large, W.G., McKenna, D.S., Santer, B.D., Smith, R.D., 2006. The Community Climate System Model version 3 (CCSM3). *J. Climate* 19 (11), 2122–2143, [http://dx.doi.org/10.1175/JCLI3761.1](https://dx.doi.org/10.1175/JCLI3761.1).
- Donelan, M.A., Drennon, W.M., Katsaros, K.B., 1997. The air-sea momentum flux in conditions of wind sea and swell. *J. Phys. Oceanogr.* 27 (10), 2087–2099, [http://dx.doi.org/10.1175/1520-0485\(1997\)027<2087:TASMF>2.0.CO;2](https://dx.doi.org/10.1175/1520-0485(1997)027<2087:TASMF>2.0.CO;2).
- Dukhovskoy, D.S., Bourassa, M.A., Peterson, G.N., Steffen, J., 2017. Comparison of the surface vector winds from atmospheric reanalysis and scatterometer-based wind products over the Nordic Seas and the northern North Atlantic and their application for ocean modeling. *J. Geophys. Res. - Oceans* 122, 1943–1973, [http://dx.doi.org/10.1002/2016JC012453](https://dx.doi.org/10.1002/2016JC012453).
- Enriquez, A.G., Friehe, C.A., 1997. Bulk parameterization of momentum, heat, and moisture fluxes over a coastal upwelling area. *J. Geophys. Res. - Oceans* 102 (C3), 5781–5798, [http://dx.doi.org/10.1029/96JC02952](https://dx.doi.org/10.1029/96JC02952).
- Fer, I., 2009. Weak vertical diffusion allows maintenance of cold halocline in the central Arctic. *Atmos. Oceanic Sci. Lett.* 2 (3), 148–152, [http://dx.doi.org/10.1080/16742834.2009.11446789](https://dx.doi.org/10.1080/16742834.2009.11446789).
- Foreman, R.J., Emeis, S., 2010. Revisiting the definition of the drag coefficient in the marine atmospheric boundary layer. *J. Phys. Oceanogr.* 40, [http://dx.doi.org/10.1175/2010JPO4420.1](https://dx.doi.org/10.1175/2010JPO4420.1).
- Garratt, J.R., 1977. Review of drag coefficients over oceans and continents. *Mon. Weather Rev.* 105 (7), 915–929, [http://dx.doi.org/10.1175/1520-0493\(1977\)105<0915:RODCOO>2.0.CO;2](https://dx.doi.org/10.1175/1520-0493(1977)105<0915:RODCOO>2.0.CO;2).
- Geernaert, G.L., 1990. Bulk parameterizations for the wind stress and heat flux. In: Geernaert, G.L., Plant, W.L. (Eds.), *Surface Waves and Fluxes*, vol. 1. Kluwer, 91–172.
- Geernaert, G.L., Katsaros, K.B., Richter, K., 1986. Variation of the drag coefficient and its dependence on sea state. *J. Geophys. Res.* 91 (C6), 7667–7679, [http://dx.doi.org/10.1029/JC091C06p07667](https://dx.doi.org/10.1029/JC091C06p07667).
- Geernaert, G.L., Larsen, S.E., Hansen, F., 1987. Measurements of the wind stress, heat flux, and turbulence intensity during storm conditions over the North Sea. *J. Geophys. Res. - Oceans* 92 (C13), 13127–13139, [http://dx.doi.org/10.1029/JC092iC13p13127](https://dx.doi.org/10.1029/JC092iC13p13127).
- Gerbi, G.P., Trowbridge, J.H., Edson, J.B., Plueddemann, A.J., Terray, E.A., Fredericks, J.J., 2008. Measurements of momentum and heat transfer across the air-sea interface. *J. Phys. Oceanogr.* 38 (5), 1054–1072, [http://dx.doi.org/10.1175/2007JPO3739.1](https://dx.doi.org/10.1175/2007JPO3739.1).
- Grachev, A.A., Fairall, C.W., 2001. Upward momentum transfer in the marine boundary layer. *J. Phys. Oceanogr.* 31 (7), 1698–1711, [http://dx.doi.org/10.1175/JPO2664.1](https://dx.doi.org/10.1175/JPO2664.1).
- Guan, C., Xie, L., 2004. On the linear parameterization of drag coefficient over sea surface. *J. Phys. Oceanogr.* 34 (12), 2847–2851, [http://dx.doi.org/10.1175/JPO2664.1](https://dx.doi.org/10.1175/JPO2664.1).
- Kalnay, E., Kanamitsu, M., Kistler, R., Collins, W., Daevan, D., Gandin, L., Iredell, M., Saha, S., White, G., Woollen, J., Zhu, Y., Chelliah, M., Ebisuzaki, W., Higgins, W., Janowiak, J., Mo, K.C., Ropelewski, C., Wang, J., Leetmaa, A., Reynolds, R., Jenne, R., Joseph, D., 1996. The NCEP/NCAR 40-year reanalysis project. *Bull. Am. Meteor. Soc.* 77 (3), 437–471.
- Kukulka, T., Hara, T., Belcher, S.E., 2007. A model of the air-sea momentum flux and breaking-wave distribution for strongly forced wind waves. *J. Phys. Oceanogr.* 37 (7), 1811–1828, [http://dx.doi.org/10.1175/JPO3084.1](https://dx.doi.org/10.1175/JPO3084.1).
- Large, W.G., Pond, S., 1981. Open ocean momentum flux measurements in moderate to strong winds. *J. Phys. Oceanogr.* 11 (3), 324–336, [http://dx.doi.org/10.1175/1520-0485\(1981\)011<0324:OOMFMI>2.0.CO;2](https://dx.doi.org/10.1175/1520-0485(1981)011<0324:OOMFMI>2.0.CO;2).
- Large, W.G., Yeager, S.G., 2004. Diurnal to decadal global forcing for ocean and sea-ice models: the data sets and flux climatologies. Technical Note NCAR/TN-460+STR. NCAR, Boulder, CO.
- Lüpkes, C., Gryanik, V.M., Hartmann, J., Andreas, E.L., 2012. A parameterization, based on sea-ice morphology, of the neutral atmospheric drag coefficients for weather prediction and climate models. *J. Geophys. Res. - Atmos.* 117 (D13), [http://dx.doi.org/10.1029/2012JD01763](https://dx.doi.org/10.1029/2012JD01763).
- Rieder, K.F., Smith, J.K., Weller, R.A., 1994. Observed directional characteristics of the wind, wind stress, and surface waves on the open ocean. *J. Geophys. Res. - Oceans* 99 (C11), 589–596, [http://dx.doi.org/10.1029/94JC02215](https://dx.doi.org/10.1029/94JC02215).
- Shutler, J.D., Piolle, J.-F., Land, P.E., Woolf, D.K., Goddijn-Murphy, L., Paul, F., Girard-Ardhuin, F., Chapron, B., Donlon, C.J., 2016. FluxEngine: a flexible processing system for calculating air-sea carbon dioxide gas fluxes and climatologies. *J. Atmos. Ocean. Technol.* 33 (4), 741–756, [http://dx.doi.org/10.1175/JTECH-D-14-00204.1](https://dx.doi.org/10.1175/JTECH-D-14-00204.1).
- Taylor, G.I., 1916. Skin friction of the wind on the Earth's surface. *Proc. Roy. Soc. London* A92, 196–199.
- Toba, Y., Smith, S.D., Ebuchi, N., 2001. Historical drag expressions. In: Jones, I.S.F., Toba, Y. (Eds.), *Wind Stress Over the Ocean*. Cambridge Univ. Press, New York, 35–53.
- Trenberth, K.E., Large, W.G., Olson, J.G., 1989. The effective drag coefficient for evaluating wind stress over the Oceans. *J. Climate* 2 (12), 1507–1516, <https://www.jstor.org/stable/26196243>.
- Wu, J., 1969. Wind stress and surface roughness at air-sea interface. *J. Geophys. Res.* 74 (2), 444–455, [http://dx.doi.org/10.1029/JB074i002p00444](https://dx.doi.org/10.1029/JB074i002p00444).
- Wu, J., 1980. Wind stress coefficients over the sea surface near neutral conditions – a revisit. *J. Phys. Oceanogr.* 10 (5), 727–740, [http://dx.doi.org/10.1175/1520-0485\(1980\)010<0727:WSCOSS>2.0.CO;2](https://dx.doi.org/10.1175/1520-0485(1980)010<0727:WSCOSS>2.0.CO;2).
- Wu, J., 1982. Wind-stress coefficients over sea surface from breeze to hurricane. *J. Geophys. Res.* 87 (C12), 9704–9706, [http://dx.doi.org/10.1029/JC087iC12p09704](https://dx.doi.org/10.1029/JC087iC12p09704).
- Yelland, M., Taylor, P.K., 1996. Wind stress measurements from the open ocean. *J. Phys. Oceanogr.* 26 (4), 541–558, [http://dx.doi.org/10.1175/1520-0485\(1996\)026<0541:WSMFTO>2.0.CO;2](https://dx.doi.org/10.1175/1520-0485(1996)026<0541:WSMFTO>2.0.CO;2).

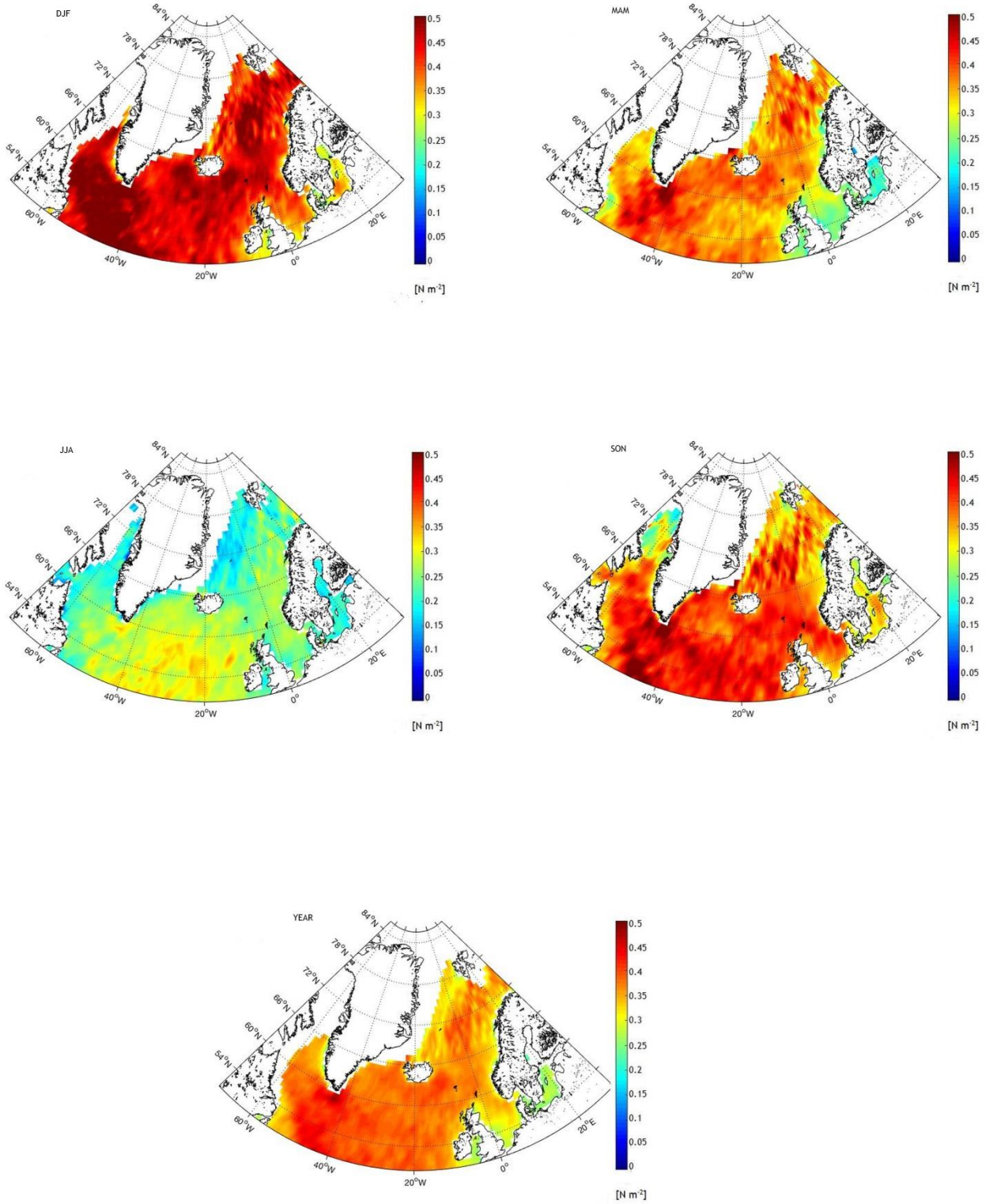
Supplementary material:

Fig. S1. Maps of seasonal and annual momentum flux [N m^{-2}] across the sea surface (wind stress) in the North Atlantic and the European Arctic for a) Wu (1969), b) Garratt (1977), c) Wu (1982), d) NCEP/NCAR, e) Yelland and Taylor (1996), f) Andreas et al., (2012). The supplementary material does not contained maps from Large and Yeager (2004) parameterization as during the transferring process the data indicate significant errors.

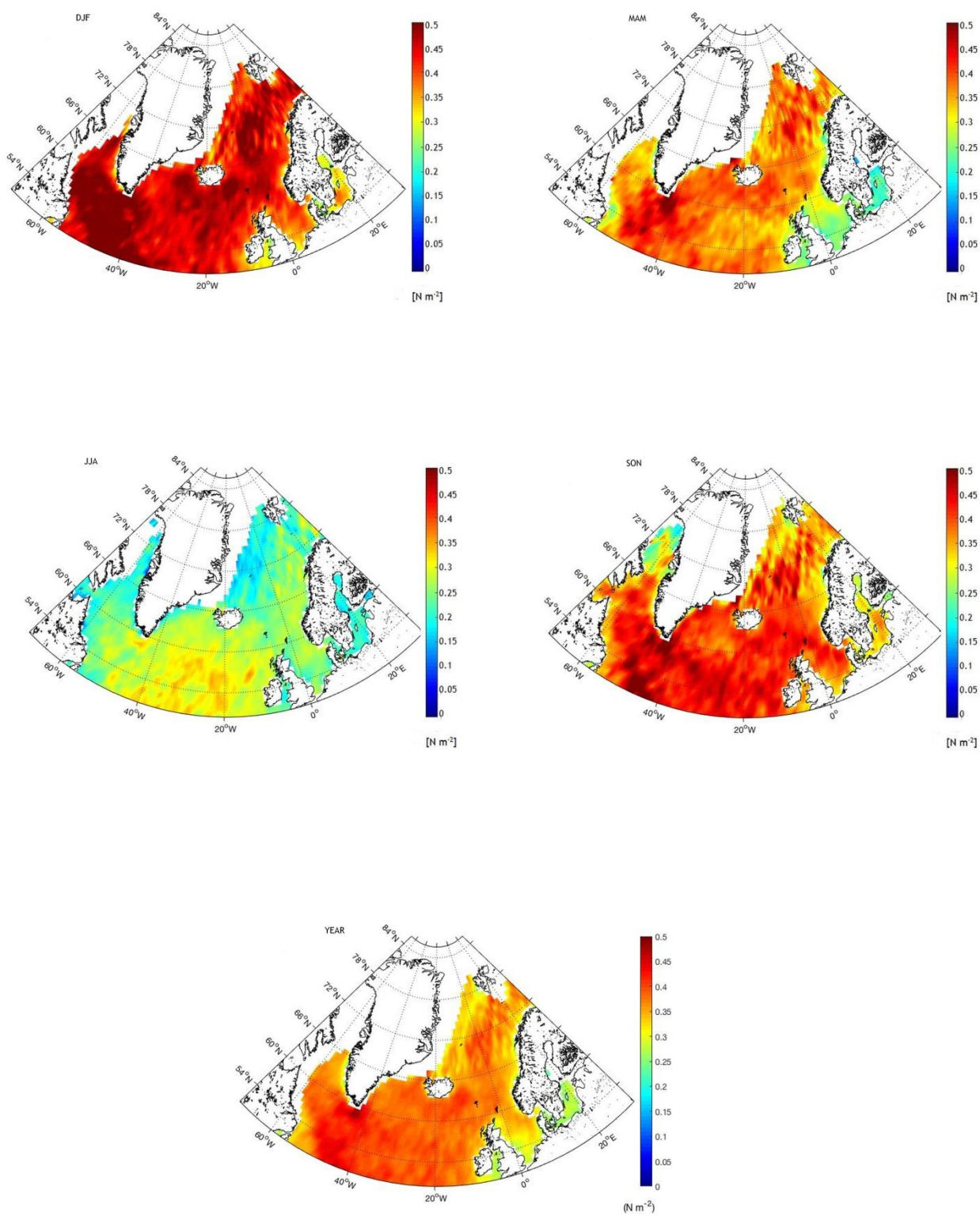
a) Wu (1969)



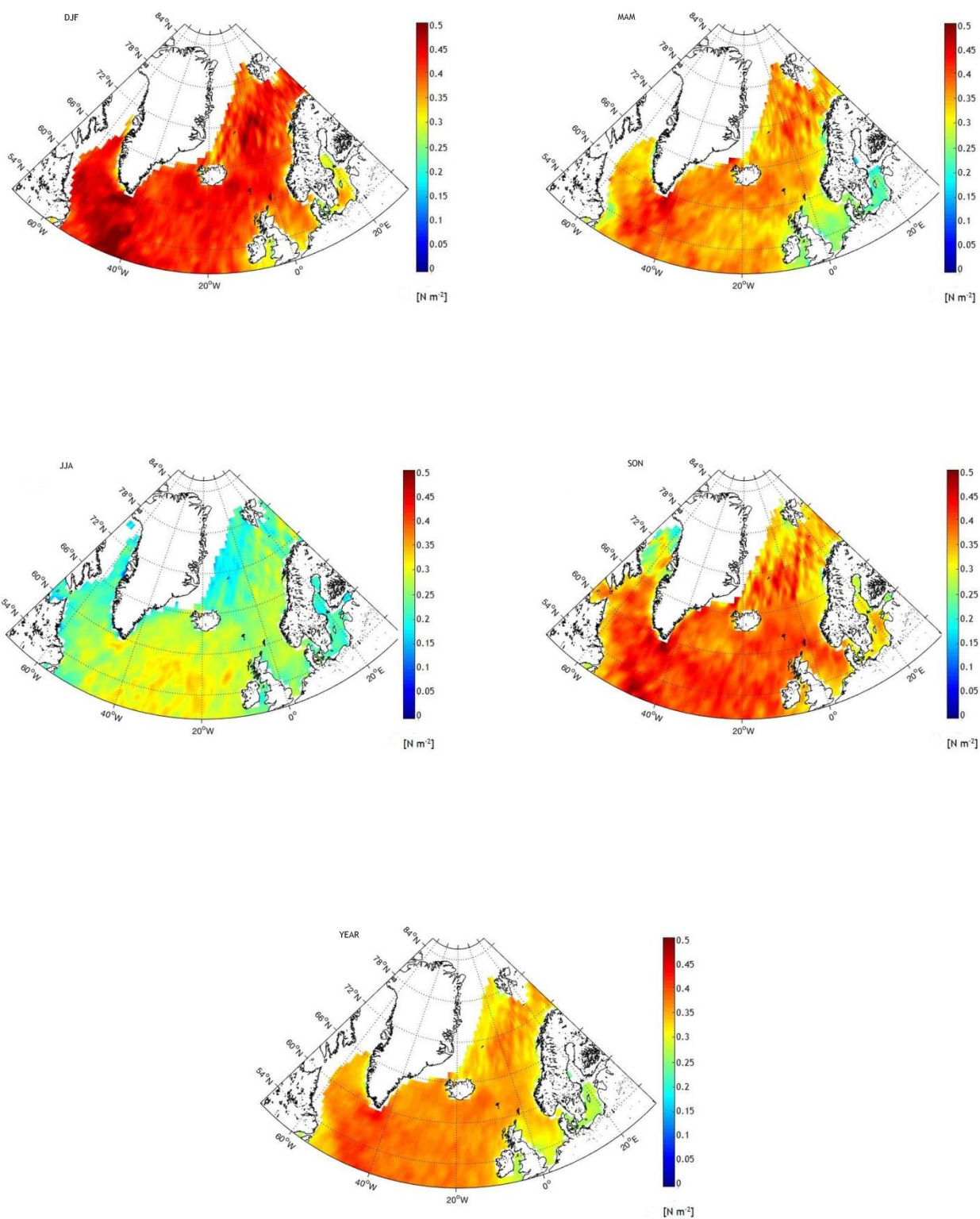
b) Garratt (1977)



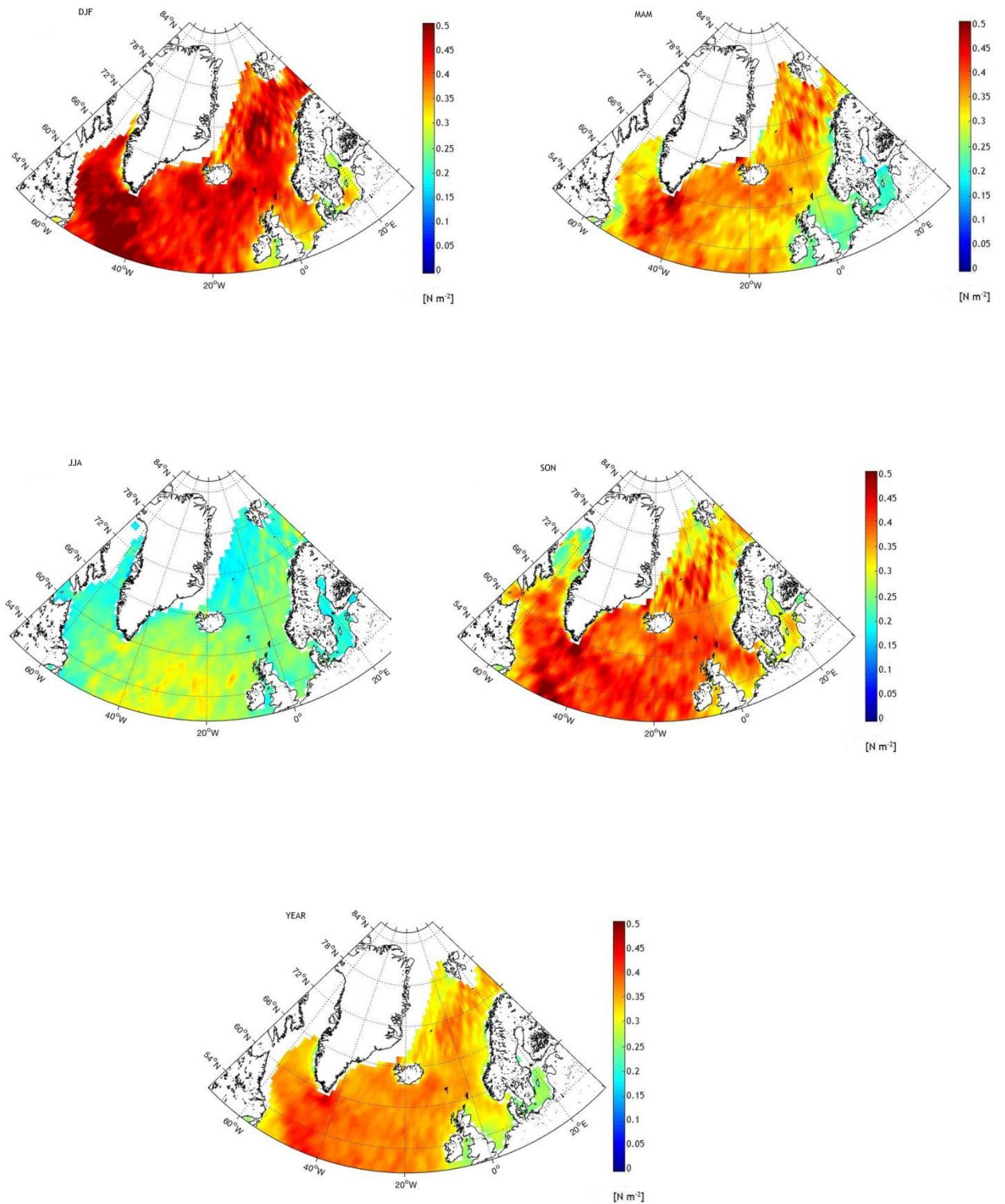
c) Wu (1982)



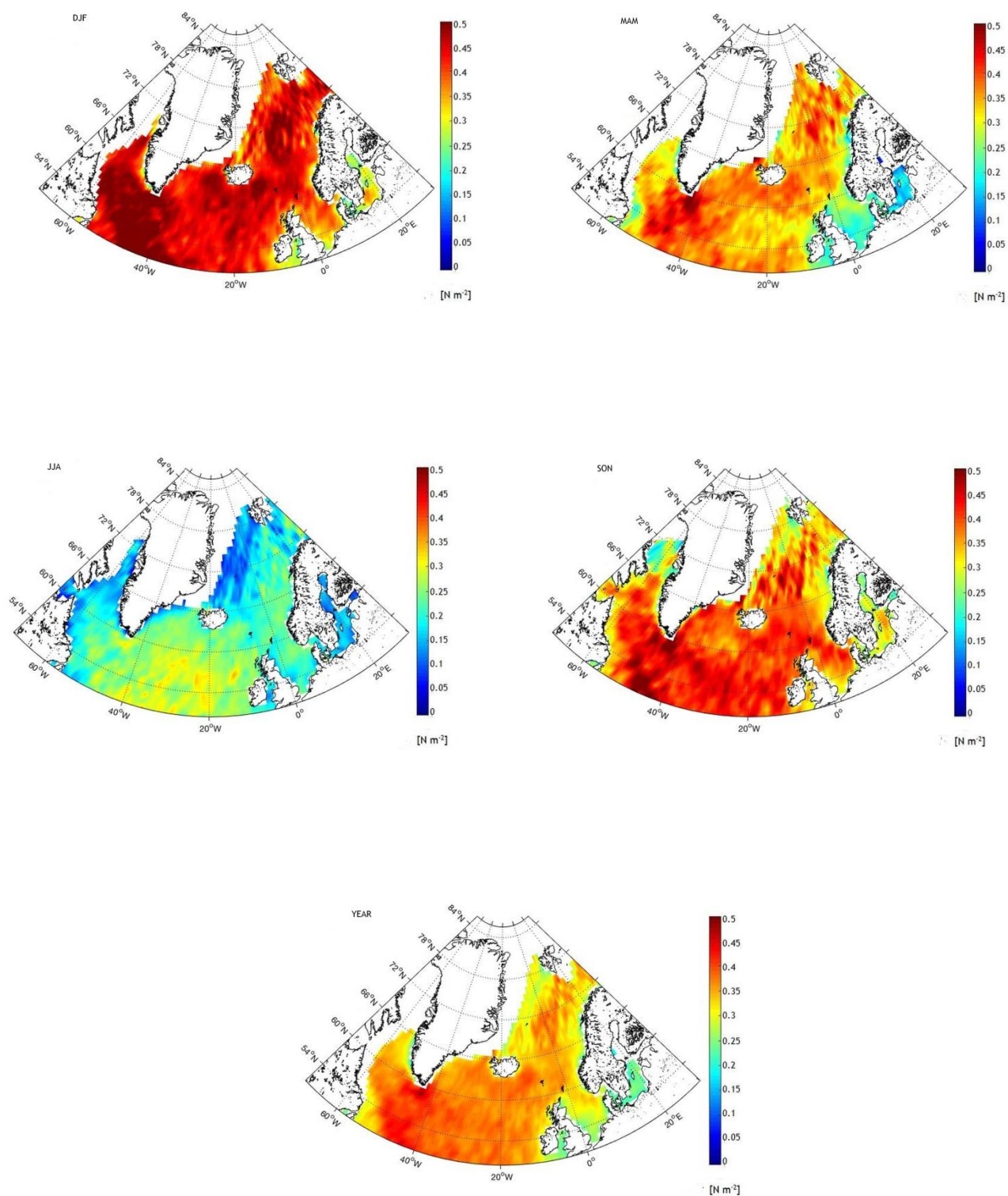
d) NCEP/NCAR



e) Yelland and Taylor (1996)



f) Andreas et al., (2012)



III. Authorship statements

mgr Iwona Niedźwiecka

Sopot, 28.05.2019

Institute of Oceanology Polish Academy of Sciences

Powstańców Warszawy 55

81-712 Sopot, Poland

AUTHORSHIP STATEMENT OF PhD CANDIDATE

I confirm that I am first and corresponding author of the articles:

1. Wróbel, I., Piskozub, J. 2016. Effect of gas-transfer velocity parameterization choice on air-sea CO₂ fluxes in the North Atlantic and the European Arctic. *Ocean Science* 12, 1091-1103.
2. Wróbel-Niedźwiecka, I., Drozdowska, V., Piskozub, J. 2019. *Effect of drag coefficient formula choice on wind stress climatology in the North Atlantic and the European Arctic*. *Oceanologia*, 61, 291-299.

I declare that my contribution (80%) to these articles included:

- design of the studies
 - data collected
 - data analysis
 - interpretation of the results
 - figures and the manuscript drafts preparation
 - writing and revisiting the manuscript
3. Wrobel, I. 2017. Monthly dynamics of carbon dioxide exchange across the sea surface of the Arctic Ocean in response to changes in gas transfer velocity and partial pressure of CO₂ in 2010. *Oceanologia*

I declare that my contribution (100%) to these articles included:

- Design of the study
- Data collected
- Data analysis

- Interpretation of the results
- Writing the manuscript
- Revisiting the manuscript

Michael Wans

dr Violetta Drozdowska

Sopot, 28.05.2019

Institute of Oceanology Polish Academy of Sciences

Powstańców Warszawy 55

81-712 Sopot, Poland

AUTHORSHIP STATEMENT OF CO-AUTHOR OF THE ARTICLES

I confirm that I am co-author of the articles:

1. Wróbel-Niedźwiecka, I., Drozdowska, V., Piskozub, J. 2019. *Effect of drag coefficient formula choice on wind stress climatology in the North Atlantic and the European Arctic*. Oceanologia, 61, 291-299.

I declare that my contribution (5%) to these articles included:

- Collecting the data
- writing and revisiting the manuscript



prof. Jacek Piskozub

Sopot, 28.05.2019

Institute of Oceanology Polish Academy of Sciences

Powstańców Warszawy 55

81-712 Sopot, Poland

AUTHORSHIP STATEMENT OF CO-AUTHOR OF THE ARTICLES

I confirm that I am co-author of the articles:

1. Wróbel, I., Piskozub, J. 2016. Effect of gas-transfer velocity parameterization choice on air-sea CO₂ fluxes in the North Atlantic and the European Arctic. *Ocean Science* 12, 1091-1103.

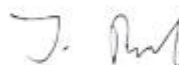
I declare that my contribution (20%) to these articles included:

- interpretation of the results
- figures preparation
- writing and revisiting the manuscript

2. Wróbel-Niedźwiecka, I., Drozdowska, V., Piskozub, J. 2019. *Effect of drag coefficient formula choice on wind stress climatology in the North Atlantic and the European Arctic*. *Oceanologia*, 61, 291-299.

I declare that my contribution (15%) to these articles included:

- interpretation of the results
- figures preparation
- writing and revisiting the manuscript



IV. Acknowledgements

Presented studies were carried out in the Physical Oceanography Department of the Institute of Oceanology Polish Academy of Sciences in Sopot, Poland.

Research described in this dissertation was supported by OceanFlux Greenhouse Gases Evolution, a project funded by the European Space Agency, ESRIN contract no. 4000112091/14/I-LG and the statutory activities of Institute of Oceanology (Sopot, Poland). Iwona Niedźwiecka, during the PhD study, was supported by the Centre for Polar Studies, KNOW-Leading National Research Centre, Sosnowiec, Poland.

I am grateful to prof. dr hab. Jacek Piskozub for taking on the role of my supervisor and further trust in research work. His guidance, suggestion and feedback allow selecting the important aspects of my research to be included into this dissertation.

Special thanks are dedicated to Employees and Colleagues from the Physical Oceanography Department , OceanFlux Greenhous Gases Evolution project, and Centre for Polar Studies, especially: Tomasz Petelski , Przemek Makuch, Drozdowska Violetta, Piotr Markuszewski, Małgorzata Kitowska, Joanna Legeżyńska, Jamie Shutler, Ian Ashton and Phil Nightingale for support and cooperation.

Finally, I would like to express my deepest gratitude to my parents and my husband for their continuous support and belief, for their love, patience and remarkable atmosphere.